

Title	DEVELOPMENT OF SYNTHETIC POLYAMPHOLYTES VIA RAFT POLYMERIZATION AND THEIR BIOMATERIAL APPLICATIONS LIKE CELL CRYOPROTECTION AND PROTEIN AGGREGATION INHIBITION
Author(s)	ROBIN, RAJAN
Citation	
Issue Date	2016-06
Type	Thesis or Dissertation
Text version	ETD
URL	<a href="http://hdl.handle.net/10119/13722">http://hdl.handle.net/10119/13722</a>
Rights	
Description	Supervisor: 松村 和明, マテリアルサイエンス研究科, 博士

# **Doctoral Dissertation**

**Development of synthetic polyampholytes via RAFT polymerization and their biomaterial applications like cell cryoprotection and protein aggregation inhibition**

**ROBIN RAJAN**

**Supervisor: Associate Prof. Dr. Kazuaki Matsumura**

School of Materials Science

Japan Advanced Institute of Science and Technology

**June 2016**

**Referee-in-chief: Associate Professor Dr. Kazuaki Matsumura**

Japan Advanced Institute of Science and Technology

**Referees: Professor Dr. Masahiro Takagi**

Japan Advanced Institute of Science and Technology

**Professor Dr. Tatsuo Kaneko**

Japan Advanced Institute of Science and Technology

**Associate Professor Dr. Yuki Nagao**

Japan Advanced Institute of Science and Technology

**Professor Dr. Koichi Kato**

Hiroshima University

## **Preface**

Nature has endowed us with many unique compounds and molecules which display extra-ordinary properties that are essential for our survival. Researchers have been trying to match nature's efficiency for many decades. Natural polymers have been known and used by people from the beginning of the human civilization in the form of rubber, papyrus, clothing, etc. The Human body is also composed of proteins and other enzymes which are polymers of amino acids. The term "polymer" was coined by Jöns Jacob Berzelius, a Swedish Scientist in 1833. His classification of polymers back then was different from what is known today. Hermann Staudinger in 1920 was the first one to develop the concept of classical polymerization, for which he won the Nobel Prize in 1953. Polyampholytes, which were developed years later, resemble proteins and enzymes because of the presence of both the charges. They are suitable substances to mimic protein folding phenomenon and for various other biomaterial applications. They exhibit several unique properties like coil-globule transitions, pH and temperature sensitivity, biocompatibility, etc. Owing to all these properties, polyampholytes have gained significant attention among all the researchers worldwide. The main purpose of this study was to develop synthetic polyampholytes and employ them for different biomaterial applications.

The first chapter deals with the general introduction for the thesis and discusses the state of the art in the field of polymers, cryopreservation and protein studies. And the latter part of this chapter explains the detailed research objective of the thesis.

The second chapter deals with the development of synthetic polyampholytes and the investigation of their cryoprotective properties. Preliminary analysis of membrane protection and biocompatibility studies has been detailed in this chapter.

The third chapter is devoted to elucidating the molecular mechanism of cryopreservation by polyampholytes. For this study, interactions of cell membrane with polyampholytes by using liposomes as cell membrane mimic and also polymer chain dynamics during freezing were investigated.

The fourth chapter presents the development of novel zwitterionic polymers for protein aggregation inhibition studies. The efficiency of this polymer was compared with previously reported compounds for protein aggregation inhibition. The effect of this polymer on the protein's secondary structure has also been investigated.

The fifth chapter deals with the transformation of zwitterionic polymer into a core-shell nanogel in order to increase the efficiency of the linear polymer. Efficiency of the nanogels have been compared with the zwitterionic polymer developed in chapter 4.

The final chapter presents the summary and scope of the thesis. It details the importance of this thesis and its contribution in the biomaterials field. The chapter also discusses the possible future impact of this thesis.

In conclusion, this thesis outlines the versatility and the multifunctional nature of the polyampholytes.

It is needless to say that I stand solely responsible for any lapses that might have occurred in carrying out and in presentation of this work, despite all the precautions taken to the best of my ability.

## **Table of Contents**

<b>Chapter 1 INTRODUCTION .....</b>	<b>1</b>
<b>1.1 Polymers.....</b>	<b>1</b>
<b>1.1.1 Polymerization Process.....</b>	<b>2</b>
<b>1.1.2 Controlled Radical Polymerization – Living Polymerization .....</b>	<b>3</b>
<b>1.1.2.1 Fundamentals of CRP .....</b>	<b>5</b>
<b>1.1.2.2 Types of CRP's.....</b>	<b>6</b>
<b>1.1.3 RAFT Polymerization .....</b>	<b>7</b>
<b>1.1.3.1 Mechanism of RAFT polymerization .....</b>	<b>8</b>
<b>1.1.3.2 Advantages of RAFT polymerization .....</b>	<b>9</b>
<b>1.1.4 Polyampholytes and zwitterionic polymers.....</b>	<b>10</b>
<b>1.2 Cryopreservation.....</b>	<b>15</b>
<b>1.2.1 Biophysical aspects of ice formation .....</b>	<b>16</b>
<b>1.2.2 Correlation between cryoinjury and the two phenomena occurring during freezing .....</b>	<b>17</b>
<b>1.2.3 Cooling rates .....</b>	<b>17</b>
<b>1.2.4 Slow cooling.....</b>	<b>18</b>
<b>1.2.5 Cryoprotective additives .....</b>	<b>19</b>
<b>1.2.6 History of CPAs .....</b>	<b>20</b>
<b>1.2.7 Problems associated with current CPAs .....</b>	<b>20</b>
<b>1.3 Protein Stability .....</b>	<b>21</b>
<b>1.4 Objective of the thesis.....</b>	<b>22</b>
<b>1.5 References .....</b>	<b>25</b>
<b>Chapter 2 PREPARATION OF NOVEL SYNTHETIC CRYOPROTECTIVE POLYAMPHOLYTES <i>via</i> RAFT POLYMERIZATION .....</b>	<b>31</b>
<b>2.1 Introduction.....</b>	<b>31</b>
<b>2.2 Materials and methods .....</b>	<b>32</b>

2.2.1 Materials.....	32
2.2.2 Synthesis of polyampholytes .....	32
2.2.3 Cell culture .....	33
2.2.4 Cryopreservation of cells .....	33
2.2.5 Cell viability and proliferation assay .....	34
2.2.6 Cytotoxicity assay .....	34
2.2.7 Liposome preparation.....	35
2.2.8 Leakage experiment .....	35
2.2.9 Statistical analysis .....	35
2.3 Results and discussion .....	36
2.3.1 Characterization.....	36
2.3.2 Cryoprotective properties of these polyampholytes .....	39
2.3.2.1 Effects of monomer ratios .....	39
2.3.2.2 Effects of hydrophobicity .....	40
2.3.2.3 Effects of molecular weight.....	42
2.3.3 Leakage experiment .....	44
2.3.4 Biocompatibility of the novel polyampholytes .....	45
2.4 Conclusion .....	46
2.5 References .....	47
<b>Chapter 3 TOWARDS A MOLECULAR UNDERSTANDING OF THE MECHANISM OF CRYOPRESERVATION: CELL MEMBRANE INTERACTION AND HYDROPHOBICITY.....</b>	<b>50</b>
3.1 Introduction.....	50
3.2 Experimental .....	54
3.2.1 Materials.....	54
3.2.2 Synthesis of Polyampholytes .....	54
3.2.2.1 Synthesis of poly-(MAA-DMAEMA) .....	54

3.2.2.2 Synthesis of poly-SPB .....	55
3.2.2.3 Synthesis of poly-CMB .....	55
3.2.2.4 Introduction of hydrophobicity .....	55
3.2.3 Molecular Weight Determination .....	57
3.2.4 Cell Culture and Cryopreservation.....	57
3.2.5 Liposome Preparation.....	58
3.2.6 DSC.....	58
3.2.7 Electron Spin Resonance Spectroscopy .....	58
3.2.8 Ice recrystallization inhibition - Cooling Splat assay .....	60
3.2.9 Leakage Experiment.....	60
3.2.10 Solid State NMR .....	61
3.3 Results and discussion .....	61
3.3.1 Cryopreservation .....	67
3.3.2 DSC.....	70
3.3.3 Electron Spin Resonance Spectroscopy .....	72
3.3.4 Ice recrystallization inhibition.....	77
3.3.5 Leakage Experiment.....	80
3.3.6 Polymer Chain Dynamics .....	81
3.4 Conclusion .....	84
3.5 References .....	84
<b>Chapter 4 ZWITTERIONIC POLYMER AS A NOVEL INHIBITOR OF PROTEIN AGGREGATION .....</b>	<b>88</b>
4.1 Introduction.....	88
4.1.1 Materials and Methods.....	90
4.1.2 Methods .....	90
4.1.3 Synthesis of Poly-SPB.....	90
4.1.4 Thioflavin T Assay.....	90



4.1.5 Residual Enzyme Activity .....	90
4.1.6 Transmission Electron Microscopy .....	91
4.1.7 Statistical Analysis .....	91
4.2 Results & discussion .....	91
4.2.1 Characterization.....	91
4.2.2 Protein aggregation Inhibition .....	96
4.2.3 Amyloid Fibril Formation.....	98
4.2.4 Enzymatic Activity .....	100
4.2.5 Preservation of Secondary Structure .....	102
4.2.5.1 ATR-FTIR.....	102
4.2.5.2 <sup>1</sup> H-NMR .....	102
4.3 Conclusion .....	105
4.4 References .....	105
<b>Chapter 5 CORE-SHELL NANOGELS AS EFFECTIVE SUPPRESSOR OF PROTEIN AGGREGATION.....</b>	<b>110</b>
5.1 Introduction.....	110
5.2 Materials and Methods .....	111
5.2.1 Methods .....	111
5.2.2 Synthesis of Poly-SPB.....	111
5.2.3 Synthesis of core-shell nanogels.....	112
5.2.4 Synthesis of Nanogel (with BuMA in the core).....	113
5.2.5 Molecular Weight Determination .....	114
5.2.6 Thioflavin T Assay .....	114
5.2.7 Residual Enzyme Activity .....	114
5.3 Results and Discussion.....	114
5.3.1 Characterization.....	114
5.3.2 Enzymatic Activity .....	117

5.3.3 Amyloid Fibril Formation.....	118
5.4 Conclusion .....	119
5.5 References .....	119
<b>Chapter 6 SUMMARY AND OUTLOOK .....</b>	<b>122</b>
6.1 Conclusion .....	122
6.2 Outlook and Scope.....	123
<b>ACHIEVEMENTS .....</b>	<b>125</b>
<b>ACKNOWLEDGEMENT .....</b>	<b>126</b>

## **List of Tables and Figures**

<b>Table 1.1.</b> Differences between controlled radical polymerization and free radical polymerization.....	4
<b>Table 1.2.</b> Classes of RAFT agents.....	7
<b>Table 1.3.</b> Comparison of NMP, ATRP and RAFT polymerization (From K. Matyjaszewski, T. Davis (Eds.), Handbook of Radical Polymerization, John Wiley & Sons, New Jersey (2002)) <sup>3</sup> .....	9
<b>Table 2.1.</b> Characteristics of various polyampholytes prepared via RAFT polymerization. a) Determined by <sup>1</sup> H-NMR, b) [monomer]:[initiator]:[RAFT agent], c) determined by GPC. ....	37
<b>Table 3.1.</b> Characteristics of various polyampholytes prepared via RAFT polymerization. a) Determined by <sup>1</sup> H-NMR, b) [monomer]:[initiator]:[RAFT agent] .....	66
<b>Table 3.2.</b> Polymer contact angle and viscosity of various polymers with and without their hydrophobic derivatives at 2.5 % polymer concentration. ....	74
<b>Table 4.1.</b> Zeta Potential values at pH 7. (Numbers in parenthesis indicate the final concentration (w/v) %). ....	97
<b>Table 5.1.</b> Characteristics of the poly-(SPB) prepared via RAFT polymerization.	115
<b>Table 5.2.</b> Characteristics of the nanogels prepared via RAFT polymerization. ...	117
 <b>Figure 1.1</b> Schematic Representation of classification of polymers is based on the arrangement of the repeating units in a copolymer. ....	2
<b>Figure 1.2.</b> Examples polymer architectures that can be obtained via CRP (From Krzysztof Matyjaszewski , James Spanswick, Controlled/living radical polymerization, Materialstoday, Volume 8, Issue 3, March 2005, Pages 26–33). <sup>3</sup> .....	5
<b>Figure 1.3.</b> The three main types of CRP's (From Krzysztof Matyjaszewski , James Spanswick, Controlled/living radical polymerization, Materialstoday, Volume 8, Issue 3, March 2005, Pages 26–33). <sup>3</sup> .....	6
<b>Figure 1.4.</b> Mechanism of RAFT polymerization (From Graeme Moad, Ezio Rizzardo, San H. Thang, Polymer, Volume 49, Issue 5, 3 March 2008, Pages 1079–1131). <sup>12</sup> .....	8

- Figure 1.5.** Comparison of the number of publications related to a) “polyampholytes” and b) “zwitterionic polymers”. (Data collected from title search in Web of science, Thomson Reuters). ..... 12
- Figure 1.6.** a) Schematic representation of the reaction of PLL succinylation. Cryoprotective properties of COOH-PLLs. (a) L929 cells were cryopreserved with 10% DMSO and 7.5% (w/w) PLL with different ratios of introduced COOH. Cell viability immediately (white bars), and 6 h (gray bars) after thawing at 37 C. (b) L929 cells were cryopreserved with various concentrations of PLL (0.65). Cell viability immediately (white bars), and 6 h (gray bars) after thawing at 37 C. Data are expressed as mean SD for 3 independent experiments (5 samples each). \*\*\*P < 0.001 vs 10% DMSO for the corresponding time period (0 or 6 h). (From Matsumura and Hyon. 2009. Biomaterials 30: 4842–4849)<sup>23</sup>14
- Figure 1.7.** Plot of the survival percent versus the cooling rate for different cell types of cells. (From Mazur, P., Cryobiology, 14, 251, 1977.)..... 18
- Figure 1.8.** Schematics of the physical events occurring in cells during freezing (From Mazur, P., Cryobiology, 14, 251, 1977). ..... 19
- Figure 2.1.** <sup>1</sup>H-NMR spectra of (a) the 1:1 copolymer polyampholyte of DMAEMA and MAA, (b) the 5% Bu-MA incorporated 1:1 polyampholyte and (c) 5% Oc-MA incorporated 1:1 polyampholyte. .... 38
- Figure 2.2.** Characterization of RAFT polymerization products. (a) Kinetic plot for the conversion vs. time of the 1:1 MAA-DMAEMA copolymer. (b) Plots of time vs.  $M_w/M_n$  and time vs.  $M_n$  for the polymerization of the 1:1 MAA-DMAEMA copolymer. (c) Plots of the content ration of RAFT agent used vs. the degree of polymerization and the concentration of RAFT agent used vs. the molecular weight. .... 39
- Figure 2.3.** Cryoprotective properties of copolymers with different copolymer ratios. L929 cells were cryopreserved with MAA-DMAEMA copolymers synthesized using different ratios of MAA and DMAEMA (15 % polymer concentration). ... 40
- Figure 2.4.** Effects of hydrophobicity of polyampholytes on cryopreservation. (a) L929 cells were cryopreserved with polyampholytes synthesized with a 1:1 ratio of MA and DMAEMA and different concentrations of Bu-MA (15% polymer concentration). (b) L929 cells were cryopreserved with polyampholytes synthesized with a 1:1 ratio of MA and DMAEMA and different concentrations of Oc-MA at various polymer concentrations. (c) L929 cells were cryopreserved with different polymers (10 % polymer concentration) and 5% Bu-MA or Oc-MA. A comparison with a polymer containing the hydrophilic monomer HEMA is shown. Data are expressed as the mean  $\pm$  SD of 3 independent experiments (5 samples each). \*\*\*p < 0.001. .... 42

<b>Figure 2.5.</b> Effects of the molecular weight of polyampholytes on cryopreservation. (a) L929 cells were cryopreserved with the 1:1 MAA-DMAEMA copolymer (10 % polymer concentration) at different molecular weights. (b) L929 cells were cryopreserved with different concentrations of polyampholytes synthesized with a 1:1 ratio of MA and DMAEMA and 8% Bu-MA having 2 different molecular weights. Data are expressed as the mean $\pm$ SD for 3 independent experiments (5 samples each). ***p < 0.001, **p < 0.05. ....	43
<b>Figure 2.6.</b> Protection of liposomes during freezing by polyampholytes. CF leakage from liposomes cryopreserved with various polyampholytes solutions at different polymer concentrations. Data are expressed as the mean $\pm$ SD for 3 independent experiments (5 samples each).....	45
<b>Figure 2.7.</b> Cytocompatibilities of polyampholytes. (a) Cytotoxicity of DMSO (open circles), 1:1 MAA-DMAEMA copolymer (closed circles), 1:1 MAA-DMAEMA copolymer with 5% Oc-MA (open triangles), and 1:1 MAA-DMAEMA copolymer with 5 % Bu-MA (closed triangles). L929 cells were incubated with the indicated concentration of each compound for 48 h, followed by CCK assay. Data are described as the percentage of viable cells as compared to the number of untreated cells. Mean values and standard deviations for independent triplicate experiments (8 samples each) are shown. (b) Growth curves of L929 cells, unfrozen control (open circles), cryopreserved with 1:1 MAA-DMAEMA copolymer (closed circles), 1:1 MAA-DMAEMA copolymer with 5% Oc-MA (open triangles), and 1:1 MAA-DMAEMA copolymer with 5% Bu-MA (closed triangles) for 7 days. Data are expressed as the mean $\pm$ SD of 3 independent experiments. ....	46
<b>Figure 3.1.</b> $^{23}\text{Na}$ -NMR spectra of (a) physiological saline solution, (b) DMSO, and (c) PLL(0.65) saline solutions during freezing (From Matsumura et al, Cryobiology. Cryotechnol., 2013, 59, 23-28). <sup>18</sup> .....	52
<b>Figure 3.2.</b> $^1\text{H}$ -NMR spectra of (a) DMSO, and (b) PLL (0.65) saline solutions during freezing (From Matsumura et al, Cryobiology. Cryotechnol., 2013, 59, 23-28). <sup>18</sup> .....	52
<b>Figure 3.3.</b> Schematic representation of the mechanism of cryopreservation by PLL (0.65). ....	53
<b>Figure 3.4.</b> Synthesis of (a) Poly-(MAA and DMAEMA) (b) Poly-SPB, (c) Poly-CMB and d) hydrophobic derivatives of polyampholytes by RAFT polymerization... ..	56
<b>Figure 3.5.</b> ESR spectra of a) 5-DSA and b) 16-DSA in EPC liposome in PBS (pH 7.4).....	60
<b>Figure 3.6.</b> Time dependent $^1\text{H}$ -NMR of b) poly-SPB and c) poly-CMB in $\text{D}_2\text{O}$ .....	63

<b>Figure 3.7.</b> Kinetic plot for the polymerization of poly-(MAA-DMAEMA), poly-SPB and poly-CMB by RAFT polymerization, followed by $^1\text{H}$ NMR spectroscopy in $\text{D}_2\text{O}$ .	64
<b>Figure 3.8.</b> NMR signal assignment of a) poly-(MAA-DMAEMA), b) poly-SPB and c) poly-CMB in $\text{D}_2\text{O}$ (900 MHz).	65
<b>Figure 3.9.</b> Cryoprotective properties of poly-(MAA-DMAEMA) and the effect of hydrophobicity. L929 cells were cryopreserved with MAA-DMAEMA copolymer with different polyampholytes at various concentrations. Data are expressed as mean $\pm$ SD for 3 independent experiments (5 samples each).	67
<b>Figure 3.10.</b> Cryoprotective properties of poly-(MAA-DMAEMA), poly-SPB and poly-CMB a) at various polymer concentration and b) with different concentration of OcMA at 10 % polymer concentration. L929 cells were cryopreserved with different polyampholytes at various concentrations. Data are expressed as mean $\pm$ SD for 3 independent experiments (5 samples each).	69
<b>Figure 3.11.</b> a) DSC heating thermograms of EPC liposomes in the presence of different amounts of i) poly-(MAA-DMAEMA), ii) poly-SPB and iii) poly-CMB. The resulting Polymer/EPC mass ratios are indicated to the right of each trace and b) Effects of poly-(MAA-DMAEMA), poly-SPB and poly-CMB on gel to liquid-crystalline transition temperature of EPC at Polymer/EPC mass ratios between 0 and 1.0.	71
<b>Figure 3.12.</b> a) ESR spectra of 5-DSA (1 mol %) incorporated in EPC in the presence of various polymers at different polymer concentrations. Numbers below denote the order parameter (S) and b) Polyampholyte concentration dependence of order parameters S for 5-DSA (1 mol %) intercalated into unilamellar dispersions of EPC in PBS buffer (pH 7.4).	73
<b>Figure 3.13.</b> a) ESR spectra of 16-DSA (1 mol %) intercalated in EPC in the presence of various polymers at different polymer concentrations. Numbers below denote the correlation time ( $\tau$ ) and b) Polyampholyte concentration dependence of correlation time $\tau$ for 16-DSA (1 mol %) intercalated into unilamellar dispersions of EPC in PBS buffer (pH 7.4).	75
<b>Figure 3.14.</b> Hydrophobic polyampholytes (with 5 % OcMA) concentration dependence of correlation time $\tau$ for 16-DSA (1 mol %) intercalated into unilamellar dispersions of EPC in PBS buffer (pH 7.4).	76
<b>Figure 3.15.</b> Schematic representation of membrane-polyampholyte interaction/localization.	77

<b>Figure 3.16.</b> a) Schematic representation of the splat assay; b) Micrographs of poly-nucleated ice crystals in PBS alone and in the presence of poly-(MAA-DMAEMA) with BuMA, after 30 minutes annealing at -6° C (scale bars = 100 μm). .....	78
<b>Figure 3.17.</b> Ice recrystallization inhibition activity of poly-(MAA-DMAEMA), poly-SPB and poly-CMB and the effect of hydrophobicity at 10 % polymer concentration. Errors bars indicate the standard deviation of the mean.....	80
<b>Figure 3.18.</b> Protection of liposomes during freezing by different polyampholytes. CF leakage from liposomes cryopreserved with various polyampholytes solutions at different polymer concentrations. Data are expressed as the mean ± SD for 3 independent experiments (5 samples each).....	81
<b>Figure 3.19.</b> <sup>1</sup> H-NMR spectra of a) poly-(MAA-DMAEMA), b) poly-SPB and c) poly-CMB in physiological saline solution (10 % w/v) during freezing. ....	83
<b>Figure 4.1.</b> Synthesis of poly-SPB by RAFT polymerization. ....	92
<b>Figure 4.2.</b> a) <sup>1</sup> H-NMR and b) <sup>13</sup> C-NMR of poly-SPB in D <sub>2</sub> O. ....	93
<b>Figure 4.3.</b> ATR-FTIR spectra of SPB monomer and poly-SPB.....	94
<b>Figure 4.4.</b> a) Time-dependent <sup>1</sup> H-NMR and b) Kinetic plot for the polymerization of SPB by RAFT polymerization, followed by <sup>1</sup> H NMR spectroscopy in D <sub>2</sub> O. ....	95
<b>Figure 4.5.</b> Photographs of lysozyme in PBS (3 mg/mL) at room temperature (top) and at 90° C (bottom); a) without additive; b) with 10 % SPB; c) with 10 % poly-SPB. Absorbance at 500 nm is shown below each image. ....	96
<b>Figure 4.6.</b> CD spectra of lysozyme (0.5 mg/mL) in PBS buffer at 30° C and 90° C. ....	97
<b>Figure 4.7.</b> TEM images of lysozyme solution after incubation at 90° C a) in PBS alone, and b) with poly-SPB. Scale bars represent 100 nm. ....	98
<b>Figure 4.8.</b> a) Protein aggregation of lysozyme (0.5 mg/mL) when heated to 90° C for 30 minutes a) in the presence of poly-SPB at various polymer concentrations, and b) in the presence of various reagents (5 % w/v). Data are expressed as the mean ± SD of 3 independent experiments (5 samples each) ***P < 0.001 vs. all other reagents. ....	99
<b>Figure 4.9.</b> a) Rate of inactivation of lysozyme when heated to 90° C when lysozyme in PBS (open triangle, slope = 0.0418); with 15 % poly-SPB (closed triangle, slope = 0.0355); with 10 % poly-SPB (open circle, slope=0.0095) and with 7.5 % poly-SPB (closed circle, slope = 0.001), and b) Enzymatic activity of lysozyme after treatment at 90 °C in the presence of poly-SPB. Data are	

expressed as the mean $\pm$ SD of 3 independent experiments (5 samples each). .....	101
<b>Figure 4.10.</b> ATR-FTIR of native lysozyme in the presence of poly-SPB and lysozyme (aggregated) after heating at 90 °C for 30 min. ....	102
<b>Figure 4.11.</b> a) <sup>1</sup> H NMR spectra of a mixture of a) lysozyme in PBS, b) lysozyme mixed with monomer SPB, and c) lysozyme mixed with poly-SPB at room temperature and after heating to 90 °C for 30 min. ....	104
<b>Figure 4.12.</b> Schematic representation of the interaction between poly-SPB and lysozyme leading to the protection of lysozyme during heating. ....	105
<b>Figure 5.1.</b> Synthesis of Macro-CTA (poly-SPB).....	111
<b>Figure 5.2.</b> Synthesis of core-shell nanogel of poly-SPB. ....	112
<b>Figure 5.3.</b> Synthesis of core-shell nanogel of poly-SPB with BuMA in the core. ....	113
<b>Figure 5.4.</b> Kinetic plot of Poly-SPB with a) DP 20 and b) DP 200. ....	115
<b>Figure 5.5.</b> Schematic Representation of nanogel formation.....	116
<b>Figure 5.6.</b> Enzymatic activity of lysozyme after treatment at 90 °C in the presence of different nanogels at 5% polymer concentration (w/v %). Data are expressed as the mean $\pm$ SD of 3 independent experiments.....	118
<b>Figure 5.7.</b> Protein aggregation inhibition of lysozyme (0.5 mg/mL) when heated to 90 °C for 30minutes in the presence of different nanogels at 5% concentration (w/v %). Data are expressed as the mean $\pm$ SD of 3 independent experiments. .....	119



## Chapter 1 INTRODUCTION

### 1.1 Polymers

Polymers are large molecules made up of several repeating units. They have found applications across-the-board, owing to their extensive properties. Hence, we are all surrounded by polymers in our day-to-day lives. Nature has endowed us with many natural polymers which are essential for our survival. The proteins inside our bodies, enzymes and a range of other natural substances are all examples of natural polymers. Polymers can also be synthetically made and they are known as synthetic polymers. Both these type of polymers are made by polymerization of numerous small molecules. When all the molecules (repeating units) are same, then those polymers are known as homopolymers. On the other hand, when the repeating units are different compounds, then the polymers are known as heteropolymers or copolymers.<sup>1</sup>

Other than the constituent repeating units, another broad classification of polymers is based on the arrangement of the repeating units in a copolymer. They are broadly classified into 4 categories (Fig. 1.1):

**Random copolymers:** When the repeating units are arranged in random fashion.

**Block copolymers:** When the repeating units are arranged in definite blocks.

**Alternating copolymers:** When the repeating units are arranged in an alternating fashion.

**Graft polymers:** When one polymer chain is grafted onto the backbone of another polymer chain.



**Figure 1.1** Schematic Representation of classification of polymers is based on the arrangement of the repeating units in a copolymer.

Apart from these broader categories, there are various other classifications of polymers depending on their stereochemistry, types of monomers, polymer structure, etc.

### 1.1.1 Polymerization Process

Polymer synthesis or polymerization can again be classified into various categories such as addition/condensation polymerization, chain growth/step growth polymerization, etc.

Chain growth polymerization and addition polymerization can sometimes be used interchangeably. The three main steps in this type of polymerization are:

**Initiation:** This is the step when the polymerization is initiated. For this process, an initiator is used.

**Propagation:** The activated chains of the repeating units attach together and longer chains are formed by the transfer of active sites.

**Termination:** In this step, polymerization reaction is terminated/stopped. This happens when two active chains add together to produce an inactive compound/chain.

This type of polymerization can take place in many ways such as anionic polymerization, cationic polymerization, free radical polymerization and coordination polymerization. The classification is quite clear from their respective names.

Free radical polymerization has the following advantages over the other types of polymerizations:

- It can be used to polymerize a wide range of vinyl, allyl and other types of monomers
- Polymerization process is not as complicated or difficult, as is the case with other types.

Almost half of the materials synthesized commercially (synthetic polymers) in industries are prepared *via* radical polymerization.<sup>2, 3</sup>

### 1.1.2 Controlled Radical Polymerization – Living Polymerization

Controlled radical polymerization (CRP) was developed because there were many drawbacks of the conventional free radical polymerizations. Some of the drawbacks of free radical polymerizations are as follows:

- There is very little control over the molecular weight of the polymer and molar mass distribution.
- It is extremely difficult to synthesize block copolymers or other polymer architectures.
- Tacticity of the polymer is very difficult to be controlled.
- Difficult to introduce different functionalities.
- Poor control over the synthesis of polymers with different architectures.<sup>3</sup>

The basic polymerization scheme is similar in both the types of polymerization. They also consist of initiation step, followed by propagation and then termination. In CRP, an additional step is present called the transfer process where an active site of the transfer agent gets attached or transferred to either a monomer, initiator or a growing polymer. Although there are some similarities, however there are some fundamental differences also between the two which are listed in Table 1.<sup>4</sup>

**Table 1.1.** Differences between controlled radical polymerization and free radical polymerization.

Features	Controlled Radical Polymerization	Free radical Polymerization
Lifetime of growing chains	More than 1 hour	<1 s
Initiation	Very fast	Slow
Growing Chains	Proportion of dead chains <10%	Almost all are dead
Polymerization rates	Relatively slower	Fast
Termination	Short chains are formed initially which grows in length with the progress of the reaction. Hence, rate of termination decreases with time	Termination takes place between the newly formed chains and the existing long chains
Achievement of steady state	Because activation and deactivation rates are balanced	Because initiation and termination rates are similar

With CRP, polymers with various architectures can be prepared (Fig. 1.2). With the ability to develop various architectures and to control molecular weight and its polydispersity has enabled researchers to enhance the properties of the existing materials.

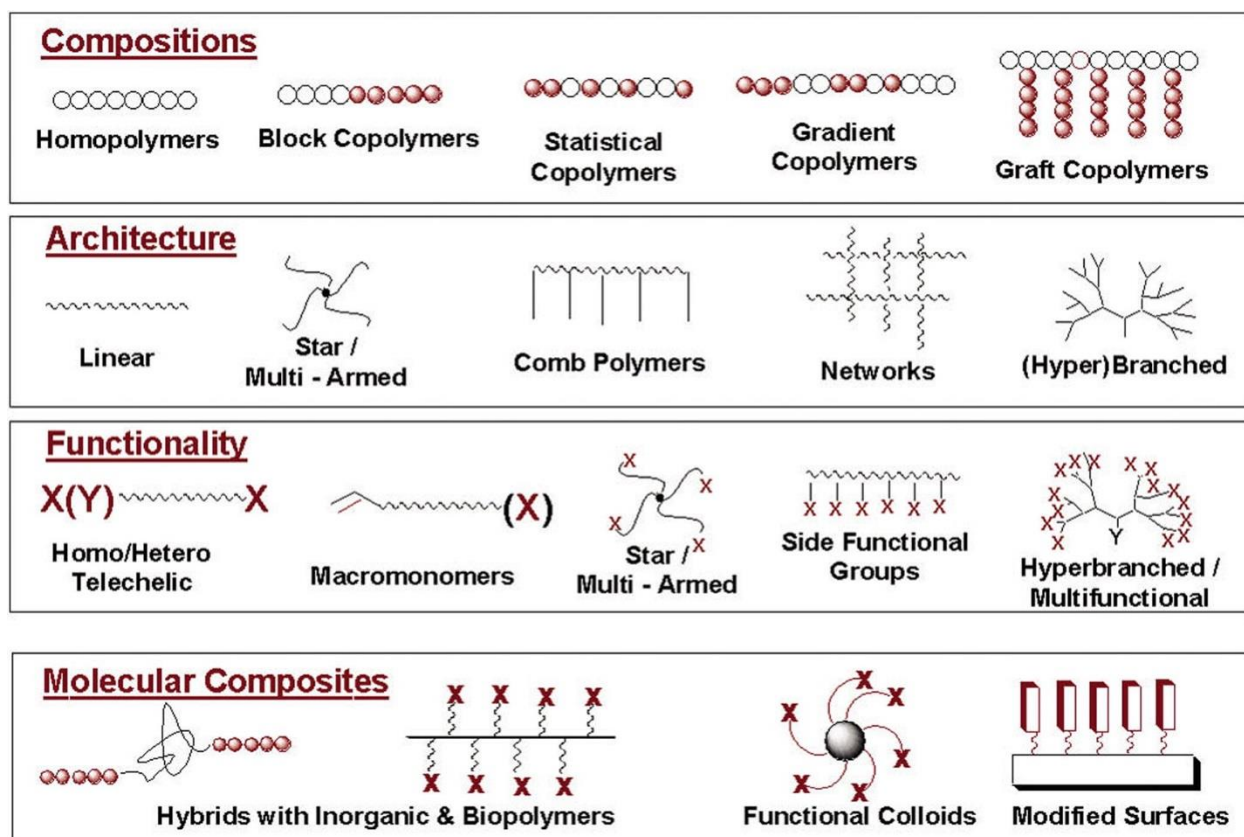


**Figure 1.2.** Examples polymer architectures that can be obtained via CRP (From Krzysztof Matyjaszewski, James Spanswick, *Controlled/living radical polymerization*, *Materialstoday*, Volume 8, Issue 3, March 2005, Pages 26–33).<sup>3</sup>

### 1.1.2.1 Fundamentals of CRP

Characteristics of an ideal CRP are as follows:

- Rate of initiation should be greater than the rate of propagation. This enables all the chains to grow at the same time and at the same rate.
- At any given time, most of the chains should be in dormant state. This is achieved by the fast exchange and the equilibrium between the dormant and the active species.
- There should not be any transfer or termination reactions.
- Molecular weight should increase linearly with the percentage conversion of the monomer. In other word, it should follow first order kinetics.

- There should be only one type of propagating chain, this eliminates the interconversion which is possible when more than one propagating chains are present.

### 1.1.2.2 Types of CRP's

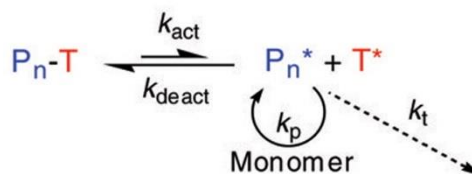
Numerous methods to carry out CRPs have been developed in the past. Not all the methods were well-accepted by the scientific community because of their inherent drawbacks. The three most widely used are:

1. Nitroxide mediated polymerization (NMP),<sup>5, 6</sup>
2. Atom transfer radical polymerization (ATRP),<sup>7, 8</sup>
3. Reversible addition-fragmentation chain transfer (RAFT).<sup>9, 10</sup>

A brief explanation of the three processes is outlined in Fig. 1.3.

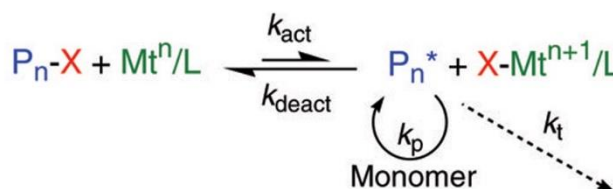
#### 1) SFRP or NMP

Thermal dissociation of dormant species ( $k_{act}$ ) provides a low concentration of radicals



#### 2) ATRP

Transition metal activation ( $k_{act}$ ) of a dormant species with a radically transferable atom



#### 3) Degenerative Transfer or RAFT

Majority of chains are dormant species that participate in transfer reactions ( $k_{exch}$ ) with a low concentration of active radicals

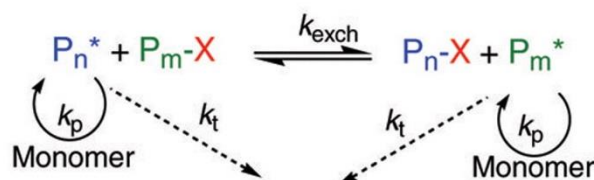


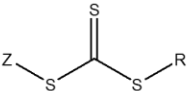
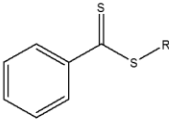
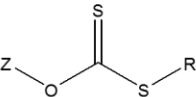
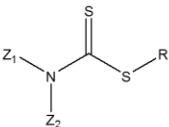
**Figure 1.3.** The three main types of CRP's (From Krzysztof Matyjaszewski, James Spanswick, *Controlled/living radical polymerization*, *Materialstoday*, Volume 8, Issue 3, March 2005, Pages 26–33).<sup>3</sup>

### 1.1.3 RAFT Polymerization

RAFT polymerization is amongst the newest and one of the most popular forms of polymerization. RAFT polymerization's versatility can be seen in its high tolerance to various reaction conditions, solvents, monomers, etc. Water soluble polymers can also be easily synthesized by this process.

RAFT is a kind of radical polymerization where monomers containing alkenes or alkynes are polymerized using a radical initiator. In this process, an extra reagent is added, known as RAFT agent, which acts as a chain transfer agent. The most widely used RAFT agents are dithiocarbamates, dithioesters, trithiocarbonates, etc.<sup>11</sup>

**Table 1.2.** *Classes of RAFT agents.*

	Trithiocarbonates	Dithiobenzoates	Xanthates	Dithiocarbamates
				
<b>Transfer Constants</b>	High	Very high	Low	Substituents on N determines the activity
<b>Reactivity</b>	High hydrolytic stability	Readily undergoes hydrolysis	More effective with electron withdrawing substituents	Effective with electron-rich monomers
<b>Polymerization Retardation</b>	Less retardation	Under high concentrations		

### 1.1.3.1 Mechanism of RAFT polymerization

The principal hallmark of RAFT polymerization is the equilibria of addition-fragmentation sequence. At first, the initiator breaks down and makes a radical ( $I^\bullet$ ) which then goes on to react with a monomer to generate a propagating radical ( $P_n^\bullet$ ). In the next step, the propagating radical adds to the RAFT agent, which leads to fragmentation and generation of the intermediate (new) radical ( $R^\bullet$ ). This new radical then adds to a monomer to generate a polymeric RAFT agent ( $P_nXC(Z)=X$ ) and new propagating radical ( $P_m^\bullet$ ). The new radical then adds to the previously formed polymeric RAFT agent and a rapid equilibrium between the propagating radicals and the dormant polymeric RAFT agent is achieved. This achievement of this equilibrium facilitates the synthesis of polymers with narrow molecular mass distribution by giving all the chains equal probability to grow (Fig. 1.4).<sup>12</sup>

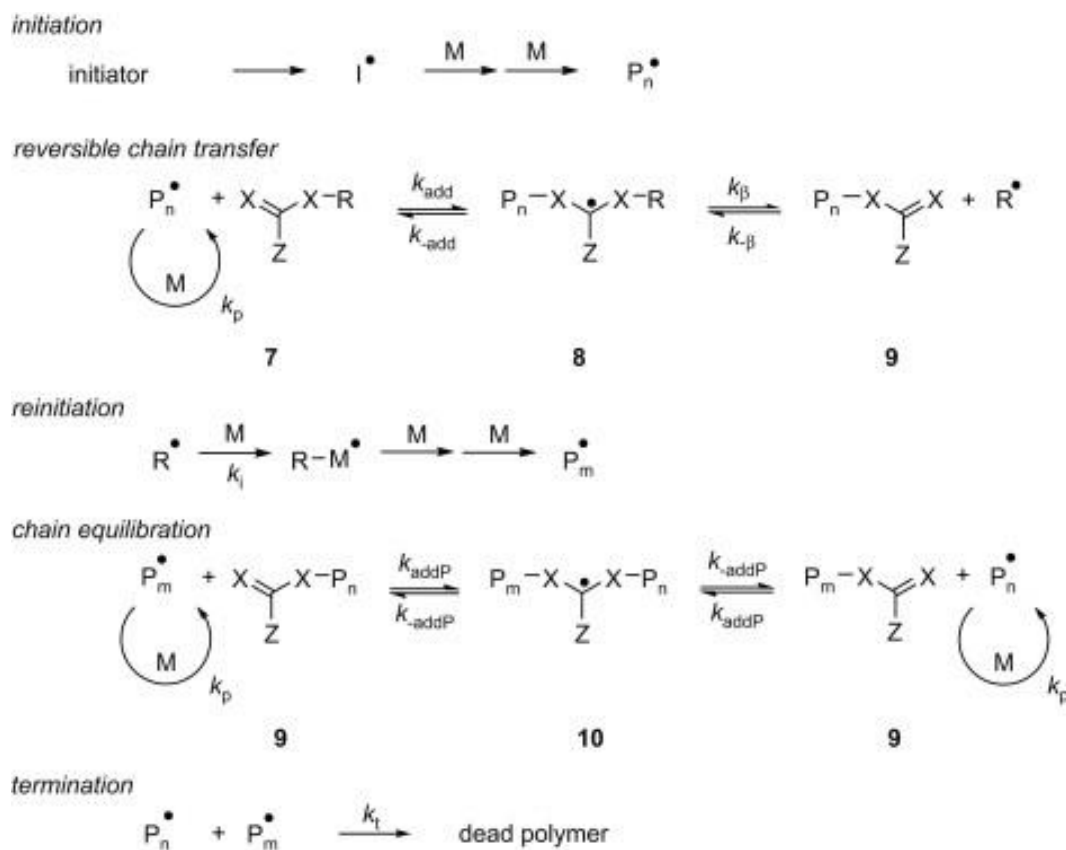


**Figure 1.4.** Mechanism of RAFT polymerization (From Graeme Moad, Ezio Rizzardo, San H. Thang, *Polymer*, Volume 49, Issue 5, 3 March 2008, Pages 1079–1131).<sup>12</sup>



### 1.1.3.2 Advantages of RAFT polymerization

All the three types of CRP's are extensively used by academic researchers and industries around the world. All of them have their own merits and demerits. In spite of their disadvantages, they are still the most convenient and effective methods of polymerization. A table outlining their versatility and their applicability is given in Table 1.3

**Table 1.3.** Comparison of NMP, ATRP and RAFT polymerization (From K. Matyjaszewski, T. Davis (Eds.), *Handbook of Radical Polymerization*, John Wiley & Sons, New Jersey (2002))<sup>3</sup>.

Feature	Systems NMP	ATRP	Degenerative Transfer (RAFT)
Monomers	Styrenes with TEMPO Also acrylates and acrylamides using new nitroxides NO methacrylates	Nearly all monomers with activated double bonds NO vinyl acetate	Nearly all monomers
Conditions	Elevated $T$ ( $>120^{\circ}\text{C}$ for TEMPO) Waterborne systems OK Sensitive to oxygen	Large $T$ range ( $-30$ – $150^{\circ}\text{C}$ ) Waterborne systems OK Some tolerance to $\text{O}_2$ and inhibitor with $\text{Mt}^0$	Elevated temperatures for less reactive monomers Waterborne systems OK Sensitive to oxygen
End Groups/ Initiators	Alkoxyamines Thermally unstable Relatively expensive Requires radical chemistry for transformations May act as a stabilizer	Alkyl (pseudo)halides Thermally and photostable Inexpensive and available Either $\text{S}_\text{N}$ , E, or radical chemistry for transformations Halogen exchange for enhanced cross-propagation	Dithioesters, iodides, and methacrylates Less thermally stable and less photo stable Relatively expensive Radical chemistry for transformations ( $\text{S}_\text{N}$ for RI) Color/odor
Additives	None NMP may be accelerated with acyl compounds	Transition metal catalyst Should be removed and recycled	Conventional radical initiator May decrease end functionality May produce too many new chains

Although the fundamental science involved is similar in the three types of CRP's, however RAFT polymerization does offer more advantages over NMP and ATRP, especially when considering biomaterial applications. The following are the advantages of RAFT polymerization:

- RAFT is applicable to a wide range of monomers, whereas in ATRP, monomers such as methacrylic acid and other monomers containing acids cannot be used. On the other hand, NMP is not suitable for di-substituted alkenes like methacrylate monomers.<sup>3</sup>
- RAFT polymers are biocompatible. Whereas, ATRP, involves copper catalyst, which is extremely cytotoxic (even when present in trace amounts). Polymers obtained by NMP are also cytotoxic.
- RAFT can tolerate various reaction conditions. Water soluble polymers can also be obtained via RAFT polymerization.
- RAFT generates end-functionalized polymers, which can later be modified according to the specific requirements.

***Due to all these advantages, RAFT polymerization was preferred over the other CRP methods in my current doctoral study.***

#### **1.1.4 Polyampholytes and zwitterionic polymers**

Polyampholytes are those polymers which encompass both the positive as well as negative charges.<sup>13, 14</sup> Alfrey et al. (1950) were the first ones to report synthetic polyampholytes. They termed polyampholytes as “***analogs of proteins***”.<sup>15</sup> Since then, numerous groups around the world have focused their attention on the study of polyampholytes and their solution properties. Few groups have suggested that the size of the coil of the polyampholytes and its corresponding viscosity as well as its solubility increases when salt is added to the solution. This is termed as “***anti-polyelectrolyte effect***”<sup>16</sup> Polyampholytes have a collapsed or a globule like conformation in a salt-free solution which is due to the attractive interaction (interchain) present between the oppositely charged atoms. When salt is added, disassociation of this attractive interaction takes place (due to the increase in ionic strength), which leads to an increase in the hydrodynamic radius.<sup>17</sup>

Polyampholytes are of two types, first type is where the existence of positive and negative charges is virtue of the presence of anionic and cationic monomers and the second type is where the presence of a zwitterionic species is responsible for the two charges.<sup>18</sup> Polyampholytes refer to a broader term of polymers which includes both the types mentioned above, but in recent times, zwitterionic polymers have emerged in itself as a new class of polymers. The main difference between the two types of polyampholytes is that in the former case, the charge of the polymer backbone can be easily tuned by changing the ratio of the two monomers. So in these cases, one charge can dominate and the net charge of the polymer may be either positive, negative or zero, while in the latter case, the net charge is usually zero under normal conditions. This is due to the presence of equal number of positive and negative charges on the polymer, and therefore it displays hybrid-like property profile, which is due to the presence of a high population of polymer-bound ion pairs attached to the polymer chain.<sup>19</sup> Zwitterionic polymers are governed by strong Coulomb interactions resulting in high hydrophilicity.<sup>20</sup> Due to the presence of a mixed charged state in zwitterionic polymers, they exhibit properties similar to those of proteins.<sup>21</sup>

Due to these properties, various polyampholytes and zwitterionic polymers have been receiving great attention from researchers across the world, as seen by the increasing number of research articles in the field (Fig. 1.5). The biomedical application of polyampholytes has been greatly studied in a review by Zurick and Bernards (2014), where they explained the application of polyampholytes in various fields like tissue engineering, non-fouling agents, drug delivery, and membrane applications.<sup>22</sup>

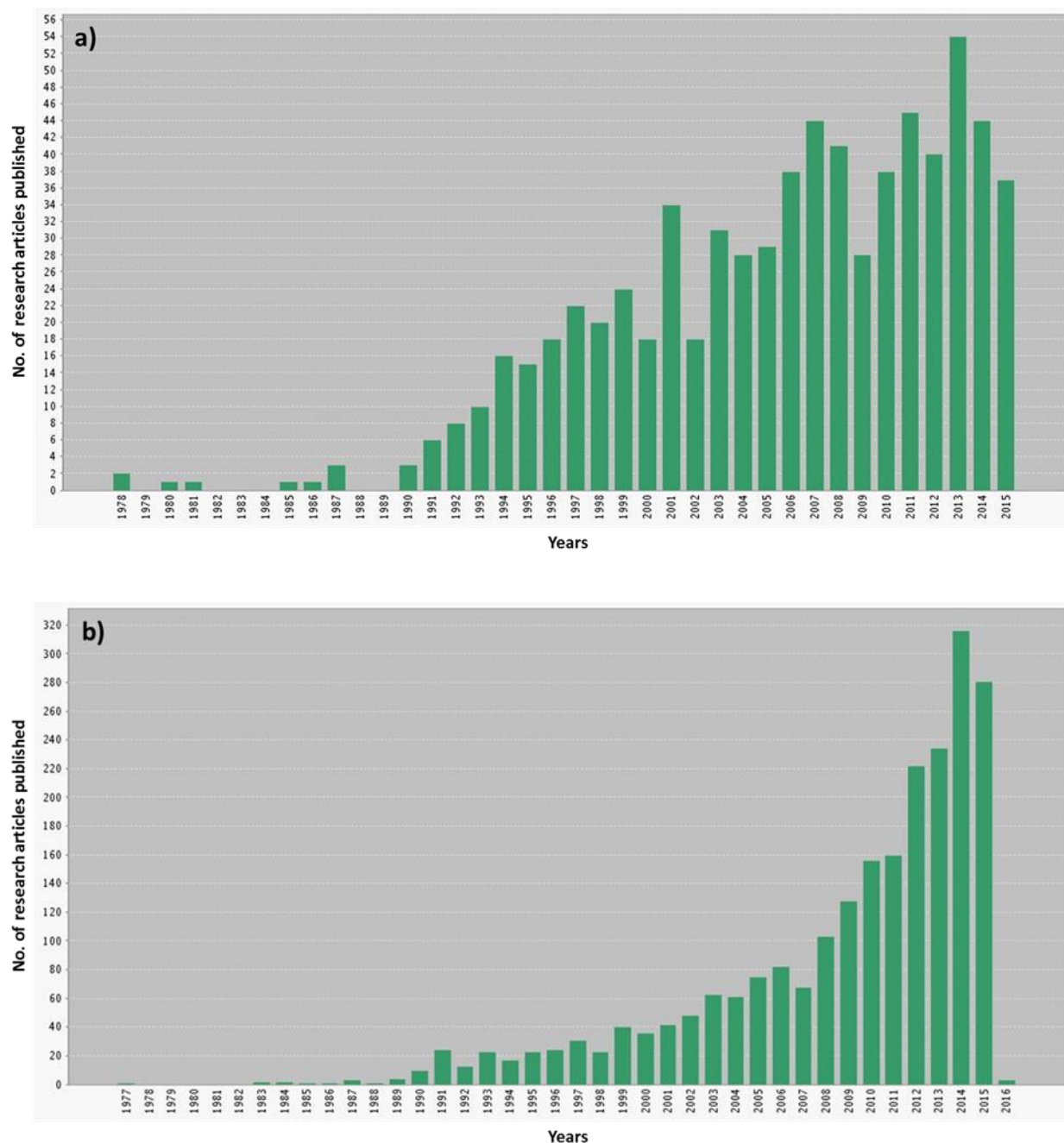


**Figure 1.5.** Comparison of the number of publications related to a) “polyampholytes” and b) “zwitterionic polymers”. (Data collected from title search in Web of science, Thomson Reuters).

Recently, our group showed that polyampholytes can be effective cryoprotective agents (Matsumura and Hyon 2009).<sup>23</sup> For this study, they synthesized succinylated-poly-L-lysine (COOH-PLL), by neutralizing cationic poly-L-lysine with anionic succinic anhydride. At

appropriate charge ratio of cation and anion (65% of the  $\alpha$ -amino group was converted into carboxyl groups), the polyampholytes showed remarkable efficiency and exhibited cell viability, which was significantly higher than dimethyl sulfoxide (DMSO). Moreover, due to the inherently lower osmotic pressure of COOH-PLL (even after neutralization by HCl or NaOH) compared to DMSO, higher concentrations of COOH-PLL can also be employed without significance loss in cell viability (see Fig. 1.6). The polyampholytes also showed excellent biocompatibility, evident by the retention of proliferation ability of the cells even after they were subjected to cryopreservation in the presence of COOH-PLL. Cytotoxicity studies revealed this DMSO has far greater cytotoxicity than COOH-PLL, which eliminates the need to immediately remove it after thawing, a problem persistent with DMSO due to its high cytotoxicity. Investigation of the cell surface affinity under cryopreservation was done by labelling COOH-PLL with fluorescein isothiocyanate (FITC) and the adsorption of the polymer to cell membrane immediately after thawing was observed. Preliminary analysis of the antifreeze properties of the polymer was also carried out, which revealed it suppresses ice recrystallization.

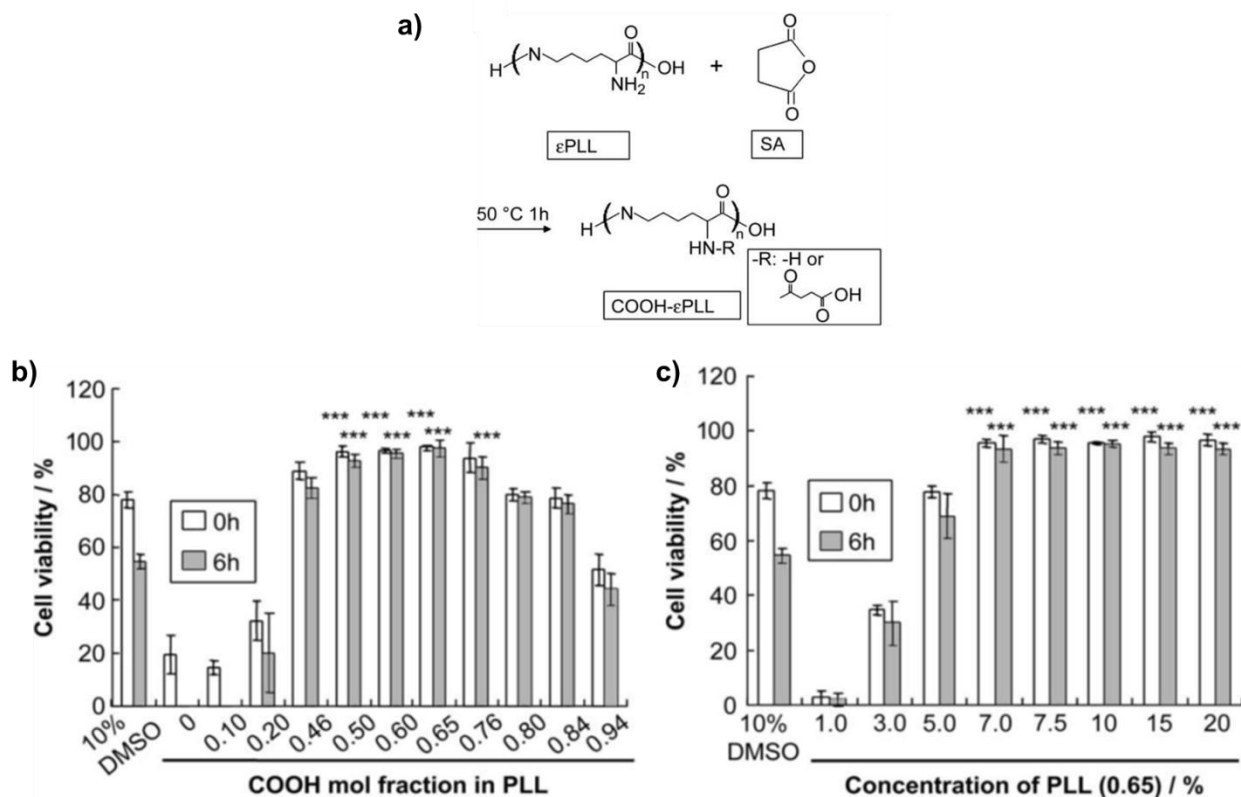


**Figure 1.6.** a) Schematic representation of the reaction of PLL succinylation. Cryoprotective properties of COOH-PLLs. (a) L929 cells were cryopreserved with 10% DMSO and 7.5% (w/w) PLL with different ratios of introduced COOH. Cell viability immediately (white bars), and 6 h (gray bars) after thawing at 37 C. (b) L929 cells were cryopreserved with various concentrations of PLL (0.65). Cell viability immediately (white bars), and 6 h (gray bars) after thawing at 37 C. Data are expressed as mean SD for 3 independent experiments (5 samples each). \*\*\* $P < 0.001$  vs 10% DMSO for the corresponding time period (0 or 6 h). (From Matsumura and Hyon. 2009. *Biomaterials* 30: 4842–4849)<sup>23</sup>

In another report, the same polyampholyte was successfully used to cryopreserved many kinds of cells, regardless of cell types including primary cells, derived cells, adhesive and floating cells, etc.<sup>24</sup> Thereafter, in another study, it was shown that COOH-PLL enables the long term cryopreservation and they successfully cryopreserved human bone marrow cells (hBMSCs) for up to 24 months. This suggested that COOH-PLL doesn't affect the phenotypic characteristics

and proliferative ability of the cells.<sup>25</sup> These studies established that polyampholytes can act as efficient cryoprotective agents.

## 1.2 Cryopreservation

Nature governs whether biological material will decay or die. The structure and function of living organelles and cells can change and be lost with time, which is a matter of concern for the researchers studying these systems. Several attempts have been made to stop the biological clock since ancient times, which was successfully achieved by controlling temperature and water content.

Refrigeration is one of the everyday life processes that have been extensively used because it provides us the means for slowing the rate of deterioration of perishable goods. Removal of water from various biological materials paves another way for arresting biological degradation, which initiates again by the addition of water.

The pioneering work in this field was conducted in 1949 by Polge and coworkers, who stored fowl semen in a freezer by adding glycerol as cryoprotectant.<sup>26</sup> Afterward, many successful experiments were carried out, such as cryopreservation of bull spermatozoa,<sup>27</sup> plant cultures,<sup>28</sup> plant callus,<sup>29</sup> and human embryos for in vitro fertilization programs.<sup>30</sup>

The application of low-temperature preservation to living organisms has revolutionized several areas of biotechnology such as plant and animal breeding. The most interesting feature of cryopreservation is that both prokaryotic and eukaryotic cells can be cryopreserved at temperatures down to  $-200^{\circ}\text{C}$ , which is a remarkable milestone for structural and molecular biologists. The most important ingredient required to achieve this goal is a cryoprotectant (CPA).

In the context of tissue cultures, simple preservation techniques like refrigeration cause limited shelf life, high risk of contamination, and genetic drift. Therefore, cryopreservation has become indispensable in biological, medical, and agricultural research fields, and in the clinical practice of reproductive medicine. In the era of microbial contaminations, natural disasters, or alteration of genetic expressions in the latter generations, cryopreservation of sperm and embryos helps to maintain a backup of the microorganisms proliferating on animals, thus saving significant space and resources that could be used to better manage the microorganisms currently used

for research. Moreover, it is an important tool to preserve strains that are not currently being used but could have potent applications in the future.

### 1.2.1 Biophysical aspects of ice formation

When biological systems are cooled to temperatures below the equilibrium melting point, ice begins to form in the extracellular medium. This extracellular ice plays an important role in the cryopreservation process because it alters the chemical environment of the cells, exerts mechanical constraints, and leads to the development of ice inside the cells.<sup>31</sup> The formation of extracellular ice has synergistic effect on the unfrozen fraction composition in the extracellular solution. Dropping temperature leads to an increase in the solute concentration in the extracellular solution, which is a driving force for the diffusion of solutes into and water flux out of the cell. At low temperature, the plasma membrane, which is more permeable to water than to the solute, behaves like a semipermeable membrane in time scale of cryopreservation.<sup>32</sup> Cells respond to this by releasing water via osmosis and undergo dehydration during freezing, the kinetic model of which was first given by Mazur.<sup>33</sup>

Solidification of the external medium can cause cell deformation because the ice matrix surrounding the cell acts as a mechanical constraint. During freezing, this mechanical force squeezes the cells into the channels of unfrozen liquid between ice crystals. Rapatz et al. have directly measured the width of the unfrozen liquid channels between ice crystals and observed that channels' diameters decrease with temperature and the cells present in the channels get deformed as the channel width reaches the cell dimensions.<sup>34</sup>

Besides these two processes, another effect of extracellular ice onto cells is the initiation of ice formation inside the cells. It has been experimentally proven that extracellular ice catalyzes the intracellular ice formation.<sup>35, 36</sup> Toner proposed that ice is formed inside the cells by nucleation on intracellular catalytic sites.<sup>35</sup>

Since the cytoplasmic supercooling and diffusion constant of intracellular water depend on the instantaneous properties of the intracellular solution, the dynamics of ice formation inside the cells are highly affected by the corresponding dehydration process.<sup>31</sup> The fate of the cellular water during cryopreservation depends on the relative magnitudes of water transport and rate



of nucleation. When cells are cooled slowly, the rate of water coming out of the cells is relatively fast, thus preventing intracellular ice formation and favoring cell dehydration. At rapid cooling rates, exosmosis of water is slow in comparison of intracellular water being supercooled, thus resulting in intracellular ice formation.

### **1.2.2 Correlation between cryoinjury and the two phenomena occurring during freezing**

Injury occurring because of intracellular ice formation during rapid cooling is believed to be due to mechanical forces.<sup>37</sup> Possible sites of injury are the plasma membrane<sup>38</sup> and the membrane of intracellular organelles.<sup>39</sup>

Cell dehydration during slow cooling is also a source of cell damage.<sup>40</sup> Lovelock reported that hypertonic solutions cause denaturation of lipoproteins, which leads to hemolysis in red blood cells (RBC).<sup>41</sup> Other theories proposed cell shrinkage as a response toward highly concentrated extracellular solution.

The two approaches used for cryopreservation are slow-rate freezing and vitrification. The core objective of the two methods is to minimize cryoinjury, intracellular ice formation, and dehydration.

Slow-rate freezing involves the pre-equilibration of cells in cryoprotectant solutions followed by slow cooling at the rate required for the particular type of cell being used. However, during the whole process, care must be taken to prevent intracellular ice formation. This complete process requires special equipment and takes 3–6 h to complete.

Vitrification is the conversion of liquid into glass. In this approach, an attempt is made to prevent ice formation throughout the entire sample. This process avoids the damaging effects of intra- and extracellular ice formation.

### **1.2.3 Cooling rates**

There are various factors affecting the efficiency of cryopreservation. One of the principal factors is the rate of freezing, which should be optimum. The relation between cell survival and cooling rate shows an inverted U-shaped curve (Fig. 1.7). Each system has an optimum cooling rate, the efficiency of which is greatly affected by whether the rate of cooling is too fast or too slow.<sup>42</sup>

<sup>43</sup> When the rate of cooling is very slow, there is minimal intracellular ice formation, which implies a high degree of cell dehydration. On the other hand, at very high cooling rates, rapid water flow through the membrane can result in rough pressure distribution across the membrane<sup>44</sup> in sudden change in size and shape of the membrane.<sup>45</sup>

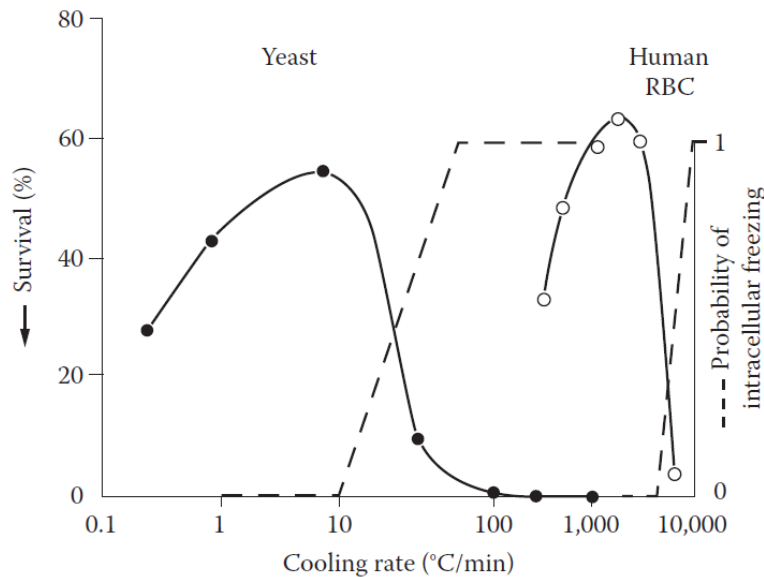


**Figure 1.7.** Plot of the survival percent versus the cooling rate for different cell types of cells. (From Mazur, P., *Cryobiology*, 14, 251, 1977.)

#### 1.2.4 Slow cooling

When cells are frozen/cooled at slow rate (controlled rate), formation of extracellular ice takes place first, followed by a differential water gradient across the cell membrane, which results in the movement of intracellular water to the outside. This has an important cryoprotective effect because it reduces the amount of water available to form ice. This process reduces the amount of water inside the cells, which could potentially form ice, thereby protecting the cells. Intracellular ice formation is lethal for cells and is the most important cause for cell death during cryopreservation. As the system is further cooled down, no further crystallization of ice is observed due to a tremendous increase in the viscosity of the unfrozen fraction (solutes), which turns into an amorphous solid lacking any ice crystals. On the other hand, slow cooling results in the increase of the solution effect, which can be damaging to the cells. The amount and rate at which water is lost from the inside of the cells depends on cell permeability; tolerance toward fast cooling is better for more permeable cells than for less permeable cells.<sup>40,46</sup> Interestingly,

there is interplay between ice crystal formation and solution effects on cell damage. Generally, a cooling rate of  $1^{\circ}\text{C}/\text{min}$  is preferred. However, there are exceptions to this requirement such as for yeast,<sup>47, 48</sup> liver,<sup>49</sup> and higher plant cells,<sup>50</sup> which shrink or become plasmolyzed when the rate of cooling is  $1^{\circ}\text{C}/\text{min}$ , but when the rate is increased to about  $200^{\circ}\text{C}/\text{min}$  or more, these cells remain in their normal state. In the case of yeast, shrinkage is the result of water loss and not of solutes loss;<sup>51, 52</sup> therefore, in these cells, water content is an estimate of the volume of the cell. However, faster cooling rates render the cells unable to maintain equilibrium with the extracellular solution due to the inability of water to leave the cells, which causes intracellular ice formation to preserve the equilibrium (Fig. 1.8).

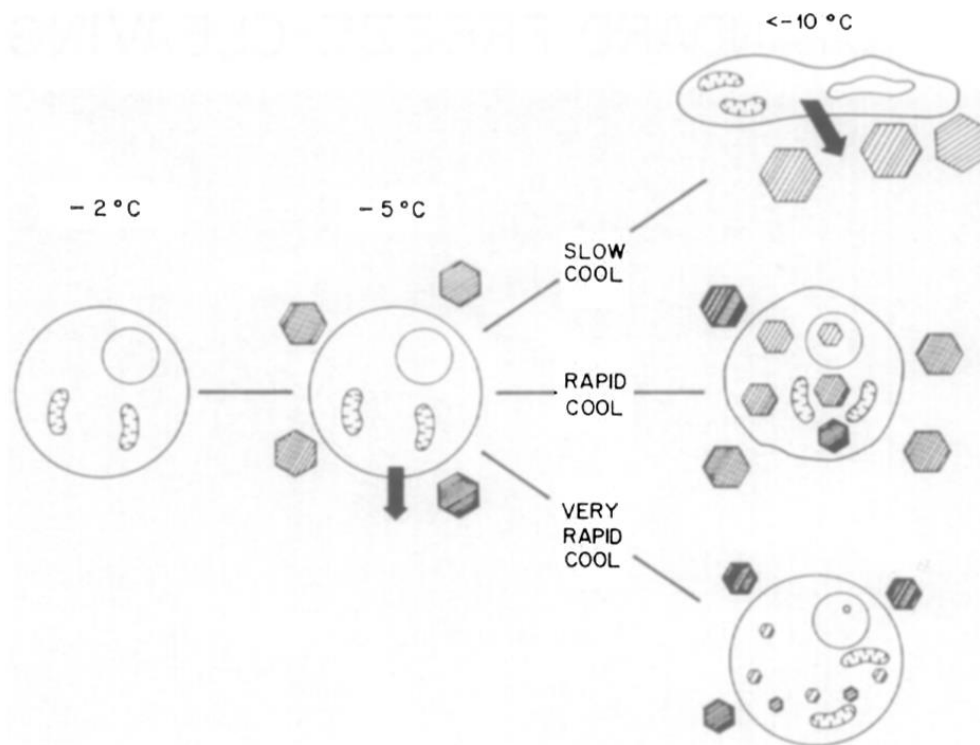


**Figure 1.8.** Schematics of the physical events occurring in cells during freezing (From Mazur, P., *Cryobiology*, 14, 251, 1977).

### 1.2.5 Cryoprotective additives

CPAs are additives provided to cells before freezing to enhance post-thaw survival.<sup>31, 53</sup>

CPA can be divided into two different groups:<sup>54, 55</sup>

1. **Low-molecular-weight CPAs** such as glycerol, ethylene (propylene) glycol, and DMSO, which can penetrate the cell membrane.
2. **Non-cell-membrane-penetrating CPAs** that usually do not enter inside the cells, like polymers such as polyvinyl propylidone, hydroxyl ethyl starch (HES), and various sugars.

### 1.2.6 History of CPAs

Ever since the discovery of the role of glycerol in cryopreservation by Polge et al. in 1949, the use of CPAs has become common practice. Lovelock and Bishop later found that the protective property shown by glycerol is due to its nontoxicity, high solubility in aqueous electrolyte solutions, and its ability to permeate living cells.<sup>56</sup> However, he found that glycerol is impermeable to bovine red blood cells and proposed DMSO as an alternative solute with greater permeability to living cells and exerting protective action against the freezing damage to human and bovine red blood cells. This CPA gained considerable attention globally and was mentioned as miracle compound. In the same period, Garzon et al.<sup>57</sup> and Knorpp et al.<sup>58</sup> independently proposed HES as a cryoprotectant for erythrocytes.<sup>59</sup> Thereafter, HES continued to be used as the CPA for RBCs,<sup>56–60</sup> granulocytes,<sup>61</sup> cultured hamster cells,<sup>62</sup> and pancreatic islets.<sup>63, 64</sup>

### 1.2.7 Problems associated with current CPAs

The cryoprotective properties of glycerol are relatively weak and DMSO, which is considered the most effective CPA, shows high cytotoxicity<sup>65</sup> and disturbs the differentiation of neuron-like cells,<sup>66</sup> cardiac myocytes,<sup>67</sup> and granulocytes.<sup>68</sup> When DMSO is used at low concentrations, it can decrease the membrane thickness and induce temporary water pores, while, when it is used at higher concentrations, it causes the disintegration of the bilayer structure of the lipid membrane.<sup>69</sup> Therefore, after thawing, it is necessary to remove it. In the current scenario, the most efficient cryopreservation technique, which is being used worldwide in cell banks, is 10% DMSO in the presence of fetal bovine serum (FBS). Importantly, it has been reported that post-thaw survival of cells decreases without the addition of FBS to the cryopreserving solution.<sup>70, 71</sup>

Indeed, it is the interplay between FBS and DMSO at the appropriate ratio that makes DMSO a potent cryoprotectant. However, the pit hole of this technique is that animal-derived proteins should be avoided for clinical usage due to high risk of infection. Therefore, these issues stimulated the development of new CPAs.

### 1.3 Protein Stability

Proteins are one of the most complex biomolecules and are essential for almost all the functions in the body. They are aptly called the building blocks. For proteins to be functional, they must fold properly into their respective native states. Any defect in the protein folding or its unfolding from its native state leads to protein instability, which usually manifests itself in the form of protein aggregation. Its effect can be seen directly and indirectly. In the academic and research environment, aggregation can pose great technical and economic problems in many industries like pharmaceutical and biotechnology. Its presence is often unnoticed or ignored and which may lead to a discrepancy in the experimental outcome. In humans, it manifests in several dreadful diseases, primarily neurodegenerative conditions like Parkinson's and Alzheimer's diseases, prions, etc.<sup>72-76</sup> Misfolding of newly synthesized proteins can be extremely lethal to cells; in such instances, molecular chaperones come into play to inhibit aggregation and simultaneously stimulate proper folding.

Protein aggregation is complex phenomenon in which proteins which have not been folded properly tend to aggregate. This process can occur both in vivo and in vitro and as a consequence fibrils are formed.

Hen egg white lysozyme (HEWL) is generally used as a model protein for such kind of studies. This is due to its easy availability, solubility in aqueous solutions and its low cost. Moreover, it is a preferred protein also because it's complete structure, including primary<sup>77</sup> and three-dimensional<sup>78</sup> structure which has already been elucidated by researchers before. Hence, it is easier to investigate the aggregation studies using this protein. It is a complex protein which comprises 129 amino acid residues accompanied by four intramolecular disulphide bridges.<sup>79</sup>

Over the years, many organic compounds have been employed like arginine,<sup>80-82</sup> proline,<sup>83</sup> cyclodextrin,<sup>84</sup> polyamines,<sup>85</sup> and a whole library of other small compounds for protein aggregation studies.

Vuillard and his co-workers have done extensive work on the role of non-detergent sulfobetaines (NDSB) as stabilizing and solubilizing agent for proteins. They found out that NDSBs can aid in the formation of protein crystals and this was suggested to be due to the ability of NDSBs to prevent amorphous aggregation. They also found out that with the addition of NDSBs, the amount of active protein recovered was increased substantially in in-vitro folding experiments.<sup>86-</sup>

90

Glycine betaine is one of the most well-known and studied osmoprotectant. They elevate the osmotic pressure in the cytoplasm and also stabilizes proteins and membranes in the conditions of adverse salt levels or temperatures.<sup>91</sup> Glycine betaine was shown to restore the activity of malate dehydrogenase.<sup>92</sup> Caldas et al. 1999, showed that glycine betaine protect  $\beta$ -galactosidase and citrate synthase against thermodenaturation in vitro, at low concentrations. It also triggers citrate synthase renaturation after urea denaturation.<sup>93</sup>

## 1.4 Objective of the thesis

In the course of my doctoral research, I have developed various polymers via RAFT polymerization. All the polymers were charged polymers containing both the charges, viz., polyampholytes. These polyampholytes were used for cryopreservation (Chapter 2 and 3) and protein aggregation inhibition studies (Chapter 4 and 5).

## Chapter 2

**Background:** DMSO and several naturally occurring polyols or their derivatives (like glycerol) have been used as cryoprotective agents (CPAs) for many years. However DMSO shows high cytotoxicity and affects differentiation of cells, so it needs to be removed immediately after thawing, whereas polyols are comparatively weaker cryoprotective agents. Furthermore, some types of cells are extremely sensitive to damage during freezing and thawing, so cannot be cryopreserved properly using current CPAs. So there is a great need to develop newer cryoprotective agents with lower cytotoxicity and high efficiency for many biological and medical purposes.

Recently, our group showed that carboxylated poly-L-lysine, which is classified as a polyampholyte, has a cryoprotective effect on cells in solution without any other cryoprotectant. Hence in this chapter, I tried to develop for the first time, a completely synthetic polyampholyte based CPA. Owing to the synthetic nature, it is easier to modify parameters like hydrophobicity, molecular weight, etc., which would enable in the understanding of the critical conditions for cryopreservation.

**Outline:** I developed a completely synthetic polyampholyte cryoprotectant with cationic and anionic monomers via RAFT polymerization. The neutralized random polyampholyte, which had an equal composition ratio of monomers, showed high cryoprotective properties in mammalian cells. Introduction of a small amount of hydrophobic monomer enhanced cell viability after cryopreservation, indicating the importance of hydrophobicity. Leakage experiments confirmed that these polyampholytes protected the cell membrane during cryopreservation. Due to low cytotoxicity, this polyampholyte has the potential to replace the convention cryoprotective agent DMSO. The present study is the first to show that it is possible to design a polymeric cryoprotectant that will protect the cell membrane during freezing using appropriate polymerization techniques.

### **Chapter 3**

**Background:** In Chapter 2, I had designed a synthetic polyampholyte based CPA. But the mechanism of cryopreservation by polyampholytes could not be explained, which is very crucial for its further evolution. Establishment of molecular mechanism can assist in the employment of these polyampholytes for various regenerative medicines like stem cell cryopreservation, tissue engineering and for development of cellular scaffolds. Moreover, it can help in more efficient design of CPA's in the future wherein newer materials can be put into use with the current knowledge and also, these polymers can be tuned to be administered to cryopreservation of cell-containing constructs. Hence in this chapter, I tried to establish the mechanism of cryopreservation.

**Outline:** I synthesized and investigated the cryoprotective property of three different synthetic polyampholytes (random copolymer and zwitterionic polymers) prepared via RAFT polymerization. Results indicated that the polymer structure has a strong influence on the cryoprotective behavior. At the same time, the introduction of hydrophobicity significantly

enhances viability, owing to its high affinity for ice recrystallization inhibition. The mechanism of cryopreservation was unveiled using numerous studies. The interaction of the polymers with cells during cryopreservation was studied using both liposomes (as cell membrane mimic) and by observing the response of polymer solution during freezing. Study of membrane localization revealed that polymer structure governs its position around/within the cell membrane. Solid state proton NMR studies exhibited that membrane protection during freezing is a manifestation of the protective reversible matrix/gel formation around the membrane; suggested by the loss in polymer chain mobility.

## **Chapter 4**

**Background:** In chapter 2 and 3, I had investigated the cryoprotective property of the polyampholytes. In this chapter, I intended to check the versatility of synthetic polyampholytes and to establish when it can be employed for any other biomaterial application. Hence, I investigated the protein aggregation studies using polyampholytes.

Protein aggregation studies are very crucial for the development of protein biopharmaceutics. To deliver proteins to a body for protein therapeutics, there should not be any aggregation of proteins. So inhibiting aggregation is very crucial. There are small organic compounds available which can inhibit the aggregation. To my knowledge, there are few reports on the use of polymers for this purpose. A previous report investigated the use of the triangular-structured monodisperse polyethylene glycol to inhibit lysozyme aggregation, but synthesis requires 15 steps and various reagents. Hence in this chapter, I prepared an effective suppressor of protein aggregation by a single step polymerization reaction.

**Outline:** I developed a zwitterionic polymer, poly-sulfobetaine, via RAFT polymerization. Lysozyme did not aggregate when heated in presence of this polymer. Amyloid formation, the cause of many diseases, was also suppressed. The zwitterionic polymer was significantly more efficient than previously described inhibitors of protein aggregation. Lysozyme heated in the presence of poly-sulfobetaine retained its solubility and very high enzymatic efficiency, even after prolonged heating. The secondary structures of lysozyme change with increasing temperature, accompanied by an increase in  $\beta$ -structure. This change was prevented by mixing the polymer with lysozyme.  $^1\text{H}$ -NMR before and after aggregation revealed the conformational changes taking place in the lysozyme: during aggregation, lysozyme is transformed into a



random coil conformation, thus losing its secondary structure. Presence of the polymer facilitates retention of partial higher order structures and lysozyme solubility at higher temperatures. The high efficiency of the polyampholyte was ascribed to its ability to prevent collisions between aggregating species by acting as molecular shield.

## **Chapter 5**

**Background:** In Chapter 4, I synthesized a linear zwitterionic polymer which proved effective against thermal denaturation of lysozyme. Although its activity was surprisingly higher than some of the previously known reagents, however for use in clinical applications, we need to further increase its efficiency, where a much lower concentration of the materials could show equal or even higher efficiency.

**Outline:** I developed various core-shell nanogels of zwitterionic polymer, poly-sulfobetaine (poly-SPB) by RAFT polymerization. The nanogels were prepared by using a chemical cross-linker and by using the RAFT-synthesized poly-SPB as the new chain transfer agent. The nanogels exhibited much higher efficiency than poly-SPB prepared in Chapter 4. Presence of only a small amount of nanogel was sufficient for lysozyme to retain very high enzymatic activity even after heating at very high temperatures. Amyloid fibril formation was also suppressed. The higher activity of nanogels can be ascribed to its ability to act as artificial molecular chaperones which protects proteins under severe conditions.

## **1.5 References**

- 1 F. W. Harris, *J. Chem. Educ.*, 1981, **58**, 837-843.
- 2 K. Matyjaszewski and J. Spanswick, *Mater. Today*, 2005, **8**, 26–33.
- 3 K. Matyjaszewski and T. Davis (Eds.), *Handbook of Radical Polymerization*, John Wiley & Sons, New Jersey, 2002.
- 4 V. Mishra, R. Umar, *J. Sci. Res.*, 2012, **56**, 141–176.
- 5 M. K. Georges, R. P. N. Veregin, P. M. Kazmaier and G. K. Hamer, *Macromolecules*, 1993, **26**, 2987–2988.
- 6 C. J. Hawker, A. W. Bosman and E. Harth, *Chem. Rev.*, 2001, **101**, 3661–3688.

- 7 M. Kato, M. Kamigaito, M. Sawamoto and T. Higashimura, *Macromolecules*, 1995, **28**, 1721–1723.
- 8 J. -S. Wang and K. Matyjaszewski, *J. Am. Chem. Soc.*, 1995, **117**, 5614–5615.
- 9 J. Chiefari, Y. K. Chong, F. Ercole, J. Krstina, J. Jeffery, T. P. T. Le , R. T. A. Mayadunne, G. F. Meijs, C. L. Moad, G. Moad, E. Rizzardo, and S. H. Thang, *Macromolecules*, 1998, **31**, 5559–5562.
- 10 M. Destarac, D. Charmot, X. Franck and S. Z. Zard, *Macromol. Rapid Comm.*, 2000, **21**, 1035–1039.
- 11 E. Rizzardo, J. Chiefari, R. T. A. Mayadunne, G. Moad and S. H. Thang, *ACS Symp. Ser.*, 2000, **768**, 278-296.
- 12 G. Moad, E. Rizzardo and S. H. Thang, *Polymer*, 2008, **49**, 1079–1131.
- 13 S. E. Kudaibergenov, *Adv. Polym. Sci.*, 1999, 144, 115-197.
- 14 E. A. Bekturov, S. E. Kudaibergenov, S. R. Rafikov, *J. Macromol. Sci. Rev. Macromol. Chem. Phys.*, 1990, C30, 233-303.
- 15 T. Jr. Alfrey, H. Morawetz, E. B. Fitzgerald and R. M. Fuoss, *J. Am. Chem. Soc.*, 1950, **72**, 1864.
- 16 S. Kudaibergenov, W. Jaeger and A. Laschewsky, *Adv. Polym. Sci.*, 2006, **201**, 157–224.
- 17 R. Kumar and G. H. Fredrickson, *J. Chem. Phys.*, 2009, **131**, 104901.
- 18 A. B. Lowe and C. L. McCormic, *Chem. Rev.*, 2002, **102**, 4177–4189.
- 19 A. Laschewsky, *Polymers*, 2014, **6**, 1544-1601.
- 20 R. G. Laughlin, *Langmuir*, 1991, **7**, 842–847.
- 21 M. Bernards and Y. He, *J. Biomater. Sci. Polym. Ed.*, 2014, **25**, 1479-1488.
- 22 M. T. Zurick, and M. T. Bernards. *J. Appl. Polym. Sci.*, 2014, **131**, 40069.
- 23 K. Matsumura, and S. H. Hyon, *Biomaterials*, 2009, *Biomaterials*, **30**, 4842–4849.
- 24 K. Matsumura, J. Y. Bae and S. H. Hyon, *Cell Transplantat.*, 2010, 19, 691–699.
- 25 K. Matsumura, F. Hayashi, T. Nagashima and S. H. Hyon, *J. Biomater. Sci. Polym. Edn.*, 2013, **24**, 1484–1497.
- 26 C. Polge, A. U. Smith and A. S. Parkes, *Nature*, 1949, **164**, 666.
- 27 A. U. Smith, and C. Polge, *Vet. Rec.*, 1950, **62**, 115-117.
- 28 R. Latta, *Can. J. Bot.*, 1974, **49**, 1253-1254.
- 29 L. J. Bannier, and P. L. Steponkus, *Hortscience*, 1972, **7**, 411-414.

- 30 J. Cohen, R. Simons, C. B. Fehily, S. B. Fishel, R. G. Edwards, J. Hewitt, G. F. Rowland, P. C. Steptoe and J. M. Webster, *J.-Lancet*, 1985, **325**, 647.
- 31 J. O. M. Karlsson and M. Toner, *Biomaterials*, 1996, **17**, 243-256.
- 32 M. E. Lynch and K. R. Diller, *Trans. ASME*, 1981, **81**, 229-232.
- 33 P. Mazur, *J. Gen. Physiol.*, 1963, **47**, 347-369.
- 34 G. Rapatz, L. J. Menz and B. J. Luyet, *Cryobiology*, 1966, **3**, 139-162.
- 35 M. Toner, *Advan. Low-Temp. Biol.*, 1993, **2**, 1-51.
- 36 P. Mazur, *Ann. N. Y. Acad. Sci.*, 1965, **125**, 658-676.
- 37 P. Mazur, *Cryobiology*, 1977, **14**, 251-272.
- 38 S. Fujikawa, *Cryobiology*, 1980, **17**, 351-362.
- 39 P. Mazur, *Cryobiology*, 1966, **3**, 214-315.
- 40 P. Mazur, S. Leibo and E. H. Y. Chu, *Exp. Cell Res.*, 1972, **71**, 345-355.
- 41 E. Lovelock, *Biochim. Biophys. Acta*, 1953, **10**, 414-426.
- 42 P. Mazur, P. Freezing and low temperature storage of living cells In Proceedings of the Workshop on Preservation of Mouse Strains. Ed. O. Miihlbock. Gustav Fischer Verlag. Stuttgart, 1976, 1-12.
- 43 M. Jacobs, H. Glassman and A. Parpart, *J. Cell. Comp. Physiol.*, 1935, **7**, 197-225.
- 44 H. Woelders, A. Matthijs and B. Engel, *Cryobiology*, 1997, **35**, 93-105.
- 45 K. Muldrew and L. McGann, *Biophys J.*, 1994, **166**, 532-541.
- 46 T. Nei, T. Araki and T. Matsusaka, Freezing injury to aerated and non-aerated cultures of *Escherichia coli* in T. Nei, Ed. Freezing and Drying of Microorganisms. University of Tokyo Press, Tokyo, Japan, 1969, 3.
- 47 T. Nei, Recent Research in Freezing and Drying, Oxford, Blackwell Scientific Publications, edited by A. Parkes and A. Smith, 1960, 78.
- 48 P. Mazur, *J. Bacteriol.*, 1961, **82**, 662-672.
- 49 H. Meryman, W. Platt and W. Naval Medical Research Institute Report Project NM 000 018.01.08, 1955, **13**, 1.
- 50 E. Asahina, The freezing process of plant cell. Contrib. Inst. Low Temp. Sci., Hokkaido Univ., 1956, **10**, 83.
- 51 P. Mazur, *Biophysic. J.*, 1963, **3**, 323-353.

- 52 P. Mazur, S. Leibo, J. Farrant, E. Chu, M. Hanna and L. Smith, Interactions of cooling rate, warming rate and protective additive on the survival of frozen mammalian cells. in Wolstenholme GEW, O'Connor M, eds. *The Frozen Cell*. London: J and A Churchill, 1970, 69-88.
- 53 E. Lovelock, *Proc. R. Soc. Lond. B Biol. Sci.*, 1957, **147**, 427-433.
- 54 A. Karow, *J. Pharm. Pharmacol.*, 1969, **21**, 209-223.
- 55 A. Stolzing, Y. Naaldijk, V. Fedorova and S. Seethe, *Transfus. Apher. Sci.*, 2012, **46**, 137-147.
- 56 E. Lovelock and M. W. Bishop, *Nature*, 1953, **183**, 1349-1355.
- 57 A. A. Garzon, C. Cheng, B. Lerner, S. Lichtenstein and K. E. Karlson, *J. Trauma*, 1967, **7**, 757-766.
- 58 C. T. Knorpp, W. R. Merchant, P. W. Gikas, H. H. Spencer and N. W. Thompson, *Science*, 1967, **157**, 1312-1313.
- 59 F. J. Lionetti and S. M. Hunt, *Cryobiology*, 1975, **12**, 110-118.
- 60 H. Kim, S. Tanaka, S. Une, M. Nakaichi, S. Sumida and Y. A. Taura, *J. Vet. Med. Sci.*, 2004, **66**, 1543-1547.
- 61 F. J. Lionetti, S. M. Hunt, J. M. Gore and W. A. Curby, *Cryobiology*, 1975, **12**, 181-191.
- 62 M. J. Ashwood, C. Warby, K. W. Connor and G. Becker, *Cryobiology*, 1972, **9**, 441-449.
- 63 T. Kenmochi, T. Asano, M. Maruyama, K. Saigo, N. Akutsu, C. Iwashita, K. Ohtsuki, A. Suzuki and M. Miyazaki, *Cell Transplant.*, 2008, **17**, 61-67.
- 64 M. Maruyama, T. Kenmochi, K. Sakamoto, S. Arita, C. Iwashita and H. Kashiwabara, *Transplant. Proc.*, 2004, **36**, 1133-1134.
- 65 G. M. Fahy, *Cryobiology*, 1986, **123**, 1-13.
- 66 J. E. Oh, R. K. Karlmark, J. H. Shin, A. Pollak, M. Hengstschlager and G. Lubec, *Amino Acids*, 2006, **31**, 289-298.
- 67 D. A. Young, S. Gavrilov, S., C. J. Pennington, R. K. Nuttall, D. R. Edwards, R. N. Kitsis, I. M. Clark, *Biochem. Biophys. Res. Commun.*, 2004, **322**, 759-765.
- 68 G. Jiang, K. Bi, T. Tang, J. Wang, Y. Zhang, W. Zhang, H. Ren, H. Bai and Y. Wang, *Int. Immunopharmacol.*, 2006, **6**, 1204-1213.
- 69 A. A. Gurtovenko and J. Anwar, *J. Phys. Chem. B*, 2011, **111**, 10453-10460.
- 70 H. Men, Y. Agca, E. S. Critser and J. K. Critser, *Theriogenology*, 2005, **64**, 1340-1349.

- 71 J. H. Son, K. H. Kim, Y. K. Nam, J. K. Park and S. K. Kim, *Biotechnol. Lett.*, 2004, **26**, 829-833.
- 72 W. Wang, *Int. J. Pharm.*, 1999, **185**, 129–188.
- 73 C. A. Ross and M. A. Poirier, *Nat. Med.*, 2004, **10**, S10–S17.
- 74 P. T. Lansbury and H. A. Lashuel, *Nature*, 2006, **443**, 774-779.
- 75 E. H. Koo, P. T. Lansbury, Jr., and J. W. Kelly, *Proc. Natl. Acad. Sci. U.S.A.*, 1999, **96**, 9989-9990.
- 76 V. Sluzky, J. A. Tamada, A. M. Klibanov, and R. Langer, *Proc. Natl. Acad. Sci. U S A.*, 1991, **88**, 9377–9381.
- 77 R. E. Canfield, *J. Biol. Chem.*, 1963, **238**, 2698–2707.
- 78 C. C. F. Blake, D. F. Koenig, G. A. Mair, A. C. T. North, D. C. Phillips and V. R. Sarma, *Nature*, 1965, **206**, 757–761.
- 79 L. R. Wetter and H. F. Deutsch, *J. Biol. Chem.*, 1951, **192**, 237–242.
- 80 S. Taneja and F. Ahmad, *Biochem. J.*, 1994, **303**, 147-153.
- 81 D. Das, J. Kriangkum, L. P. Nagata, R. E. Fulton and M. R. Suresh, *J. Virol. Meth.*, 2004, **117**, 169-177.
- 82 R. Asano, T. Kudo, K. Makabe, K. Tsumoto and I. Kumagai,, *FEBS Lett.*, 2002, **528**, 70–76.
- 83 D. Samuel, T. K. Kumar, G. Ganesh, G. Jayaraman, P. W. Yang, M. M. Chang, V. O. Trivedi, S. L. Wang, K. C. Hang, D. K. Chang and C. Yu, *Protein Sci.*, 2000, **9**, 344-352.
- 84 N. Karuppiyah and A. Sharma, *Biochem. Biophys. Res. Commun.*, 1995, **21**, 6066-6072.
- 85 Motonori Kudou, K. Shiraki, S. Fujiwara, T. Imanaka and M. Takagi, *Eur. J. Biochem.*, 2003, **270**, 4547-4554.
- 86 M. E. Goldberg, N. E. Bezançon, L. Vuillard and T. Rabilloud, *Fold. Des.*, 1996, **1**, 21–27.
- 87 L. Vuillard, T. Rabilloud, R. Leberman, C. B.Colominas and S. Cusack, *FEBS Lett.*, 1994, **353**, 294-296.
- 88 L. Vuillard, D. Madern, B. Franzetti and T. Rabilloud, *Anal. Biochem.*, 1995, **230**, 290–294.
- 89 L. Vuillard, C. B. Breton and T Rabilloud, *Biochem. J.*, 1995, **305**, 337–343.
- 90 L. Vuillard, B. Baalbaki, M. Lehmann, S. Nørager, P. Legrand and M. Roth, *J.Cryst Growth*, 1996, **168**, 150-154.
- 91 S. D. McNeil, M. L. Nuccio and A.D. Hanson, *Plant Physiol.*, 1999, **120**, 945-50.
- 92 A. Pollard and R. G. W Jones, *Planta*, 1979, **144**, 291–298.

93 T. Caldas, N. D.-Caulet, A. Ghazi and G. Richarme, *Microbiology*, 1999, **145**, 2543-2548.

## Chapter 2 PREPARATION OF NOVEL SYNTHETIC CRYOPROTECTIVE POLYAMPHOLYTES *via* RAFT POLYMERIZATION

### 2.1 Introduction

Cryopreservation is a process through which different types of cells, tissues, or organs are preserved at very low temperatures in such a way as to allow them to be restored with all their original functions whenever required. Cryopreservation is of paramount importance in various medicinal and biological contexts. Polge et al. were the first to report the preservation of living cells at very low temperatures after the accidental discovery of the cryoprotective properties of glycerol on fowl sperm.<sup>1</sup> Some years later, the cryopreservation of red blood cells was achieved using dimethyl sulfoxide (DMSO) as a cryoprotectant.<sup>2</sup> These common cell membrane-penetrating cryoprotectants (i.e. glycerol and DMSO) protect cells from lethal damage caused by the formation of intracellular ice during freezing and thawing. However, the cryoprotective properties of glycerol are relatively weak, and DMSO shows high toxicity,<sup>3</sup> and affects the differentiation of various types of cells.<sup>4-6</sup> Thus, there is a great need to develop newer cryoprotective agents, especially in applications of regenerative medicine.

The polyampholyte carboxylated poly-L-lysine (COOH-PLL) shows excellent post-thaw survival efficiency<sup>7-9</sup> and cryoprotective properties against human mesenchymal stem cells, while retaining the cells' full differentiation capacity without the addition of any other low-molecular-weight cryoprotectants or proteins.<sup>10</sup> However, the mechanisms through which a non-membrane-penetrating polymer, such as COOH-PLL, could exhibit substantial cryoprotective properties are still not clear. From our previous studies demonstrating that polyampholytes are absorbed on the cell membrane during freezing,<sup>10</sup> I hypothesized that the mechanisms of such polyampholytes are likely related to the induction of membrane protection against mechanical damage from ice formation.

Controlled radical polymerization techniques, such as ATRP,<sup>11, 12</sup> NMP,<sup>13, 14</sup> and RAFT polymerization,<sup>15-17</sup> have been studied extensively in recent years. Among them, RAFT polymerization has the advantage that it can be applied to a wide range of functional and nonfunctional monomers under a variety of conditions and solvents to yield polymers with predetermined molecular weights, narrow molecular weight distributions, and complex

architecture.<sup>18, 19</sup> Moreover, it does not require the use of any toxic organometallic catalysts. Recently, many researchers have attempted to achieve RAFT polymerization in aqueous media.<sup>20–23</sup> In the present study, I sought to examine whether a completely synthetic polyampholyte (different from COOH-PLLs), synthesized using RAFT polymerization, could exhibit cryoprotective properties in murine L929 cells, which would allow us to elucidate the molecular mechanisms of these effects by synthesizing various polymers. I also investigated the membrane-protective properties of the newly synthesized polyampholyte and evaluated the effects of hydrophobicity on enhanced membrane protection and cryopreservation. This report is the first to reveal that a completely synthetic polymer possesses cryoprotective properties and to demonstrate the relationship between the cryoprotective properties of a polymer and the cell membrane protection of these polyampholytes.

## **2.2 Materials and methods**

### **2.2.1 Materials**

2-(Dimethylamino)ethyl methacrylate (DMAEMA), methacrylic acid (MAA), and n-butyl methacrylate (Bu-MA) were purchased from Wako Pure Chemical Industries Ltd (Osaka, Japan). N-Octyl methacrylate (Oc-MA) was purchased from NOF Corporation (Tokyo, Japan). All of these monomers were distilled under reduced pressure prior to use to remove inhibitors. 2-(dodecylthiocarbonothioylthio)-2-methylpropionic acid (RAFT agent) and carboxyfluorescein (CF), obtained from Sigma–Aldrich (St. Louis, MO, USA), were used as provided without further purification. 4–4'-Azobis-(4-cyanovaleric acid) (V-501, initiator) was purchased from TCI (Tokyo, Japan). All other reagents were reagent grade and were used without further purification.

### **2.2.2 Synthesis of polyampholytes**

I synthesized various amphoteric copolymers and terpolymers by changing the monomer ratios of the components added or by changing the molar ratio of total monomer/ RAFT agent/initiator to obtain polymers with various molecular weights. To synthesize a 1:1 copolymer, DMAEMA (4 mmol), MAA (4 mmol), 2-(dodecylthiocarbonothioylthio)-2-methylpropionic acid (0.2 mmol), and V-501 (0.04 mmol) were added to reaction vial, and 20 mL of water–methanol mixture (1:1 [v/v]) was then added. To introduce hydrophobic moieties to the polyampholytes, 1–10 % of the total



monomer amount of Bu-MA or Oc-MA was added in the reaction mixture. Alternatively, 5 % HE-MA was added to the reaction mixture to introduce hydrophilicity. The solution was then purged with nitrogen gas for 1 h and stirred at 70 °C. Samples were removed periodically (25 µL), and the conversion at each reaction time was obtained by <sup>1</sup>H NMR (400MHz, Bruker). After 24 h, the reaction mixture was precipitated using 2-propanol, the precipitates were collected by centrifugation, and the compound was dried over vacuum. The molecular weight and distribution (polydispersity index, PDI) of the polymers was determined by gel permeation chromatography (GPC, column, BioSep-s2000, Phenomenex, Inc., CA, USA) and was measured on a Shimadzu high-performance liquid chromatography data system using a refractive index detector. Phosphate buffer solution (pH 7.4, 0.1 M) was used as the mobile phase (flow rate, 1 mL/ min) and pullulan was used as the standard. The chemical structures of the compounds were confirmed by <sup>1</sup>H NMR using D<sub>2</sub>O as solvent.

### **2.2.3 Cell culture**

L929 cells (American Type Culture Collection, Manassas, VA, USA) were cultured in Dulbecco's modified Eagle's medium (DMEM, Sigma Aldrich) supplemented with 10 % fetal bovine serum (FBS). Cells were cultured at 37 °C in a CO<sub>2</sub> incubator in a humidified atmosphere. When the cells were confluent, they were washed with phosphate buffered saline (PBS) and then treated with trypsin solution (0.25 % [w/v] trypsin containing 0.02 % [w/v] ethylenediaminetetraacetic acid in PBS) to detach the cells. The cell pellet was then collected by centrifugation, mixed with fresh DMEM, and subsequently transferred to a new culture plate for subculture.

### **2.2.4 Cryopreservation of cells**

Polyampholyte solutions were prepared in DMEM without FBS at 5–15 % concentrations. The pH of the solution was adjusted to 7.4, and the osmotic pressure was adjusted to 500 mmol/kg by the addition of sodium chloride using a vapor pressure Osmometer (VAPRO Model 5660, WESCOR Biomedical Systems, UT, USA). These solutions were filter sterilized using a MILLEX GP Filter Unit 0.22 µm (Millipore Corp., Billerica, MA, USA). One million L929 cells were

suspended in 1 mL of this cryopreservation solution and stored at -80 °C without controlling the cooling rate.<sup>7, 8</sup>

### 2.2.5 Cell viability and proliferation assay

After 24 h, the cells were thawed by immersing the vial into a water bath at 37 °C. The cell suspension was then diluted 10-fold with DMEM followed by centrifugation at 1000 rpm for 5 min. The supernatant was discarded, and fresh DMEM was added. The cells were then centrifuged again, and the cell pellet was suspended in a small amount of fresh DMEM. A portion of the suspension was then removed to determine cell viability, which was determined by staining with trypan blue. The remaining cells were plated in 6-well culture plates at a cell density of  $1 \times 10^4/\text{cm}^2$  ( $n = 5$ ). To determine cell survival, the medium, including dead floating cells, was collected, and the attached cells were trypsinized. All cells were stained with trypan blue and counted using a haemocytometer immediately post-thawing (0 h) and at 6 h after thawing. The reported values are the ratios of living cells to the total number of cells. To study cell proliferation capacity after thawing, the cells were seeded in 24-well culture plates at a cell density of  $5.0 \times 10^4/\text{cm}^2$  with 2 mL of DMEM ( $n = 3$ ). Cell numbers were counted at 2, 4, 5, and 7 days after seeding.<sup>7</sup>

### 2.2.6 Cytotoxicity assay

L929 cells suspended in 0.1 mL medium at a concentration of  $1.0 \times 10^4/\text{mL}$  were placed in 96-well culture plates. After 72 h of incubation at 37° C, 0.1 mL medium containing different concentrations of polyampholyte solution was added to the cells, followed by incubation for 48 h. To evaluate cell viability, the supernatant was discarded from each of the wells, and 10  $\mu\text{L}$  of Cell Counting Kit-8 reagent (Dojindo Molecular Technologies, Inc., Kumamoto, Japan) and 90  $\mu\text{L}$  DMEM were added to the cultured cells. Cells were then further incubated for 3 h at 37 °C. The resulting color intensity, which was proportional to the number of viable cells, was recorded at 450 nm using a microplate reader (MTP-300 Corona Electric). The cytotoxicity was represented as the concentration of copolymers that caused a 50 % decrease in the reduction of WST-8 (in CCK-8) by dehydrogenases present in the cell and was compared with the untreated control culture ( $\text{IC}_{50}$ ).

### 2.2.7 Liposome preparation

Lecithin (Wako Pure Chemical Industries, Osaka, Japan), dissolved in diethyl ether, and poured into a glass test tube. Organic solvent was then evaporated under a gentle stream of N<sub>2</sub>, and the precipitate was dried under a vacuum overnight. The resulting lipid film was hydrated in 300  $\mu$ L of 0.1 M CF/PBS solution, and liposomes were formed using a mini-extruder set (Avanti Polar Lipids) and membranes with a 0.1  $\mu$ m pore size.<sup>24</sup>

### 2.2.8 Leakage experiment

The external CF from the liposomes was removed by passing the solution obtained after extrusion through a Sephadex G-25 column (NAP-5, GE Healthcare). Liposomes were eluted from the column using PBS and collected in a small vial. The liposomes were then suspended in polyampholyte solutions of various concentrations and stored at -80 °C. After 24 h, the solution was thawed by immersing the vial in a 37 °C water bath. The solution was then diluted 1000-fold. CF fluorescence was measured using a Fluololog-3 instrument (Horiba Jobin-Yvon, Japan) with an excitation wavelength of 450 nm and a detection wavelength of 520 nm at 25 °C. When liposomes remain intact, the fluorescence is strongly quenched, but when liposomes are damaged, the fluorescence increases as CF is released into the surrounding buffer. The maximum CF fluorescence (around 100 % leakage) was determined after lysis of the liposomes with Triton X-100, and the percent leakage was calculated relative to these values.<sup>25</sup>

### 2.2.9 Statistical analysis

All data are expressed as the mean  $\pm$  standard deviation (SD). All experiments were conducted in triplicate. To compare data among more than 3 groups, the Tukey–Kramer test was used. To compare data between two groups, Student's t-test was used.

## 2.3 Results and discussion

### 2.3.1 Characterization

MAA, DMAEMA, and other monomers were polymerized in water-methanol (1:1 [v/v]) solvent. The results of the polymerization are summarized in Table 1. The compositions of each monomer in the polymers were well controlled and similar to the feed ratio. Fig. 2.1 shows representative  $^1\text{H}$  NMR charts of poly (DMAEMA-*r*-MAA) and 5% Bu-MA and Oc-MA incorporated into poly-(DMAEMA-*r*-MAA). The kinetic plots of conversion to polymerization time of poly (DMAEMA-*r*-MAA) indicated that 80 % monomer conversion had been reached after 6 h (Fig. 2.2(a)). I selected the RAFT agent for this polymerization according to a previous report,<sup>26</sup> and succeeded in obtaining not only amphoteric copolymers, but also amphoteric terpolymers harboring hydrophobic moieties in the same solvent and with the same initiator. Although, I also tested another RAFT agent (4-cyano-4-(phenylcarbonothioylthio) pentanoic acid) for the same polymerization, the reaction did not proceed, even after 24 h. These results suggested that the combination of monomers, RAFT agents, and solvents is important to achieve successful living polymerization. The molecular weight and polydispersity ( $M_w/M_n$ ) are shown in Fig. 2.2 (b). The  $M_n$  values of the 1:1 DMAEMA-MAA copolymer increased linearly with time, while the  $M_w/M_n$  ratio remained below 1.4. Furthermore, GPC curves showed that all copolymers had a unimodal distribution with  $M_n$  in the range of 2–15 kDa and low polydispersities of 1.2–1.3 (Table 1). The PDIs were relatively high, but comparable with those in another study for polymers synthesized using the same RAFT agent.<sup>26</sup> After 24 h, the NMR charts of all the copolymers and terpolymers showed no peaks ascribed to vinyl protons, indicating that the reaction was completed in 24 h. Fig. 2.2(c) depicts the relationships among the RAFT agent/monomer ratio, molecular weight, and degree of polymerization of the 1:1 DMAEMA-MAA copolymer. The degree of polymerization was proportionally decreased with the increase in RAFT agent/monomer ratio. These results suggested that these amphoteric polymers were successfully synthesized with controlled radical polymerization.

**Table 2.1.** Characteristics of various polyampholytes prepared *via* RAFT polymerization.a) Determined by  $^1\text{H-NMR}$ , b)  $[\text{monomer}]:[\text{initiator}]:[\text{RAFT agent}]$ , c) determined by GPC.

Entry		Composition					Molar ratio <sup>b)</sup>	$M_n \times 10^{-3,c)}$	$M_w/M_n^c)$
		DMAEMA	MAA	Bu-MA	Oc-MA	HEMA			
1	In feed	50	50	0	0	0	100:1:5	4.9	1.21
	In polymer <sup>a)</sup>	50.3	49.7	0	0	0			
2	In feed	50	50	0	0	0	250:1:5	14.7	1.49
	In polymer <sup>a)</sup>	50.4	49.6	0	0	0			
3	In feed	66	33	0	0	0	125:1:5	7.12	1.57
	In polymer <sup>a)</sup>	67.5	32.5	0	0	0			
4	In feed	33	66	0	0	0	125:1:5	4.2	1.20
	In polymer <sup>a)</sup>	32.2	67.8	0	0	0			
5	In feed	49	49	2	0	0	102:1:5	4.9	1.32
	In polymer <sup>a)</sup>	49.3	48.7	2.0	0	0			
6	In feed	47.5	47.5	5	0	0	105:1:5	5.05	1.36
	In polymer <sup>a)</sup>	47.7	47.3	5.0	0	0			
7	In feed	46	46	8	0	0	54:1:5	2.3	1.19
	In polymer <sup>a)</sup>	46.1	45.5	8.4	0	0			
8	In feed	46	46	8	0	0	108:1:5	4.9	1.28
	In polymer <sup>a)</sup>	46.6	45.2	8.2	0	0			
9	In feed	49	49	0	2	0	102:1:5	4.95	1.23
	In polymer <sup>a)</sup>	49.4	48.6	0	2.0	0			
10	In feed	48.5	48.5	0	3	0	103:1:5	5.03	1.14
	In polymer <sup>a)</sup>	48.2	48.3	0	3.5	0			
11	In feed	48	48	0	4	0	104:1:5	5.15	1.25
	In polymer <sup>a)</sup>	48.5	47.6	0	3.9	0			
12	In feed	47.5	47.5	0	5	0	105:1:5	5.36	1.32
	In polymer <sup>a)</sup>	47.6	47.5	0	4.9	0			
13	In feed	47.5	47.5	0	0	5	105:1:5	4.3	1.31
	In polymer <sup>a)</sup>	48.1	46.5	0	0	5.4			

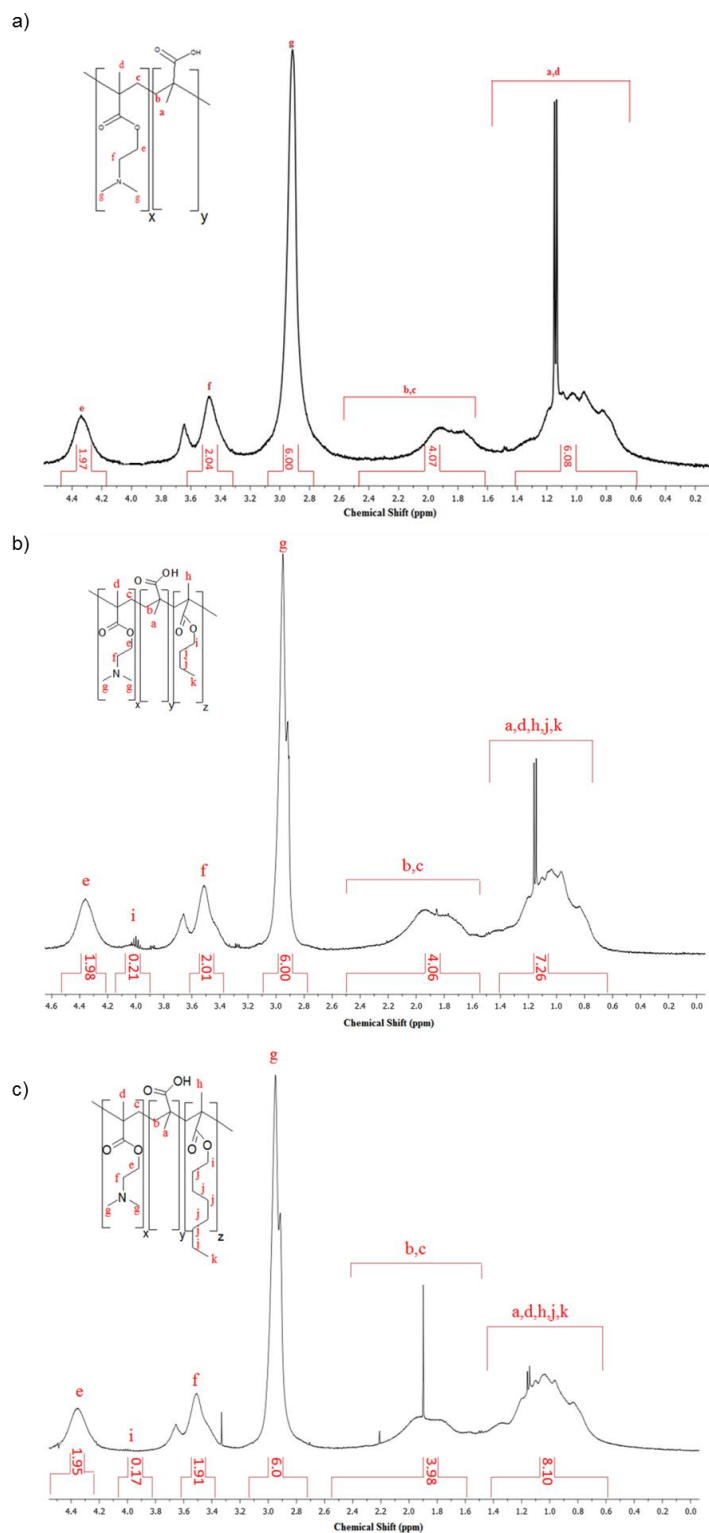


**Figure 2.1.**  $^1\text{H}$ -NMR spectra of (a) the 1:1 copolymer polyampholyte of DMAEMA and MAA, (b) the 5% Bu-MA incorporated 1:1 polyampholyte and (c) 5% Oc-MA incorporated 1:1 polyampholyte.

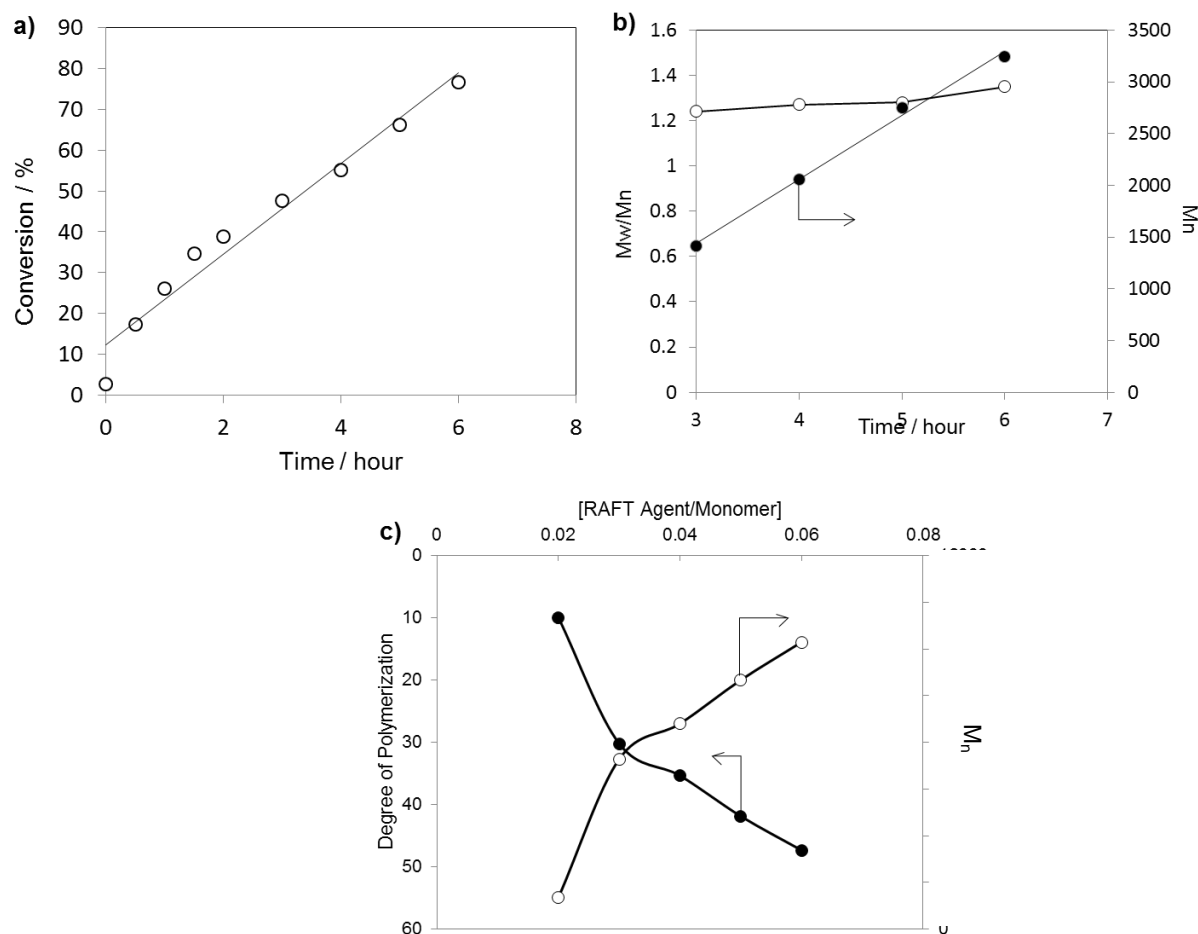


**Figure 2.2.** Characterization of RAFT polymerization products. (a) Kinetic plot for the conversion vs. time of the 1:1 MAA-DMAEMA copolymer. (b) Plots of time vs.  $M_w/M_n$  and time vs.  $M_n$  for the polymerization of the 1:1 MAA-DMAEMA copolymer. (c) Plots of the content ratio of RAFT agent used vs. the degree of polymerization and the concentration of RAFT agent used vs. the molecular weight.

## 2.3.2 Cryoprotective properties of these polyampholytes

### 2.3.2.1 Effects of monomer ratios

The ratio of monomers (MAA and DMAEMA) in the copolymer was varied in order to optimize conditions for cryoprotection. For this, 3 different types of copolymers with different ratios of monomers were prepared, and cell viability after cryopreservation with 15 % polymer/DMEM solutions without FBS was calculated. The copolymer synthesized with a 1:1 ratio of MAA to

DMAEMA showed the highest cell viability (Fig. 2.3), as compared to copolymers synthesized with 2:3 and 3:2 ratios. This result was similar to the results presented in our previous report,<sup>7, 8</sup> which showed that appropriate amounts of positively and negatively charged groups were needed to confer high cryoprotective properties. A cell viability of over 90 %, as achieved in the current study, was similar to that achieved with the commonly used cryoprotectant DMSO. After 6 h of culture, cell viability did not decrease, indicating that live cells were well protected immediately after thawing and that the evaluation by trypan blue staining was appropriate for viability measurement. Thus, for subsequent experiments, I prepared and modified the polyampholyte based on that synthesized with positive and negative monomers in a 1:1 ratio.

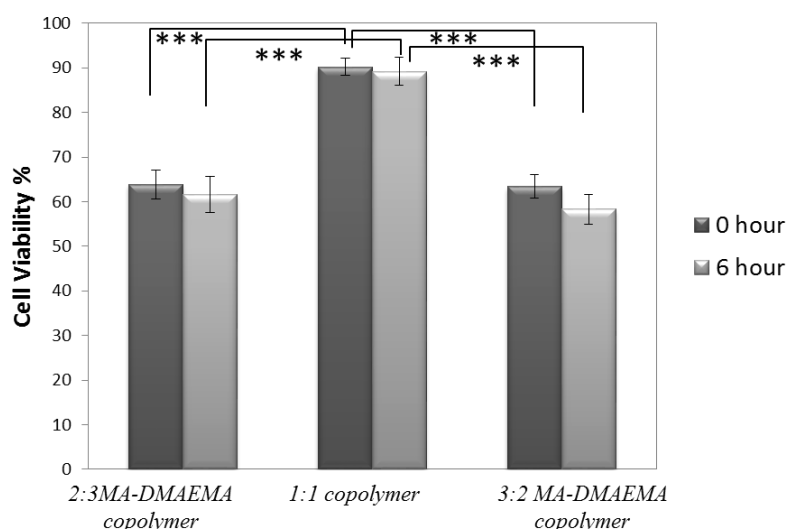


**Figure 2.3.** Cryoprotective properties of copolymers with different copolymer ratios. L929 cells were cryopreserved with MAA-DMAEMA copolymers synthesized using different ratios of MAA and DMAEMA (15 % polymer concentration).

### 2.3.2.2 Effects of hydrophobicity

In our previous report, when cells were frozen in a polyampholyte solution, the polyampholyte molecules were attached onto the cell membrane, as determined by fluorescent-conjugated polyampholyte detection with confocal laser microscopy.<sup>10</sup> This indicates that the mechanism through which the polyampholyte acts as a cryoprotectant probably differs from that of DMSO. Other non-penetrating polymeric cryoprotectants, such as hydroxymethyl starch (HES), have also been reported.<sup>27</sup> Previous studies have shown that HES attracts and absorbs water. Its viscosity is then reduced, and the rate of dehydration increases, which allows cells to be cooled



rapidly, thereby avoiding intracellular ice crystal formation as well as chilling injury. However, HES showed various cryopreservation properties that depended on the type of cell line used, and therefore, its use as a cryoprotectant is limited by its weak cryoprotective properties.<sup>28</sup> Thus, the cryoprotective mechanism of HES may be similar to that of polyampholytes by providing extracellular protection of the cell membrane. To enhance the cryoprotective properties of these membrane-protective cryoprotectants, I sought to increase the cell membrane interaction of the polyampholytes by the introduction of hydrophobic group(s) in the polymer backbone. The alkyl chain is highly hydrophobic, and amphiphilic polymers, such as polyethylene glycol and polyvinyl alcohol, in which the alkyl chain was introduced, show cell membrane attachment via hydrophobic interactions between membrane lipids and the alkyl chain.<sup>29</sup> To identify the effects of hydrophobicity, a small amount of a hydrophobic alkyl chain monomer, i.e., n-butyl methacrylate (Bu-MA) or n-octyl methacrylate (Oc-MA), was introduced into the 1:1 copolymer. Different amounts of Bu-MA were introduced, and cell viability after cryopreservation was measured. As shown in Fig. 2.4(a), the viability of L929 cells cryopreserved with 15 % poly (DMAEMA-co-MAA) solution including various concentrations of Bu-MA was enhanced. A similar effect was observed in cells frozen in 7.5 % polymer with 5 % Oc-MA (Fig. 2.4(b)), which showed almost double the viability of cells frozen in the polyampholyte without the hydrophobic moiety. Fig. 2.4(c) shows the cell viability after cryopreservation with hydrophilic and hydrophobic polyampholyte solutions at the same polymer concentration (10 %). Under these conditions, and with the same ratio of hydrophilic and hydrophobic moieties, the cryoprotective properties of the solution were strongly correlated with hydrophobicity.

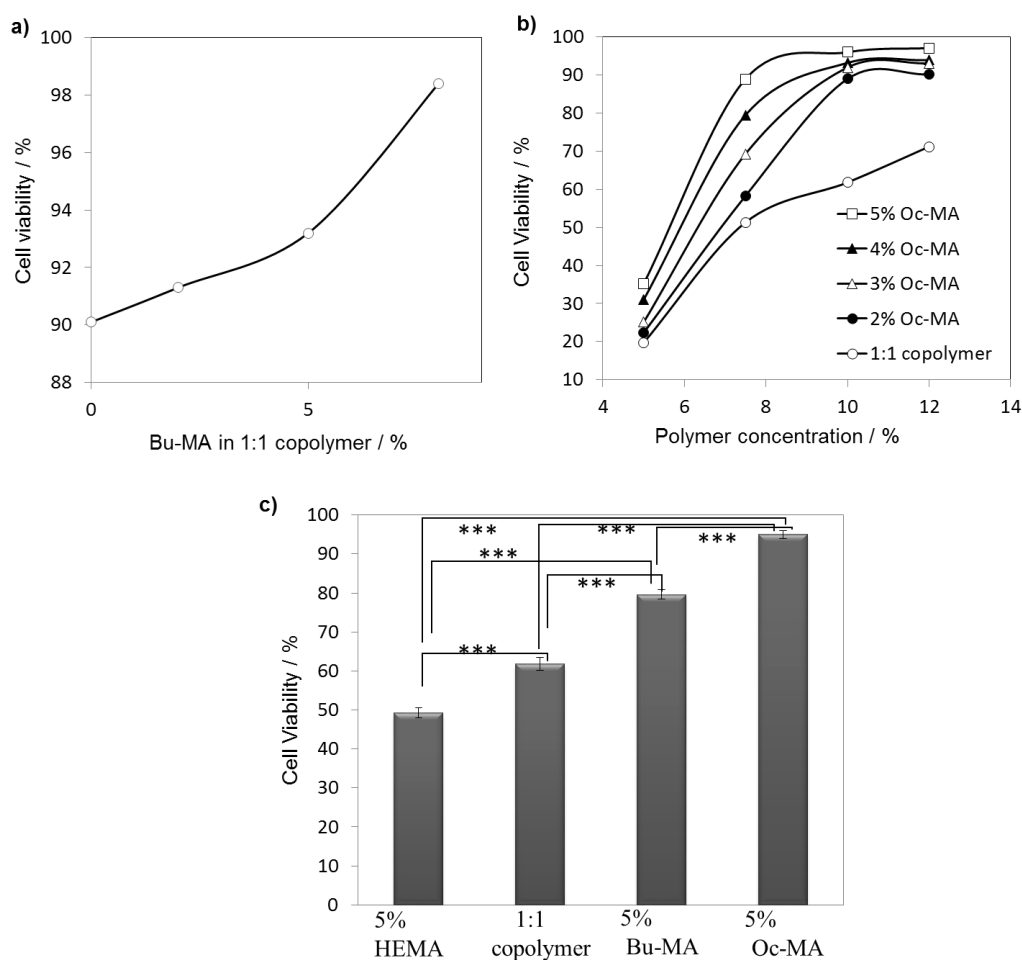


**Figure 2.4.** Effects of hydrophobicity of polyampholytes on cryopreservation. (a) L929 cells were cryopreserved with polyampholytes synthesized with a 1:1 ratio of MA and DMAEMA and different concentrations of Bu-MA (15% polymer concentration). (b) L929 cells were cryopreserved with polyampholytes synthesized with a 1:1 ratio of MA and DMAEMA and different concentrations of Oc-MA at various polymer concentrations. (c) L929 cells were cryopreserved with different polymers (10 % polymer concentration) and 5% Bu-MA or Oc-MA. A comparison with a polymer containing the hydrophilic monomer HEMA is shown. Data are expressed as the mean  $\pm$  SD of 3 independent experiments (5 samples each). \*\*\* $p < 0.001$ .

### 2.3.2.3 Effects of molecular weight

Next, I examined variations in the viability of L929 cells after cryopreservation with 1:1 copolymer solutions having different molecular weights. As shown in Fig. 2.5(a), cell viability increased with

increasing molecular weight of the copolymer. One more copolymer, i.e. 1:1 copolymer with 8 % Bu-MA, was also synthesized at different molecular weights, and its effects on cell viability were also examined in L929 cells. Again, cell viability increased when the molecular weight of the copolymer was increased (Fig. 2.5(b)). A previous study also demonstrated that high-molecular-weight HES was more effective as a cryoprotectant than low-molecular-weight HES in Chinese hamster cells.<sup>30</sup> In general, the cryoprotective effects of polymers such as HES depend on its ability to absorb water molecules and keep these thermally inert in a glassy state without experiencing any phase transitions during cooling. Absorption of water molecules depends on the molecular weight and concentration of the molecule. Although further research should be conducted, our current data strongly support the hypothesis that the protective properties of these cryoprotectants may be related to water absorption, which is dependent on the molecular weight of the compound. Thus, careful control of molecular weight using RAFT polymerization may be effective in the development of polyampholyte cryoprotectants.

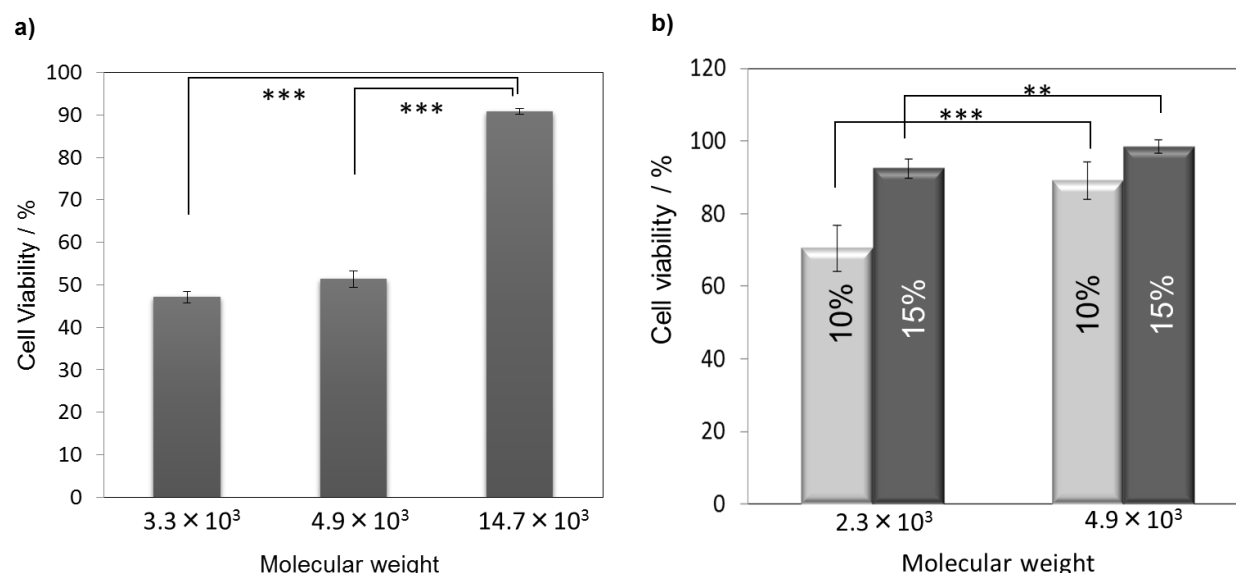


**Figure 2.5.** Effects of the molecular weight of polyampholytes on cryopreservation. (a) L929 cells were cryopreserved with the 1:1 MAA-DMAEMA copolymer (10 % polymer concentration) at different molecular weights. (b) L929 cells were cryopreserved with different concentrations of polyampholytes synthesized with a 1:1 ratio of MA and DMAEMA and 8% Bu-MA having 2 different molecular weights. Data are expressed as the mean  $\pm$  SD for 3 independent experiments (5 samples each). \*\*\* $p < 0.001$ , \*\* $p < 0.05$ .

### 2.3.3 Leakage experiment

Our research group previously used a soluble fluorescent dye, carboxyfluorescein (CF), to investigate the protective effect that polyampholytes provide against leakage during freezing and thawing.<sup>31</sup> In the present study, I also used CF to analyze leakage in L929 cells. When no polyampholyte was added to L929 cells before cryopreservation, fluorescent leakage was maximal (Fig. 2.6). However, when the amount of polyampholyte solution was increased, leakage began to decrease, indicating that liposomes were protected when the polyampholyte solution was added. This trend was again observed when a small amount of hydrophobic monomer (Bu-MA) was introduced into the 1:1 copolymer; the fluorescent intensity decreased compared to the intensity when no hydrophobic monomer was present. Introduction of Oc-MA in particular yielded the highest liposome protection properties, and less than 10 % leakage was seen with a 10 % polymer solution, in accordance with the results of cell viability after cryopreservation. These results indicated that hydrophobicity provided more efficient protection of the cell membrane during cryopreservation. Since freezing is a biologically relevant stress factor that involves a dramatic decrease in water activity, as shown in many previous publications,<sup>32</sup> freezing of liposomes without a protectant results in complete lysis of the vesicles. Thus, our experiment using freeze/thaw cycles directly showed that polyampholytes are able to stabilize phospholipid bilayers under freezing stress conditions. These results strongly supported our hypothesis that polyampholytes protect the cell membrane during freezing. In the literature, many proteins that protect cells from the damage induced during freezing have been reported, especially in freezing-tolerant plants, anhydrobiotic invertebrates, and fungi.<sup>33</sup> Interestingly, these proteins share many common characteristics, including highly charged polyampholytes with hydrophobic moieties.<sup>34, 35</sup> According to a report by Tolleter et al., polyampholytic protein,<sup>31</sup> which is classified as late embryogenesis abundant (LEA) protein, protects the liposome from desiccation and freezing damage with membrane attachments via electrostatic interactions between LEA protein molecules, which have many positive and negative charges, and phospholipid molecules. Although the mechanisms of protection are still unknown, a relationship may exist between these proteins and our synthesized polyampholytes.

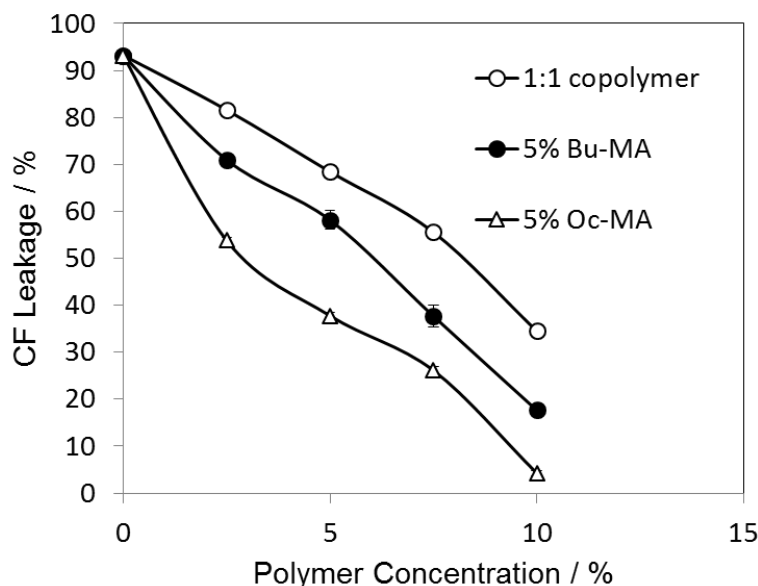


**Figure 2.6.** Protection of liposomes during freezing by polyampholytes. CF leakage from liposomes cryopreserved with various polyampholytes solutions at different polymer concentrations. Data are expressed as the mean  $\pm$  SD for 3 independent experiments (5 samples each).

### 2.3.4 Biocompatibility of the novel polyampholytes

The novel polyampholytes had a much higher  $IC_{50}$  in L929 cells than DMSO ( $IC_{50} = 2.519\%$ ) at 48 h after thawing (Fig. 2.7(a)), indicating that these synthetic polyampholytes were much less cytotoxic than DMSO. This result agrees with our previous report, which concluded that polyampholytes whose positive and negative charges are balanced have low cytotoxicity.<sup>7</sup> Moreover, introduction of a small amount of hydrophobic moiety to the completely synthetic polyampholyte further increased biocompatibility over that of DMSO. When L929 cells were cryopreserved with the polyampholytes and subsequently cultured in DMEM supplemented with 10 % FBS, the cells proliferated well after 7 days (Fig. 2.7(b)). After 7 days of culture, cell numbers for cryopreserved cells were not significantly reduced compared to those of the unfrozen control. These data suggested that the novel polyampholytes may be useful for cell cryopreservation in research and clinical applications due to its lower cytotoxicity and negligible effects on cell proliferation after thawing. The advantages of the polyampholytes synthesized by RAFT polymerization in terms of cryoprotective properties were clearly indicated, and I expect

that the control of dispersity, composition, and precise polymerization, such as block copolymerization, may enable researchers to prepare cryoprotective agents with high cell viability and to elucidate the mechanisms of cryoprotection of polyampholytes.

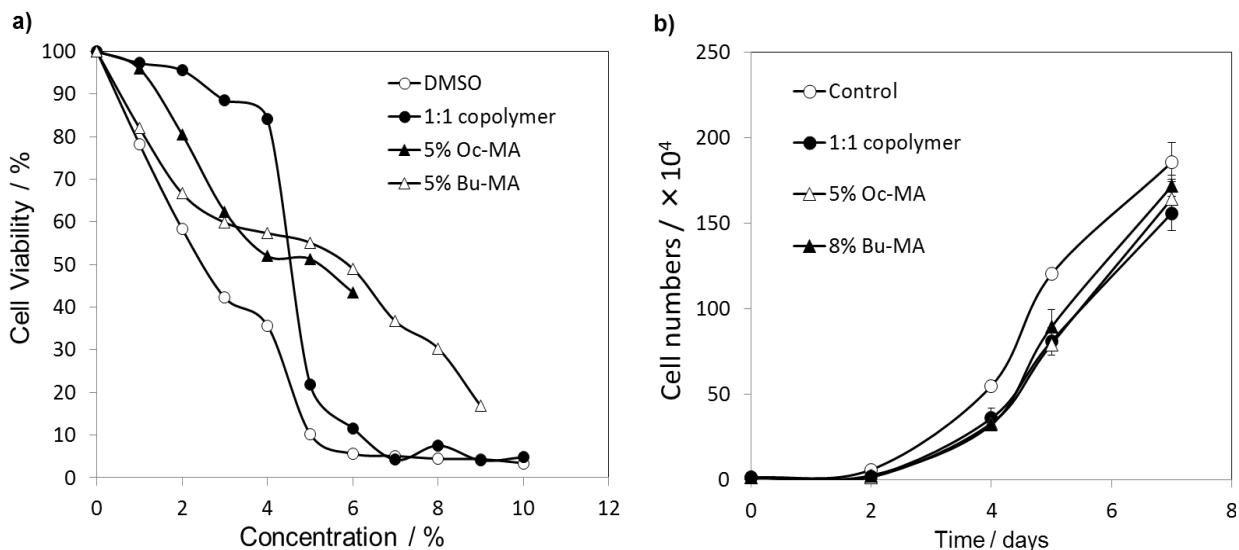


**Figure 2.7.** Cytocompatibilities of polyampholytes. (a) Cytotoxicity of DMSO (open circles), 1:1 MAA-DMAEMA copolymer (closed circles), 1:1 MAA-DMAEMA copolymer with 5% Oc-MA (open triangles), and 1:1 MAA-DMAEMA copolymer with 5 % Bu-MA (closed triangles). L929 cells were incubated with the indicated concentration of each compound for 48 h, followed by CCK assay. Data are described as the percentage of viable cells as compared to the number of untreated cells. Mean values and standard deviations for independent triplicate experiments (8 samples each) are shown. (b) Growth curves of L929 cells, unfrozen control (open circles), cryopreserved with 1:1 MAA-DMAEMA copolymer (closed circles), 1:1 MAA-DMAEMA copolymer with 5% Oc-MA (open triangles), and 1:1 MAA-DMAEMA copolymer with 5% Bu-MA (closed triangles) for 7 days. Data are expressed as the mean  $\pm$  SD of 3 independent experiments.

## 2.4 Conclusion

I have successfully demonstrated that synthetic polyampholytes made of methacrylic acid and 2-(dimethylamino)ethyl methacrylate can efficiently cryopreserve various types of cells without the requirement for any other cryoprotectants. Additionally, introduction of hydrophobicity and

an increase in molecular weight promoted cell viability after thawing. Leakage experiments suggested that polyampholytes protected the cell membrane during cryopreservation, and this effect was enhanced by increased hydrophobicity. Moreover, due to low cytotoxicity, these polyampholytes have the potential to replace the conventionally used cryoprotective agent DMSO. The present study is the first to show that it is possible to design a polymeric cryoprotectant that will protect the cell membrane during freezing using appropriate polymerization techniques.

## 2.5 References

- 1 C. Polge, A. U. Smith and A. S. Parkes, *Nature*, 1949, **164**, 666.
- 2 J. E. Lovelock and M. W. Bishop, *Nature*, 1959, **183**, 1394–1395.
- 3 G. M. Fahy, *Cryobiology*, 1986, **23**, 1–13.
- 4 J. E. Oh, R. K. Karlmark, J. H. Shin, A. Pollak, M. Hengstschlager and G. Lubec, *Amino Acids*, 2006, **31**, 289–298.
- 5 D. A. Young, S. Gavrilov, C. J. Pennington, R. K. Nuttall, D. R. Edwards, R. N. Kitsis and I. M. Clark, *Biochem. Biophys. Res. Commun.*, 2004, **322**, 759–765.
- 6 G. S. Jiang, K. H. Bi, T. H. Tang, J. W. Wang, Y. K. Zhang, W. Zhang, H. Q. Ren, H. Q. Bai and Y. S. Wang, *Int. Immunopharmacol.*, 2006, **6**, 1204–1213.
- 7 K. Matsumura and S. H. Hyon, *Biomaterials*, 2009, **30**, 4842–4849.
- 8 K. Matsumura, J. Y. Bae JY and S. H. Hyon, *Cell Transplant.*, 2010, **19**, 691–699.
- 9 N. Vrana, K. Matsumura, S. H. Hyon, L. Geever, J. Kennedy, J. Lyons, C. L. Higginbotham, P. A. Cahill and G. B. McGuinness, *J. Tissue. Eng. Regen. Med.*, 2012, **6**, 280–290.
- 10 K. Matsumura, F. Hayashi, T. Nagashima and S. H. Hyon SH, *J. Biomater. Sci. Polym. Ed.*, 2013, **24**, 1484–97.
- 11 J. S. Wang and K. Matyjaszewski, *J. Am. Chem. Soc.*, 1995, **117**, 5614–5615.
- 12 M. Kato, M. Kamigaito, M. Sawamoto and T. Higashimura, *Macromolecules*, 1995, **28**, 1721–1723.
- 13 M. K. Georges, R. P. N. Veregin, P. M. Kazmaier and G. K. Hamer, *Macromolecules*, 1993, **26**, 2987–2988.

- 14 J. Nicolas, Y. Guillaneuf, C. Lefay, D. Bertin, D. Gigmes and B. Charleux, *Prog. Polym. Sci.*, 2013, **38**, 63–235.
- 15 J. F. Quinn, T. P. Davis and E. Rizzardo, *Chem. Commun.*, 2001, **11**, 1044–1045.
- 16 A. Goto, K. Sato, Y. Tsujii, T. Fukuda, G. Moad, E. Rizzardo and S. H. Thang, *Macromolecules*, 2001, **34**, 402–408.
- 17 J. Chiefari, Y. K. Chong, F. Ercole, J. Krstina, J. Jeffery, T. P. Le, R. T. A. Mayadunne, G. F. Meijs, C. L. Moad, G. Moad, E. Rizzardo and S. H. Thang, *Macromolecules*, 1998, **31**, 5559–5562.
- 18 Y. Mitsukami, M. S. Donovan, A. B. Lowe and C. L. McCormick, *Macromolecules*, 2001, **34**, 2248–2256.
- 19 M. S. Donovan, A. B. Lowe, T. A. Sanford and C. L. McCormick, *J. Polym. Sci. Polym. Chem.*, 2003, **41**, 1262–1281.
- 20 C. L. McCormick and A. B. Lowe, *Acc. Chem. Res.*, 2004, **37**, 312–325.
- 21 D. B. Thomas, B. S. Sumerlin, A. B. Lowe and C. L. McCormick, *Macromolecules*, 2003, **36**, 1436–1439.
- 22 C. Ladavière, N. Dörr and J. P. Claverie, *Macromolecules*, 2001, **34**, 5370–5372.
- 23 B. S. Sumerlin, A. B. Lowe, D. B. Thomas and C. L. McCormick, *Macromolecules*, 2003, **36**, 5982–5987.
- 24 R. C. MacDonald, R. I. MacDonald, B. P. M. Menco, K. Takeshita, N. K. Subbarao and L. R. Hu, *Biochim. Biophys. Acta.*, 1991, **1061**, 297–303.
- 25 D. K. Hinch, E. Zuther, E. M. Hellwege and A. G. Heyer, *Glycobiology*, 2002, **12**, 103–110.
- 26 H. Kitano, T. Kondo, T. Kamada, S. Iwanaga, M. Nakamura and K. Ohno, *Colloids Surf. B.*, 2011, **88**, 455–462.
- 27 A. Stolzing, Y. Naaldijk, V. Fedorova and S. Sethe, *Transfus. Apher. Sci.*, 2012, **46**, 137–147.
- 28 P. J. Stiff, A. J. Murgo, C. G. Zaroulis, M. F. Derisi and B. D. Clarkson, *Cryobiology*, 1983, **20**, 17–24.
- 29 O. Inui, Y. Teramura and H. Iwata, *ACS Appl. Mater. Interfaces*, 2010, **2**, 1514–1520.
- 30 K. Luo, G. Wu, Q. Wang, Y. Sun and H. Liu, *Cryobiology*, 1994, **31**, 349–354.
- 31 D. Tolleter, D. K. Hinch and D. Macherel, *Biochim. Biophys. Acta.*, 2010, **1798**, 1926–1933.



- 32 D. K. Hinch, A. V. Popova and C. Cacula, Effects of sugars on the stability and structure of lipid membranes during drying. Vol. 3. In: Tien HT, Ottova-Leitmannova A, editors. Advances in planar lipid bilayers and liposomes. Amsterdam: Elsevier, 2006, 189–217.
- 33 A. Tunnacliffe and M. J. Wise, *Naturwissenschaften*, 2007, **94**, 791–812.
- 34 T. Shimizu, Y. Kanamori, T. Furuki, T. Kikawada, T. Okuda, T. Takahashi, H. Mihara and M. Sakurai, *Biochemistry*, 2010, **16**, 1093–1104.
- 35 T. Furuki, T. Shimizu, S. Chakrabortee, K. Yamakawa, R. Hatanaka, T. Takahashi, T. Kikawada, T. Okuda, H. Mihara, A. Tunnacliffe and M. Sakurai, *Biochim. Biophys. Acta.*, 2012, **1824**, 891–897.

## Chapter 3 TOWARDS A MOLECULAR UNDERSTANDING OF THE MECHANISM OF CRYOPRESERVATION: CELL MEMBRANE INTERACTION AND HYDROPHOBICITY

### 3.1 Introduction

Our current cognizance of cryopreservation stems from the studies carried out in the last two centuries. The first successful cryopreservation was reported by Polge et al. in 1949 when he accidentally discovered the cryoprotective property of glycerol on fowl sperm.<sup>1</sup> Few years later, Lovelock et al. reported dimethyl sulfoxide (DMSO) as an efficient cryoprotectant for red blood cells.<sup>2</sup> This was a major breakthrough because DMSO is still used frequently as the preferred cryoprotective agent (CPA) in many biological applications. Since then, numerous research groups undertook investigations to explain the physical phenomenon<sup>3, 4</sup> and kinetics behind cryopreservation.<sup>5-9</sup>

Cryoprotectants can be divided into two classes: those which penetrate the cell membrane (penetrating CPAs) and those which cannot penetrate the cell membrane during freezing (non-penetrating CPAs). Penetrating CPAs are small molecules which include DMSO, glycerol, ethylene glycol, etc. These two classes act very differently from each other in cryopreserving cells. Penetrating CPAs reduces or avoids intracellular ice formation during freezing and thereby controlling the salt concentration.<sup>10</sup> On the other hand, non-penetrating CPAs are usually high molecular weight compounds such as polyethylene oxide, polyvinyl propylidone, hydroxyl ethyl starch (HES), sugars, etc. They assist in dehydrating the cells faster at low temperatures, which in turn prevents the chilling injury caused by slow freezing.<sup>11</sup>

Recently, Matsumura et al. developed a non-penetrating polymer based cryoprotectant carboxylated Poly-L-lysine (COOH-PLL) which has both positive and negative charges on the polymer chain (polyampholyte).<sup>12-14</sup> It was found to be an excellent CPA, even in the absence of any antifreeze proteins like fetal bovine serum (FBS), and thereby eliminating the perils associated with it. Various kinds of cells were successfully cryopreserved with it. The cells showed a good survival rate even after cryopreservation for 24 months.<sup>15</sup> Dextran based polyampholytes also exhibited excellent cryoprotective property.<sup>16</sup>

In Chapter 2, I developed synthetic polyampholyte cryoprotectant via living radical polymerization, which showed good cell viability and biocompatibility. Supplementing the polyampholytes with a small dose of hydrophobicity (incorporation of hydrophobic moieties) led to a significant increase in cell viability.<sup>17</sup> But the mechanism of cryopreservation by polyampholytes could not be explained, which is very crucial for its further evolution. Establishment of molecular mechanism can assist in the employment of these polyampholytes for various regenerative medicines like stem cell cryopreservation, tissue engineering and for development of cellular scaffolds. Moreover, it can help in more efficient design of CPA's in the future wherein newer materials can be put into use with the current knowledge and also, these polymers can be tuned to be administered to cryopreservation of cell-containing constructs.

Matsumura et al. investigated the probable mechanism of cryoprotection of polyampholytes by using solid state NMR spectroscopy in the magic angle spinning condition (MAS).<sup>18</sup> As can be seen through Fig. 3.1, they proposed when DMSO was used, water and solutes retained high mobility even at low temperature in ice, and this finding is similar with the mechanism of cryopreservation reported previously that DMSO prevents intracellular ice formation by penetrating into cells. In contrast, the PLL (0.65) polymer immediately formed soluble aggregates in ice and probably trapped water and salt and played a role as a buffer for preventing drastic changes of the osmotic environment and crystal formation during freezing.

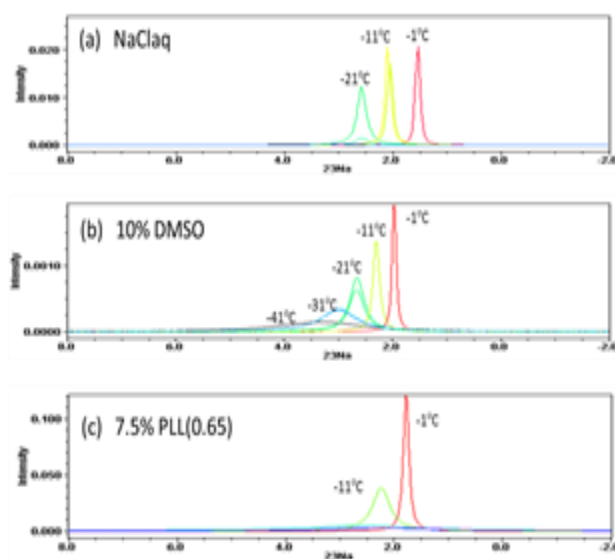


**Figure 3.1.**  $^{23}\text{Na}$ -NMR spectra of (a) physiological saline solution, (b) DMSO, and (c) PLL(0.65) saline solutions during freezing (From Matsumura et al, *Cryobiolol. Cryotechnol.*, 2013, 59, 23-28).<sup>18</sup>

Also,  $^1\text{H}$ -NMR results demonstrated that DMSO produced very narrow signals at ultra-low temperatures ( $-41^\circ\text{C}$ ), suggesting that it remained highly diffusible at these temperatures in ice. On the other hand, polymer chain in PLL (0.65) loses its mobility when cooled down to ultra-low temperature (Fig. 3.2). It was also suggested that disappearance of these signals was not due to precipitation but due to some intermolecular interaction.

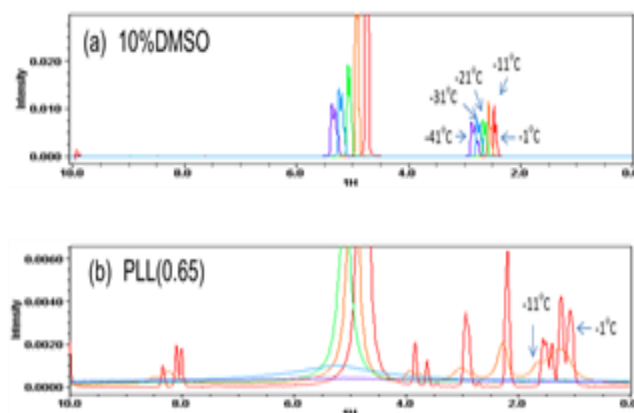


**Figure 3.2.**  $^1\text{H}$ -NMR spectra of (a) DMSO, and (b) PLL (0.65) saline solutions during freezing (From Matsumura et al, *Cryobiolol. Cryotechnol.*, 2013, 59, 23-28).<sup>18</sup>

They hypothesized that this is due to reversible gel formation around the cell matrix which protects it from various freeze-induced damages. In this article they concluded that PLL

(0.65) acts as a cryoprotective agent by protecting cells from stresses such as drastic changes in soluble space size and osmotic pressure (Fig. 3.3). But this is not the complete mechanism; it needs to be studied more in future. Since polyampholytes are non-penetrating in nature and remain on membrane surface, therefore a deeper understanding of the interaction of polyampholytes with cell membrane is required.

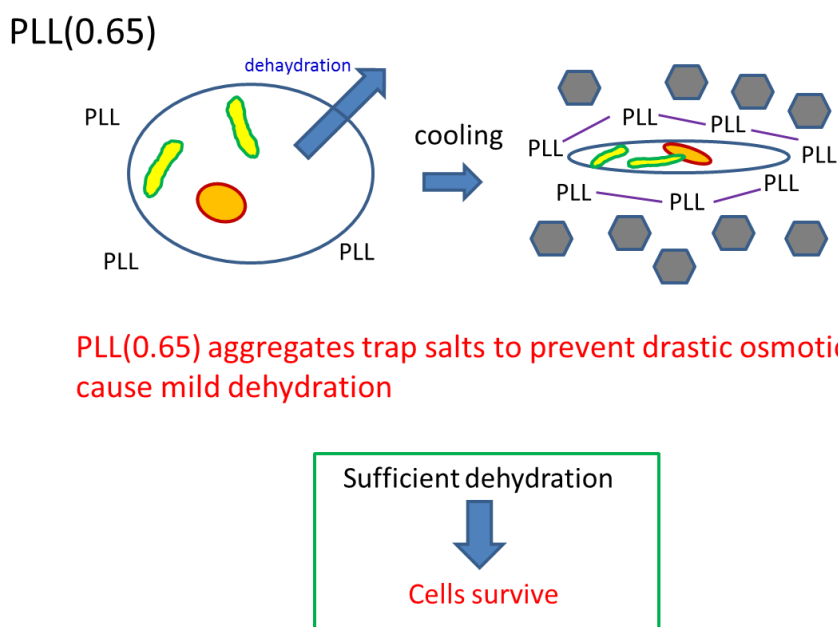


**Figure 3.3.** Schematic representation of the mechanism of cryopreservation by PLL (0.65).

In this chapter, I have tried to ascertain the role of polymer structure in cryopreservation, and for this we formulated structurally analogous polyampholytes with a modest structural difference by RAFT polymerization and compared their activity with the previously synthesized polyampholyte.<sup>18</sup> Hydrophobicity was also induced in the polymers by virtue of hydrophobic moieties like n-butyl methacrylate (BuMA) and n-octyl methacrylate (OcMA). To investigate the molecular mechanism of cryopreservation, various physicochemical techniques were employed. Liposomes were used to probe the interaction of polyampholytes with the cell membrane during freezing. Liposomes are closed vesicles made up of phospholipid bilayers and enclose an aqueous solution and hence they are used as a cell membrane mimic. Polymer response on freezing was also evaluated by studying the ice recrystallization during thawing (by cryomicroscopy), which is lethal to cell membrane and subsequently causes cell death. We

reckoned that this structural activity relationship study of the polymers with respect to its propensity for cryopreservation can steer us further in the elucidation of molecular mechanism.

## **3.2 Experimental**

### **3.2.1 Materials**

2-(Dimethylamino)ethyl methacrylate (DMAEMA), methacrylic acid (MAA), n-butyl methacrylate (BuMA) was purchased from Wako Pure Chemical Industries Ltd (Osaka, Japan). N-octyl methacrylate (OcMA) was purchased from NOF Corporation (Tokyo, Japan). All of these monomers were distilled under reduced pressure prior to use to remove inhibitors. Sulfobetaine (SPB) and carboxymethyl betaine (CMB) was donated by Osaka Organic Chem. Ind. Ltd., Osaka, Japan. 2-(Dodecylthiocarbonothioylthio)-2-methylpropionic acid, 5- and 16-doxyl stearic acid (DSA) and carboxyfluorescein (CF) were purchased from Sigma–Aldrich (St. Louis, MO, USA), were used as provided without further purification. 4–4'-Azobis-(4-cyanovaleric acid) (V-501, initiator) was purchased from TCI (Tokyo, Japan). Azobisisobutyronitrile (AIBN) was purchased from Wako. AIBN was recrystallized with methanol before using. Egg phosphatidylcholine (EPC) was purchased from NOF Corporation. Ethanol, methanol, 2-propanol and Triton® X-100 were purchased from nacalai tesque Inc., Kyoto, Japan.

### **3.2.2 Synthesis of Polyampholytes**

#### **3.2.2.1 Synthesis of poly-(MAA-DMAEMA)**

Synthesis of poly-(MAA-DMAEMA). Poly-(MAA-DMAEMA) was prepared as described in our previous study.<sup>18</sup> Briefly, DMAEMA, MAA, 2-(dodecylthiocarbonothioylthio) -2-methylpropionic acid (RAFT agent), and V-501 (initiator) were added to a reaction vial, and 20 mL of water–methanol mixture (1:1 [v/v]) was then added. The solution was purged with nitrogen gas for 1 hour and stirred at 70° C. After 24 h, the reaction mixture was precipitated using 2-propanol, the precipitates were collected by centrifugation, and the compound was dried over vacuum (Fig. 3.1a).

### 3.2.2.2 Synthesis of poly-SPB

SPB monomer, 2-(dodecylthiocarbonothioylthio)-2-methylpropionic acid and AIBN were dissolved in methanol-water mixture (3:1 v/v %). The solution was then purged with nitrogen gas for 1 hour and stirred at 70° C. After 6 hours, the reaction mixture was dialyzed against methanol and water successively for 24 hours each with constant change of solvent. The polymer was then obtained after lyophilization (Fig. 3.4b).

### 3.2.2.3 Synthesis of poly-CMB

CMB monomer, 2-(dodecylthiocarbonothioylthio)-2-methylpropionic acid and AIBN were dissolved in ethanol. The solution was purged with nitrogen gas for 1 hour and stirred at 70° C. After 48 hours, the reaction mixture was precipitated using 2-propanol, the precipitates were collected by centrifugation, and the compound was dried over vacuum (Fig. 3.4c).

### 3.2.2.4 Introduction of hydrophobicity

Hydrophobic derivatives of the above three polymers were synthesized by including either of the two hydrophobic monomers (BuMA or OcMA) to the reaction mixture and then proceeding with the polymerization. 2-5 % of hydrophobicity was incorporated by adding different amounts of hydrophobic monomers (Fig. 3.4d).

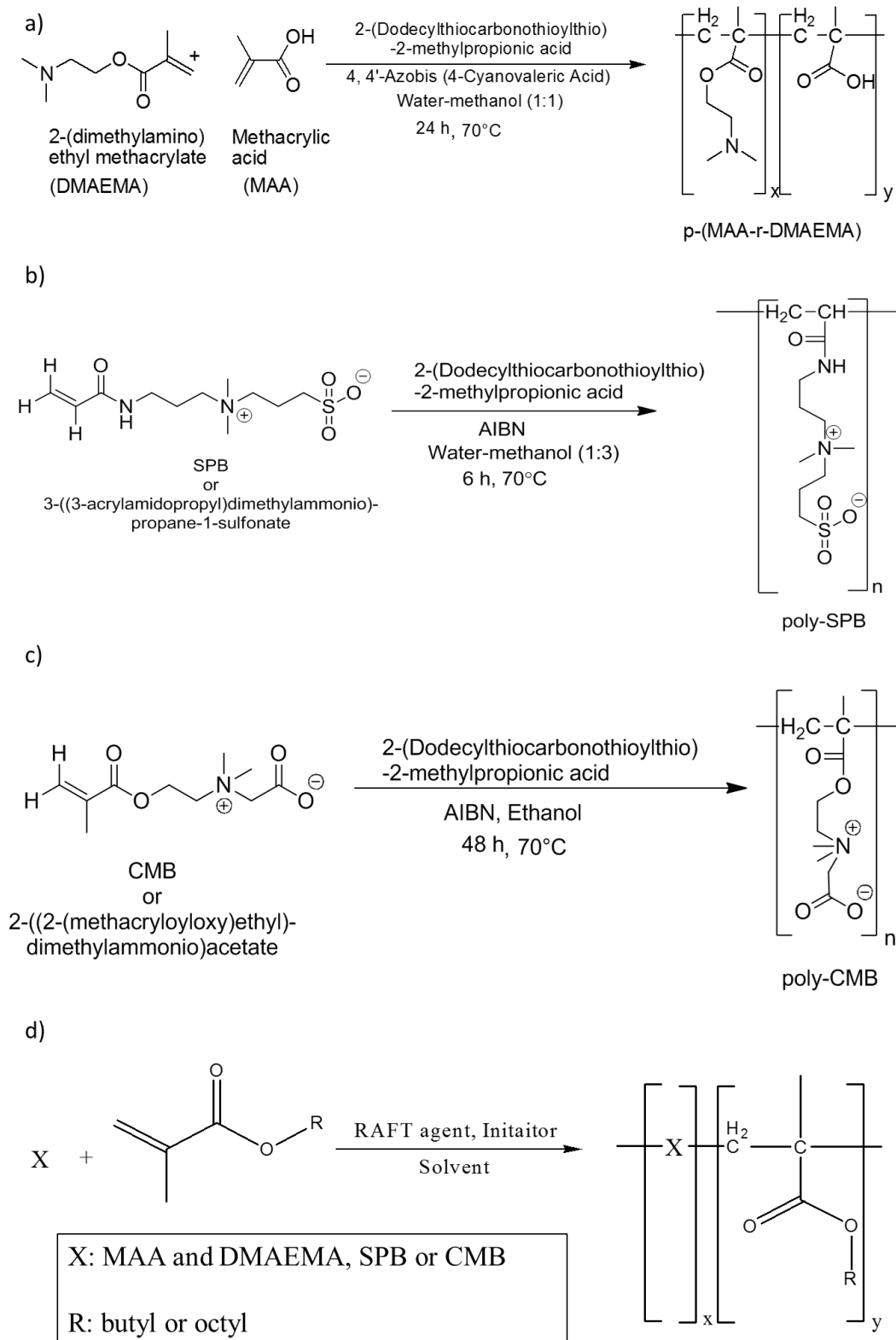


**Figure 3.4.** Synthesis of (a) Poly-(MAA and DMAEMA) (b) Poly-SPB, (c) Poly-CMB and d) hydrophobic derivatives of polyampholytes by RAFT polymerization.



### 3.2.3 Molecular Weight Determination

The molecular weight and distribution (polydispersity index, PDI) of the polymers were determined by gel permeation chromatography (GPC, column, BioSeps2000; Phenomenex, Inc., CA, USA) and was measured using Shimadzu high-performance liquid chromatography data system incorporating a refractive index detector. A phosphate buffer (pH 7.4, 0.1 M) was used in the case of poly-(MAA-DMAEMA) and NaBr solution (pH 7.4, 0.1 M) for poly-CMB and poly-SPB as the mobile phase (flow rate, 1 mL min<sup>-1</sup>) and Pullulan (Shodex Group, Tokyo, Japan) was used as the standard.

### 3.2.4 Cell Culture and Cryopreservation

L929 cells (American Type Culture Collection, Manassas, VA, USA) were cultured in Dulbecco's modified Eagle's medium (DMEM, Sigma Aldrich) supplemented with 10% FBS. Cells were cultured at 37 °C in a CO<sub>2</sub> incubator in a humidified atmosphere. When the cells were confluent, they were washed with phosphate buffered saline (PBS) and then treated with trypsin solution (0.25 % [w/v] trypsin containing 0.02% [w/v] ethylenediaminetetraacetic acid in PBS) to detach the cells. The cell pellet was then collected by centrifugation, mixed with fresh DMEM, and subsequently transferred to a new culture plate for subculture.

Polyampholyte solutions were prepared in DMEM without FBS at 2.5–15 % concentrations. The pH of the solution was adjusted to 7.4, and the osmotic pressure was adjusted to 500 mmol/kg by the addition of sodium chloride using a vapor pressure Osmometer (VAPRO Model 5660, WESCOR Biomedical Systems, UT, USA). These solutions were filter sterilized using a MILLEX GP Filter Unit 0.22 µm (Millipore Corp., Billerica, MA, USA). One million L929 cells were suspended in 1 mL of this cryopreservation solution in a vial and stored at -80 °C without controlling the cooling rate. After one week, the vials were thawed in a water bath maintained at 37 °C with gentle shaking. Cell suspension was then diluted tenfold and mixed well and then the cell pellet was collected after centrifugation. The cells were stained with trypan blue and counted on a hemocytometer. Cell viability was reported as the ratio of the living cells to the total number of cells and subsequently percentage cell viability was evaluated.

### 3.2.5 Liposome Preparation

EPC (12 mg) was dissolved in chloroform, in a glass test tube. Organic solvent was evaporated under a gentle stream of nitrogen gas to produce a thin lipid film. The film was subsequently dried under vacuum overnight. The resulting lipid film was hydrated in aqueous solution, and single unilamellar vesicles were obtained using a mini-extruder set (Avanti Polar Lipids) and membranes with a 0.1- $\mu\text{m}$  pore size.<sup>19</sup>

### 3.2.6 DSC

Thermal behavior of the lipids in the presence of polyampholytes was studied by DSC. Thermograms were obtained of EPC liposome with polyampholytes at polymer/EPC mass ratios between 0 and 1.0. 50  $\mu\text{L}$  of the sample was transferred to an alodined aluminum pan and measurements were carried out using a Seiko Instrument EXTAR SII-6200 DSC system in a temperature range of -30 °C to 80 °C with a heating rate of 20 °C/min in a constant nitrogen flow. The gel to liquid phase transition temperature of the lipid was recorded as the temperature at the peak minimum.

### 3.2.7 Electron Spin Resonance Spectroscopy

EPC (0.013mmol) was dissolved in 1 mL chloroform and to it  $1 \times 10^{-4}$  mmol of 5- or 16- DSA to prepare the corresponding spin labelled liposome. Organic solvent was evaporated under a gentle stream of nitrogen gas to produce a thin lipid film. The film was subsequently dried under vacuum overnight. The resulting lipid film was hydrated in aqueous solution, and single unilamellar vesicles were obtained using a mini-extruder set (Avanti Polar Lipids) and membranes with a 0.1- $\mu\text{m}$  pore size. The liposomes were suspended in polyampholyte solutions of various concentrations and stored at -78 °C. After 24 h, solutions were thawed in a 37 °C water bath. Solutions were then transferred to an ESR quartz flat cell equipped with a screw knob (ES-LC12; JEOL, Ltd., Tokyo, Japan). The flat cell was placed in the cavity of the spectrometer, and ESR spectra were recorded on a JEOL JES-FA100 ESR SPECTROMETER using the following parameters: sweeping field,  $333 \pm 10$  mT; microwave power, 10 mW; modulation width, 0.02 mT; sweep time, 2 min; total sweep, 10; time constant, 0.03 sec; and amplitude, 1000.

We have introduced two kinds of nitroxide probes, viz., 5- and 16-DSA, which are free fatty acids. Nitroxide group of the 5-DSA acid gets located near the polar head group region of the membrane,<sup>20</sup> so a change in probe mobility can assist in detection of polyampholyte in this region. Meanwhile, molecular motion in the 5-position of fatty acid chain is anisotropic and produces spectra where both outer and inner hyperfine extrema are defined,<sup>21, 22</sup> and order parameter,  $S$ , may be calculated according to the following equation (Fig. 3.5a).

$$S = \frac{A_{II} - A_I}{a} \times 0.5407, a = (A_{II} + 2A_I)/3$$

where  $A_{II}$  and  $A_I$  are the apparent parallel and perpendicular hyperfine splitting parameters respectively.  $S$  represents the anisotropy of motion or in other words, it represents the ordering along the long molecular axis.<sup>23</sup>

On the other hand, radical group of 16-DSA gets localized near the lipid core region of the phospholipid membranes. Molecular motion is isotropic and spectra are highly disordered, and as such correlation time ( $\tau_c$ ) is calculated, according to the following equation (Fig. 3.5b).

$$\tau_c = \left(6.6 \times 10^{-10} W_0\right) \left[ \sqrt{\frac{h_0}{h_{-1}}} - 1 \right]$$

where  $h_0/h_{-1}$  is the ratio of the peak heights of the central and high field lines respectively and  $W_0$  is the peak-to-peak width of the central line.  $\tau_c$  represents the motional rate parameters.<sup>23</sup>

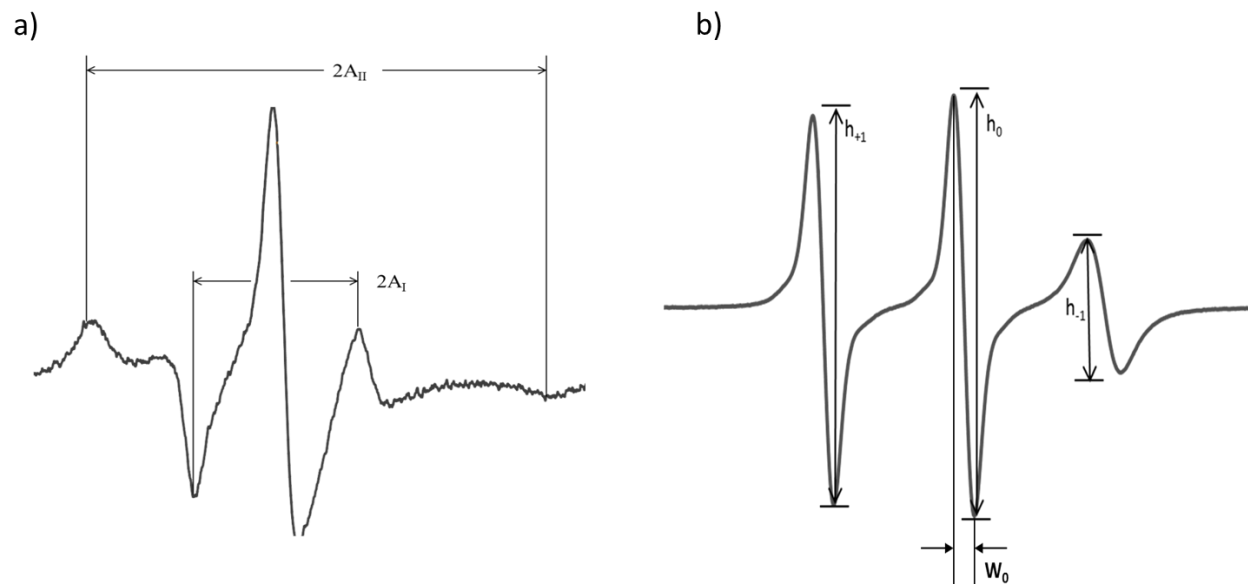


**Figure 3.5.** ESR spectra of a) 5-DSA and b) 16-DSA in EPC liposome in PBS (pH 7.4).

### 3.2.8 Ice recrystallization inhibition - Cooling Splat assay

The potential of the polymers to inhibit ice recrystallization during freezing was examined using the modified splat assay. 20  $\mu$ L of a polymer sample dissolved in PBS was released from 1.5 m above a glass coverslip placed on a thin aluminum sheet on dry ice. With the splatting of the droplet onto the chilled coverslip, a thin wafer with a diameter of 10-12 mm was formed immediately which was composed of very fine-grained ice. The glass coverslip was then transferred to a Linkam cryostage maintained at -6 °C. It was then allowed to stabilize for 30 minutes under nitrogen atmosphere. Photographs were captured using Nikon DS Fi2 microscope fitted with crossed polarizers. The images were then processed using ImageJ software. Degree of recrystallization was quantitatively analyzed by measuring mean largest grain size (MLGS) from five individual wafers and was calculated relative to the size obtained from PBS control.<sup>24</sup>

### 3.2.9 Leakage Experiment

Liposome thin lipid film was prepared by the procedure described above. The resulting lipid film was hydrated in 600  $\mu$ L of 0.1 M CF/PBS solution, and uniform liposomes were obtained by using a mini-extruder set (Avanti Polar Lipids) and membranes with a 0.1- $\mu$ m pore size. The

excess of the dye (CF) was removed by passing the liposome through a Sephadex G-25 column (NAP-5, GE Healthcare). The resultant liposomes were then suspended in polymer solutions of different concentrations and were stored at -80 °C. The mixture was then thawed after 24 hours in a 37 °C water bath. CF fluorescence was measured using a JASCO spectrofluorometer FP-8600 using an excitation wavelength of 450 nm and a detection wavelength of 520 nm. Fluorescence quenching represents that the membrane is intact (protected) after freeze-thaw process and the increase in fluorescence intensity represents the membrane damage due to the release of the CF into the surrounding buffer. Complete membrane lysis was determined (100 % leakage) after mixing it with Triton X-100 and the percentage leakage for the other systems were calculated relative to these values.<sup>18</sup>

### 3.2.10 Solid State NMR

Polymer solutions were prepared in physiological saline (10 % concentration) and pH was adjusted to 7.4. Solid-state NMR experiments were performed on a 700 MHz JEOL ECA spectrometer, using a Doty Scientific Inc. (DSI) 4 mm HXY CP/MAS NMR probe. The solution samples were sealed into DSI inner-sealing cells for an XC4 rotor and spun at 3.6 - 5.8 kHz with various temperature ranging from 1 to -41 °C. Sample cooling was performed by replacing spinning and bearing gases to cooled N<sub>2</sub>-gas passing through liquid nitrogen cryostat with DSI cold gas supply unit. All the data were collected with a single pulse experiment, providing sharp signals from soluble part and highly broad signals from frozen part. All the data were processed with the program NMRPipe.<sup>25</sup> NMRViewJ were employed for spectral visualization and analysis. Intensity and line width of peaks were analyzed by IGOR (WaveMetrics).<sup>26</sup>

## 3.3 Results and discussion

Characterization. Polyampholytes were prepared under various conditions and were characterized with <sup>1</sup>H NMR and GPC. Completion of the reaction was monitored by <sup>1</sup>H-NMR by observing the loss of vinyl protons of the monomer (Fig. 3.6). Conversion of the monomer to the corresponding polymer and the ratio of the initial concentration and at any given time during the reaction,  $\ln ([M]_0 / [M])$  were also evaluated using <sup>1</sup>H-NMR. Poly-SPB reacts fastest (more than 80 % of the reaction gets completed within the first 2 hours) followed by poly-CMB where reaction for 2 hours leads to around 75 % conversion (Fig. 3.7). On the other hand, poly-(MAA-DMAEMA)

reacts slowly initially with only 40 % conversion in the first 2 hours. The plot of  $\ln ([M]_0/[M])$  vs the reaction time manifested a linear relationship indicating the presence of constant number active species during the polymerization.<sup>27</sup> The final polymers obtained were characterized using 2D-NMR (Fig. 3.8). Synopsis of all the polymers are stated in Table 3.1. The compositions of each monomer in the polymers were well controlled and were in accordance with the initial feed ratio. Further, GPC curves indicated that all the polymers had a unimodal distribution with polydispersity index ( $M_w/M_n$ ) in the range of 1.1-1.5 and observed  $M_n$  being consistent with the theoretical molecular weight for the corresponding feed ratios.

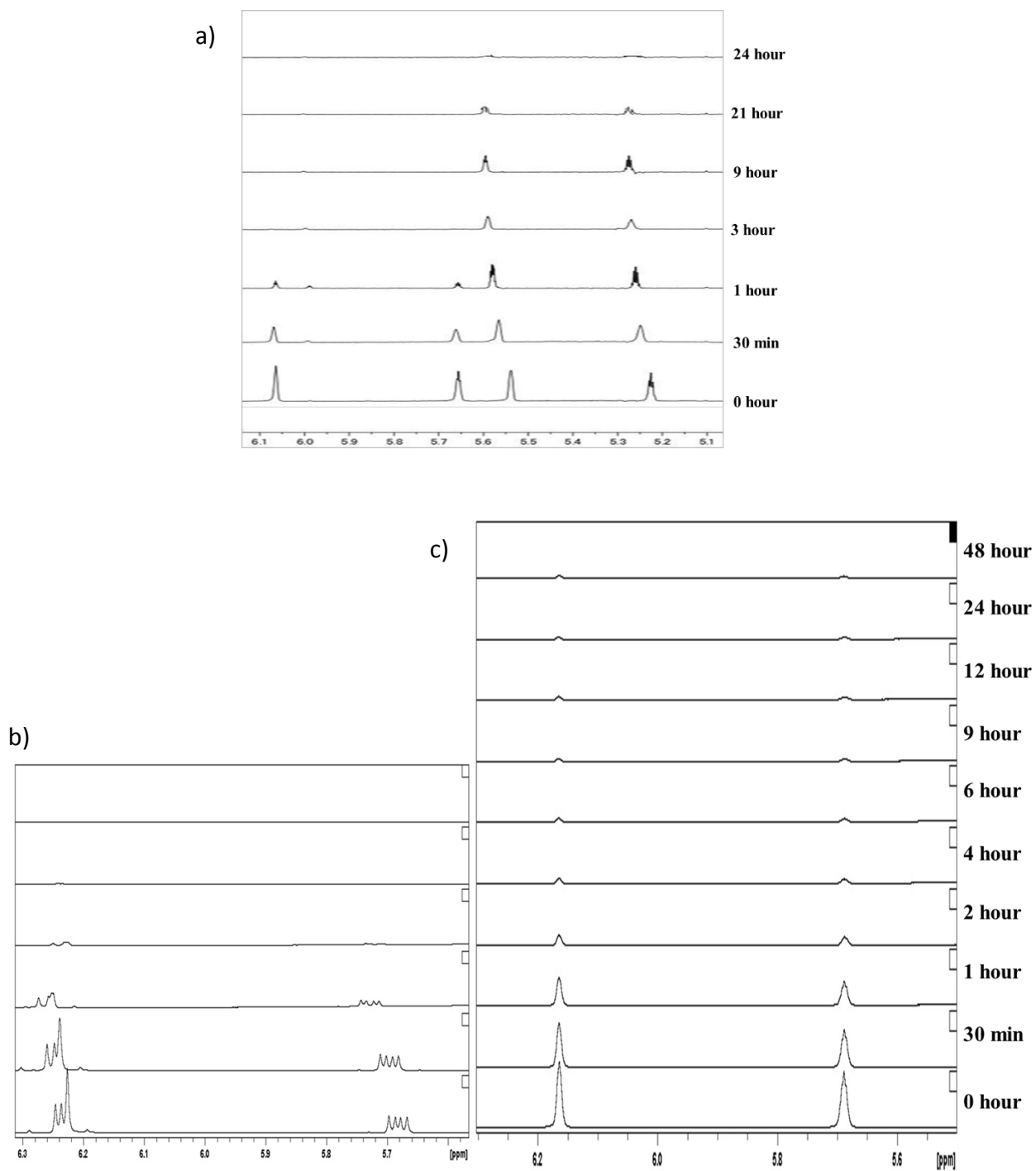


**Figure 3.6.** Time dependent  $^1\text{H}$ -NMR of b) poly-SPB and c) poly-CMB in  $\text{D}_2\text{O}$ .

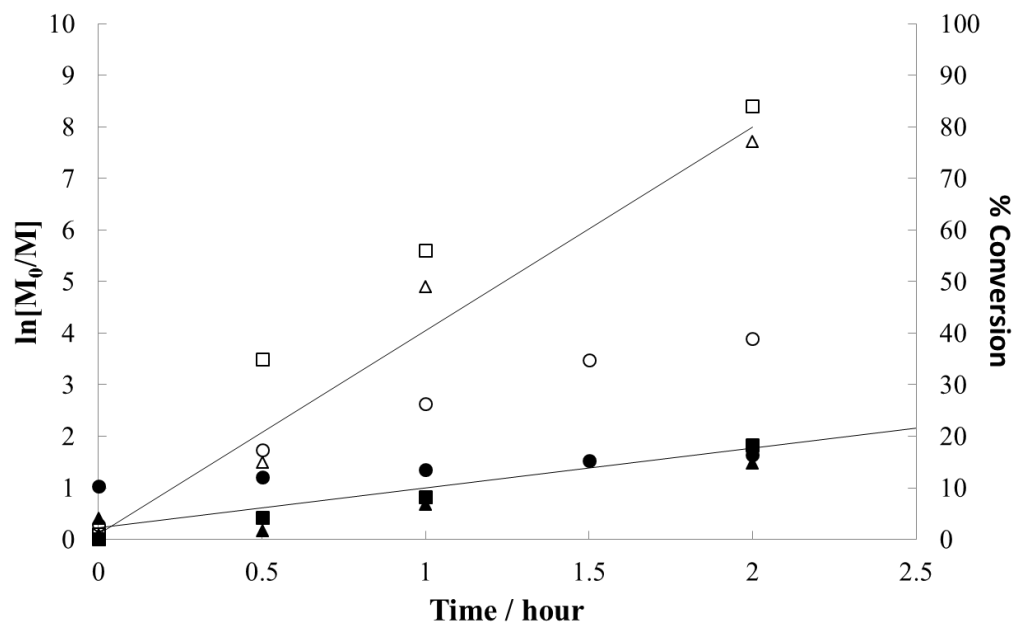


**Figure 3.7.** Kinetic plot for the polymerization of poly-(MAA-DMAEMA), poly-SPB and poly-CMB by RAFT polymerization, followed by  $^1\text{H}$  NMR spectroscopy in  $\text{D}_2\text{O}$ .



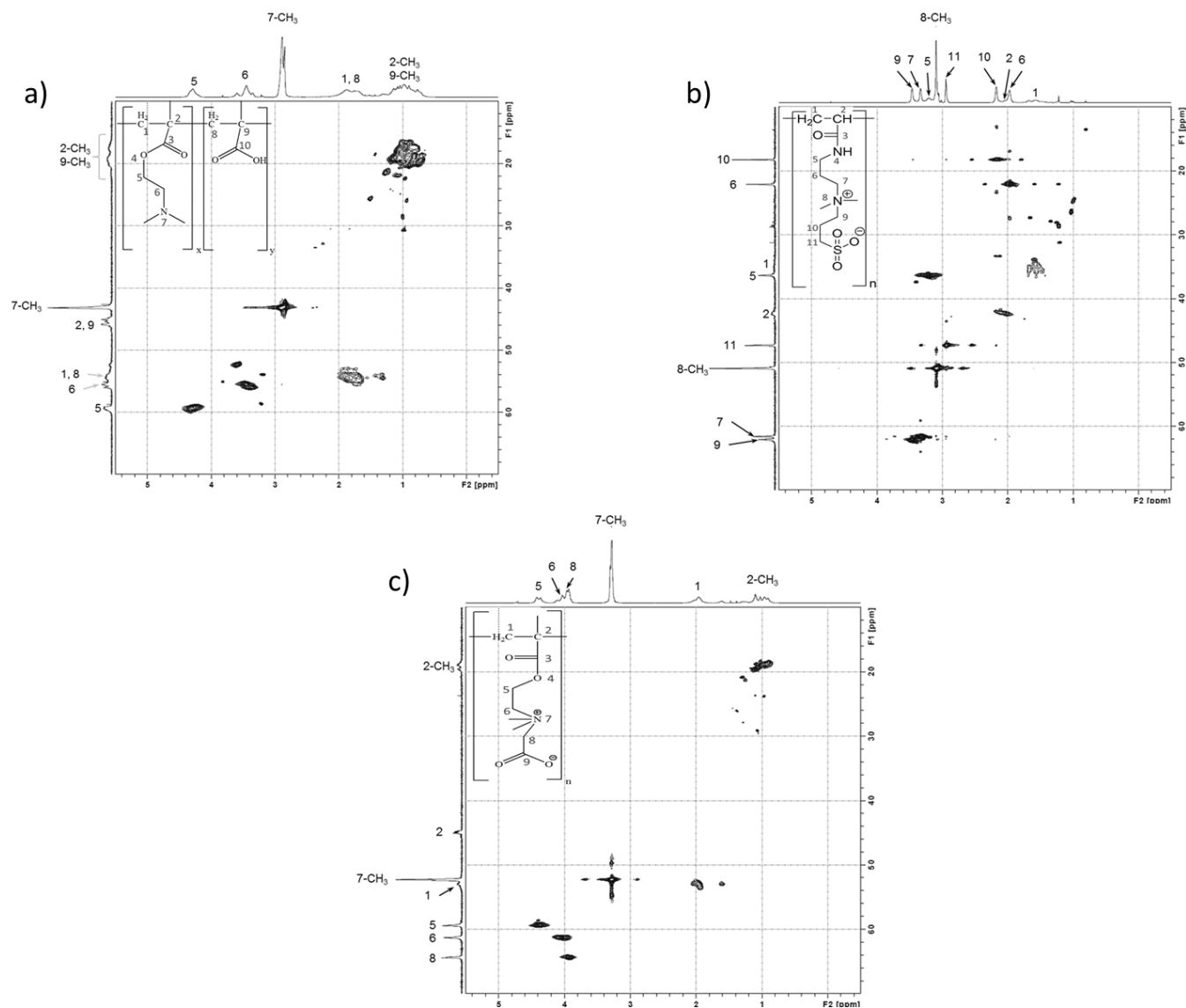


**Figure 3.8.** NMR signal assignment of a) poly-(MAA-DMAEMA), b) poly-SPB and c) poly-CMB in  $D_2O$  (900 MHz).

**Table 3.1.** Characteristics of various polyampholytes prepared via RAFT polymerization.  
a) Determined by  $^1\text{H-NMR}$ , b) [monomer]:[initiator]:[RAFT agent]

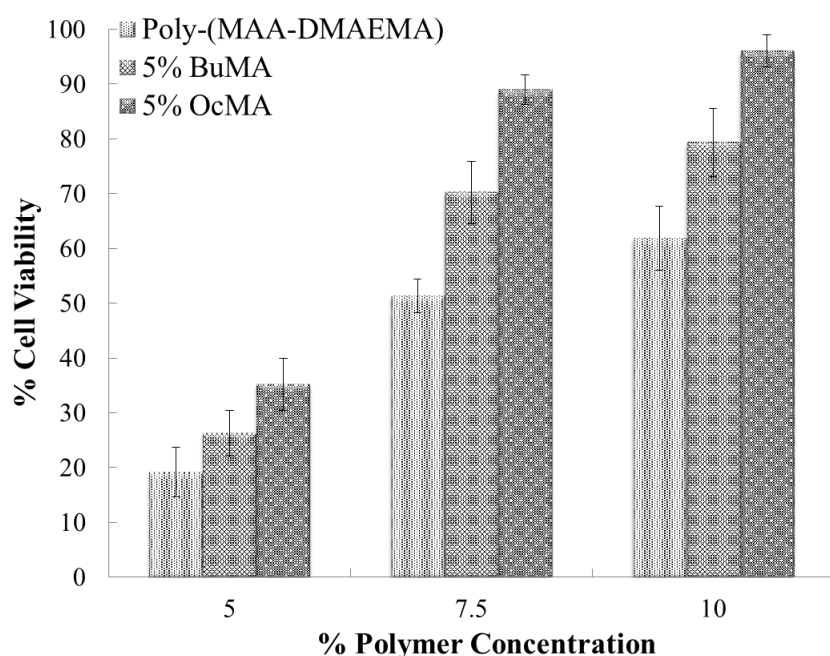
Entry		Composition				Molar ratio <sup>b</sup>	$M_n \times 10^{-3}, ^c$	$M_w/M_n ^c$
		DMAEMA	MAA	Bu-Ma	Oc-Ma			
1	In Feed	50	50	0	0	100:1:5	4.8	1.21
	In Polymer <sup>a)</sup>	50.3	49.7	0	0			
2	In Feed	49	49	2	0	102:1:5	4.9	1.32
	In Polymer <sup>a)</sup>	49.3	48.7	2.0	0			
3	In Feed	47.5	47.5	5	0	105:1:5	5.05	1.36
	In Polymer <sup>a)</sup>	47.7	47.3	5.0	0			
4	In Feed	49	49	0	2	102:1:5	4.95	1.23
	In Polymer <sup>a)</sup>	49.4	48.6	0	2.0			
5	In Feed	47.5	47.5	0	5	105:1:5	5.36	1.32
	In Polymer <sup>a)</sup>	47.6	47.5	0	4.9			

Entry		Composition				Molar ratio <sup>b</sup>	$M_n \times 10^{-3}, ^c$	$M_w/M_n ^c$
		SPB	CMB	Bu-Ma	Oc-Ma			
6	In Feed	100	0	0	0	100:1:5	5.5	1.18
	In Polymer <sup>a)</sup>	100	0	0	0			
7	In Feed	98	0	2	0	102:1:5	5.7	1.29
	In Polymer <sup>a)</sup>	98.6	0	1.4	0			
8	In Feed	95	0	5	0	105:1:5	6.0	1.42
	In Polymer <sup>a)</sup>	96.1	0	3.9	0			
9	In Feed	98	0	0	2	102:1:5	5.7	1.34
	In Polymer <sup>a)</sup>	98.3	0	0	1.7			
10	In Feed	95	0	0	5	105:1:5	6.1	1.37
	In Polymer <sup>a)</sup>	95.9	0	0	4.1			
11	In Feed	0	100	0	0	100:1:5	4.1	1.32
	In Polymer <sup>a)</sup>	0	100	0	0			
12	In Feed	0	98	2	0	102:1:5	4.3	1.44
	In Polymer <sup>a)</sup>	0	98.4	1.6	0			
13	In Feed	0	95	5	0	105:1:5	4.6	1.39
	In Polymer <sup>a)</sup>	0	96	4	0			
14	In Feed	0	98	0	2	102:1:5	4.4	1.41
	In Polymer <sup>a)</sup>	0	98.3	0	1.7			
15	In Feed	0	95	0	5	105:1:5	4.6	1.49
	In Polymer <sup>a)</sup>	0	95.9	0	4.1			

### 3.3.1 Cryopreservation

L929 cells were cryopreserved with different polymers in DMEM solution without FBS. Fig. 3.9 shows the effect of concentration and hydrophobicity of Poly-(MAA-DMAEMA) on cell viability after cryopreservation. Result unambiguously suggested that this polymer has excellent cryoprotective property and its efficiency was found to increase with increasing polymer concentration. Incorporation of hydrophobicity by virtue of BuMA and OcMA enhanced viability significantly with cell viability reaching a value of around 96 % at 10 % polymer concentration of poly-(MAA-DMAEMA) with 5 % OcMA. Cell viability observed after OcMA substitution was higher than in the case of BuMA substitution. This can be explained by the fact that OcMA contains bigger alkyl chain (more hydrophobic) than BuMA. So this confirms the fact that the introduction of hydrophobicity to poly-(MAA-DMAEMA) significantly amplifies cell viability values.



**Figure 3.9.** Cryoprotective properties of poly-(MAA-DMAEMA) and the effect of hydrophobicity. L929 cells were cryopreserved with MAA-DMAEMA copolymer with different polyampholytes at various concentrations. Data are expressed as mean  $\pm$  SD for 3 independent experiments (5 samples each).

To ascertain the relationship between polymer structure and the cryoprotective behavior, we developed two structurally similar zwitterionic polymers, poly-SPB and poly-CMB and compared

their cryoprotective property with poly-(MAA-DMAEMA). Fig. 3.10a shows that poly-SPB displays lesser cell viability than poly-(MAA-DMAEMA) and even at 15 % concentration; it shows only around 65 % cell viability. Poly-CMB on the other hand shows very weak to almost no cryoprotective properties, at 15 % concentration, it showed only around 4 % viability. So these results points to the fact that poly-(MAA-DMAEMA) shows exceptionally high cryoprotective property, whereas poly-SPB shows intermediate property and poly-CMB doesn't show any property. Moreover, Fig 3.10b shows that unlike Poly-(MAA-DMAEMA), introduction of hydrophobicity to poly-SPB and poly-CMB did not have any effect on the cell viability. From all the results, it was evident that not all polyampholytes possess cryoprotective property, which indicated that there must some molecular mechanisms behind it. Detailed discussion of this behavior is given in the succeeding sections.

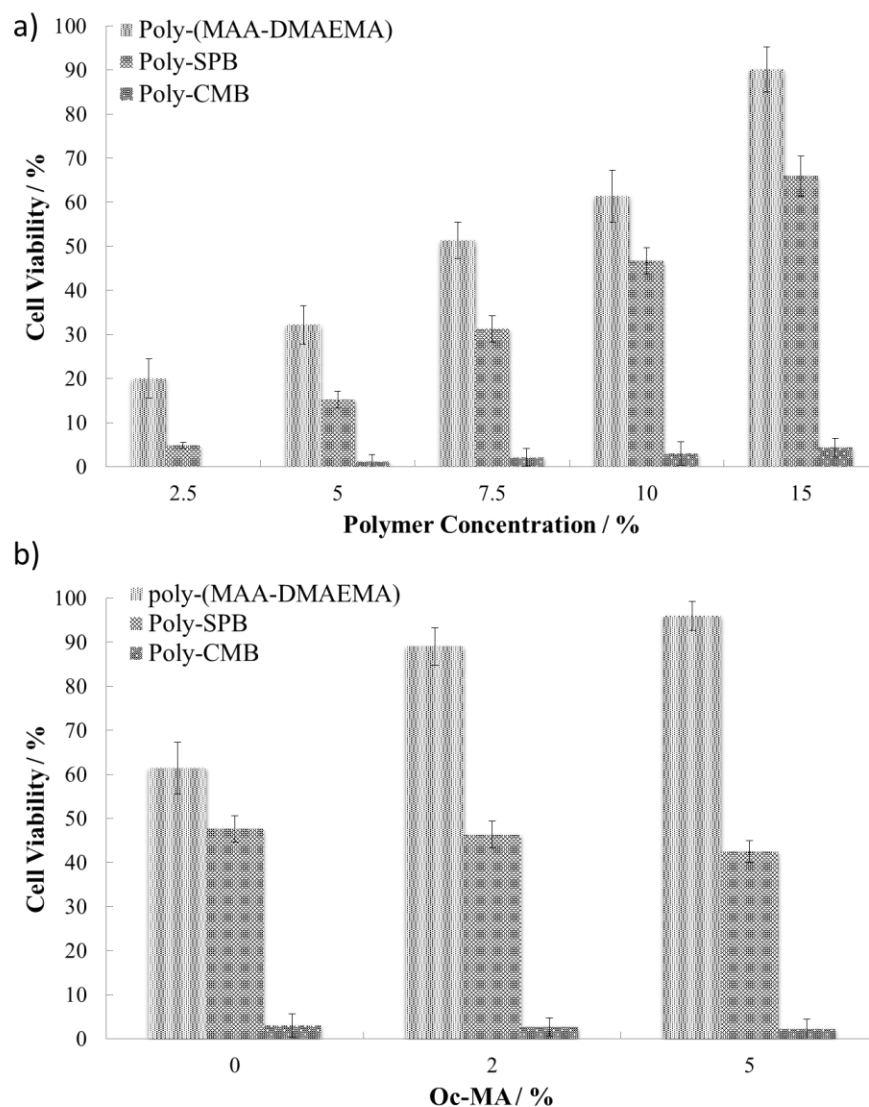


**Figure 3.10.** Cryoprotective properties of poly-(MAA-DMAEMA), poly-SPB and poly-CMB a) at various polymer concentration and b) with different concentration of OcMA at 10 % polymer concentration. L929 cells were cryopreserved with different polyampholytes at various concentrations. Data are expressed as mean  $\pm$  SD for 3 independent experiments (5 samples each).

### 3.3.2 DSC

Liposomes can exist in either gel state (lower temperature) or in a liquid state (higher temperature). In the gel state, they are tightly held by van der Waals forces. Phospholipids cooperatively melt at the inception of phase transition temperature and transforms to the liquid state, where they are more loosely held due to weaker van der Waals interaction between acyl chains.<sup>28</sup> Moreover, lateral expansion of the acyl chains and weaker interaction of polar head groups is also a reason for this weaker association in the liquid state. As a consequence of which, nature of the gel-liquid crystalline phase transition temperature is largely due the length of the acyl chain and the nature of phospholipid headgroup.<sup>29</sup>

From the results of DSC (Fig. 3.11a), it can established that polyampholytes depress the bilayer gel to liquid-crystalline transition temperature of EPC. Polyampholytes cause a depression in the transition temperature with increasing concentration of polyampholytes leading to lower transition temperature. Poly-(MAA-DMAEMA) shows a steep decrease in phase transition of EPC with a decrease of more than 6° C at polymer: lipid mass of 0.25 (Fig. 3.11b). Poly-CMB on the other hand showed lesser decrease in transition temperature. Previous studies by Crowe et al. suggested that establishment of interactions results in the depression of the gel to liquid-crystalline phase transition temperature.<sup>30</sup> This shows that poly-(MAA-DMAEMA) has a far greater interaction with the cell membrane and this may a result of an increase in spacing between the lipids in the presence of poly-(MAA-DMAEMA) which facilitates more number of gauche conformers in the fatty acyl chains.<sup>31</sup>

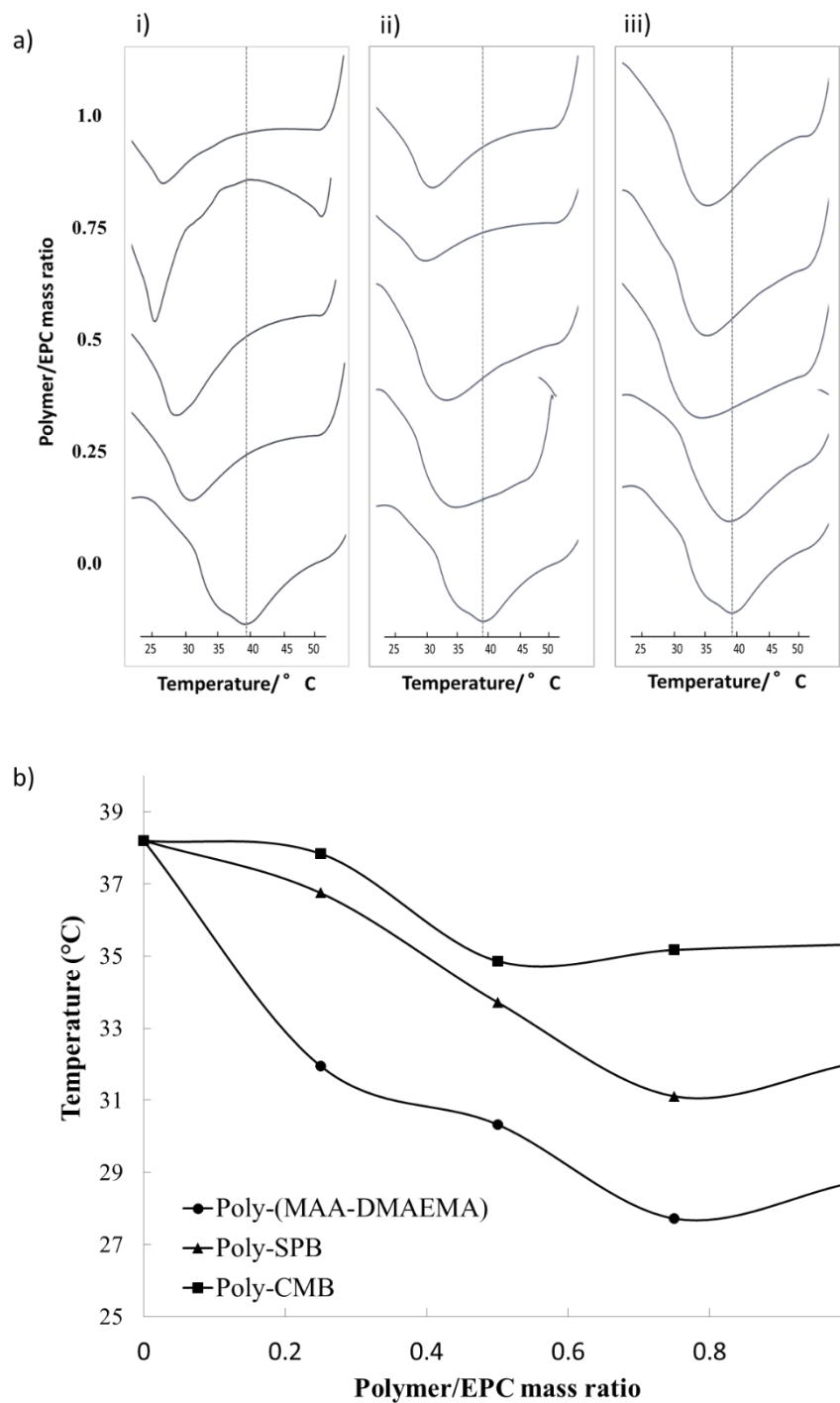


**Figure 3.11.** a) DSC heating thermograms of EPC liposomes in the presence of different amounts of i) poly-(MAA-DMAEMA), ii) poly-SPB and iii) poly-CMB. The resulting Polymer/EPC mass ratios are indicated to the right of each trace and b) Effects of poly-(MAA-DMAEMA), poly-SPB and poly-CMB on gel to liquid-crystalline transition temperature of EPC at Polymer/EPC mass ratios between 0 and 1.0.

To further investigate the detailed interactions between the polyampholytes and membrane, ESR studies was carried out.

### 3.3.3 Electron Spin Resonance Spectroscopy

ESR has greater sensitivity than NMR because of greater magnetic moment of electrons compared to the nucleus. ESR can be used to study to fast dynamics. Biological systems, including membranes, lack unpaired electrons, so they cannot be investigated by ESR in their native states.<sup>32</sup> This was overcome by spin labelling the membranes by incorporating spin-bearing probes.

The effect of the polyampholytes on the polar region of the membrane during freezing was investigated by ESR studies of the freeze-thawed 5-DSA liposomes supplemented with polymers of different concentrations. Fig. 3.12a revealed that poly-(MAA-DMAEMA) interacts with the outer surface of the membrane, indicated by a significant decrease in order parameter. Poly-SPB also showed a similar effect with a considerable interaction with membrane surface. On the other hand, poly-CMB did not exhibit a large decrease in the order parameter value signifying very less interaction with the cell surface (Fig. 3.12b). Interaction of poly-(MAA-DMAEMA) may be due to the electrostatic interaction with the membrane, whereas in the case of poly-CMB and poly-SPB, the major difference is the basicity, carboxylate group in poly-CMB is a stronger base than that of the sulfonate group of poly-SPB and as such, the carboxylate group in poly-CMB becomes non-ionic by lowering pH.<sup>33, 34</sup> Therefore, poly-SPB interacts strongly with the membrane electrostatically whereas poly-CMB does not. The ESR spectrum of the hydrophobic derivative of poly-(MAA-DMAEMA) showed lower interaction due to the effect of the hydrophobic part attached to it.



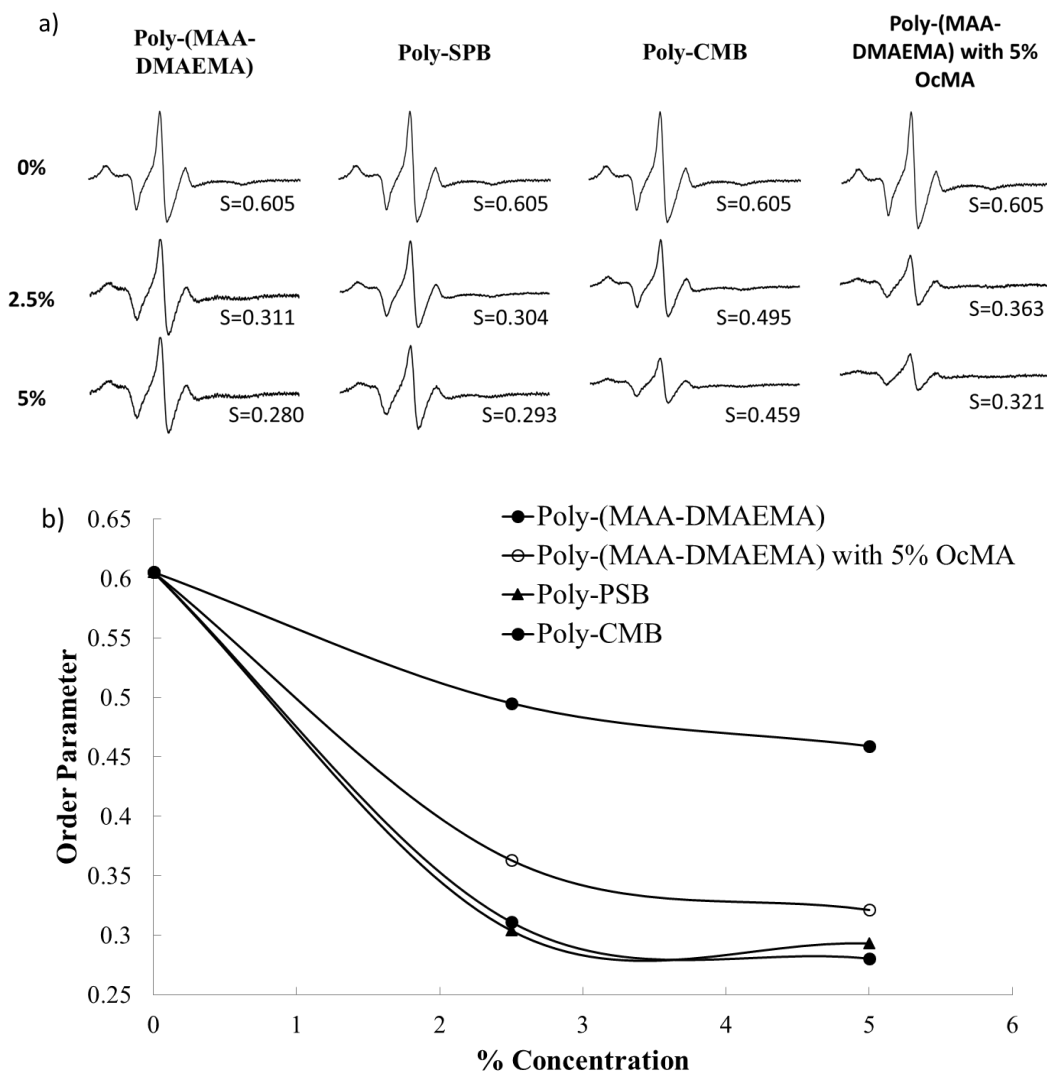


**Figure 3.12.** a) ESR spectra of 5-DSA (1 mol %) incorporated in EPC in the presence of various polymers at different polymer concentrations. Numbers below denote the order parameter ( $S$ ) and b) Polyampholyte concentration dependence of order parameters  $S$  for 5-DSA (1 mol %) intercalated into unilamellar dispersions of EPC in PBS buffer (pH 7.4).

Incorporation of 16-DSA to the membrane showed that all the three polymers do not interact with the hydrophobic region of the membrane, which is represented by almost no change in the correlation time (Fig. 3.13a). This indicated that these polymers are not present in this region. However, poly-(MAA-DMAEMA) with 5 % Oc-MA exhibited an increase in the correlation time (Fig. 3.13b), implying that this polymer shows significant interaction with the probe which is present hydrophobic core of the membrane. This could be attributed to its penetration or

localization in this region. This is supported from previous reports which revealed that hydrophobic drugs penetrate the cell membrane, whereas their hydrophilic counterparts do not.<sup>35-38</sup> Similar observations were obtained where tocopheryl polyethylene glycol succinate-coated poly(D,L-lactide-co-glycolide) nanoparticles showed greater penetration into the dipalmitoylphosphatidylcholine (DPPC) lipid membrane than polyvinyl alcohol-coated poly(D,L-lactide-co-glycolide).<sup>39</sup> Another study with polyampholytes revealed that introduction of hydrophobicity to polyampholytes facilitated adsorption onto the cell membrane and subsequent penetration.<sup>40</sup> Investigation of the change in correlation time with respect to different hydrophobic polyampholytes was also carried out. Fig. 3.14 shows that hydrophobic derivative of poly-(MAA-DMAEMA) shows the maximum deviation in correlation time values, whereas, not much change was observed in the case of poly-SPB, which could be attributed to relatively high water solubility (hydrophilicity) which was observed in poly-SPB with 5 % OcMA when compared to the corresponding hydrophobic poly-(MAA-DMAEMA). Poly-CMB with 5 % OcMA showed almost no change in correlation time value. This is because the introduction of BuMA or OcMA in the case of poly-SPB and poly-CMB did not enhance hydrophobicity significantly. Previous report by Smith and McCormick suggest that hydrophobicity increases with the increase in viscosity in aqueous polymer solutions.<sup>41</sup> Therefore, we carried out viscosity measurements (TVE-22, TOKI SANGYO CO., LTD., Tokyo, Japan) to scrutinize the hypothesis (Table 3.2), which confirmed that even with the addition of BuMA and OcMA, hydrophobicity did not increase sufficiently in the case of poly-CMB and poly-SPB, in particular, to manifest any significant changes in the correlation times.

**Table 3.2.** Polymer contact angle and viscosity of various polymers with and without their hydrophobic derivatives at 2.5 % polymer concentration.

Polymer	Viscosity (mPa.s)		
		BuMA	OcMA
<b>Poly-(MAA-DMAEMA)</b>	1.25 ± 0.02	1.30 ± 0.03	1.41 ± 0.02
<b>Poly-SPB</b>	0.999 ± 0.04	1.024 ± 0.03	1.032 ± 0.06
<b>Poly-CMB</b>	1.076 ± 0.1	1.148 ± 0.15	1.173 ± 0.18

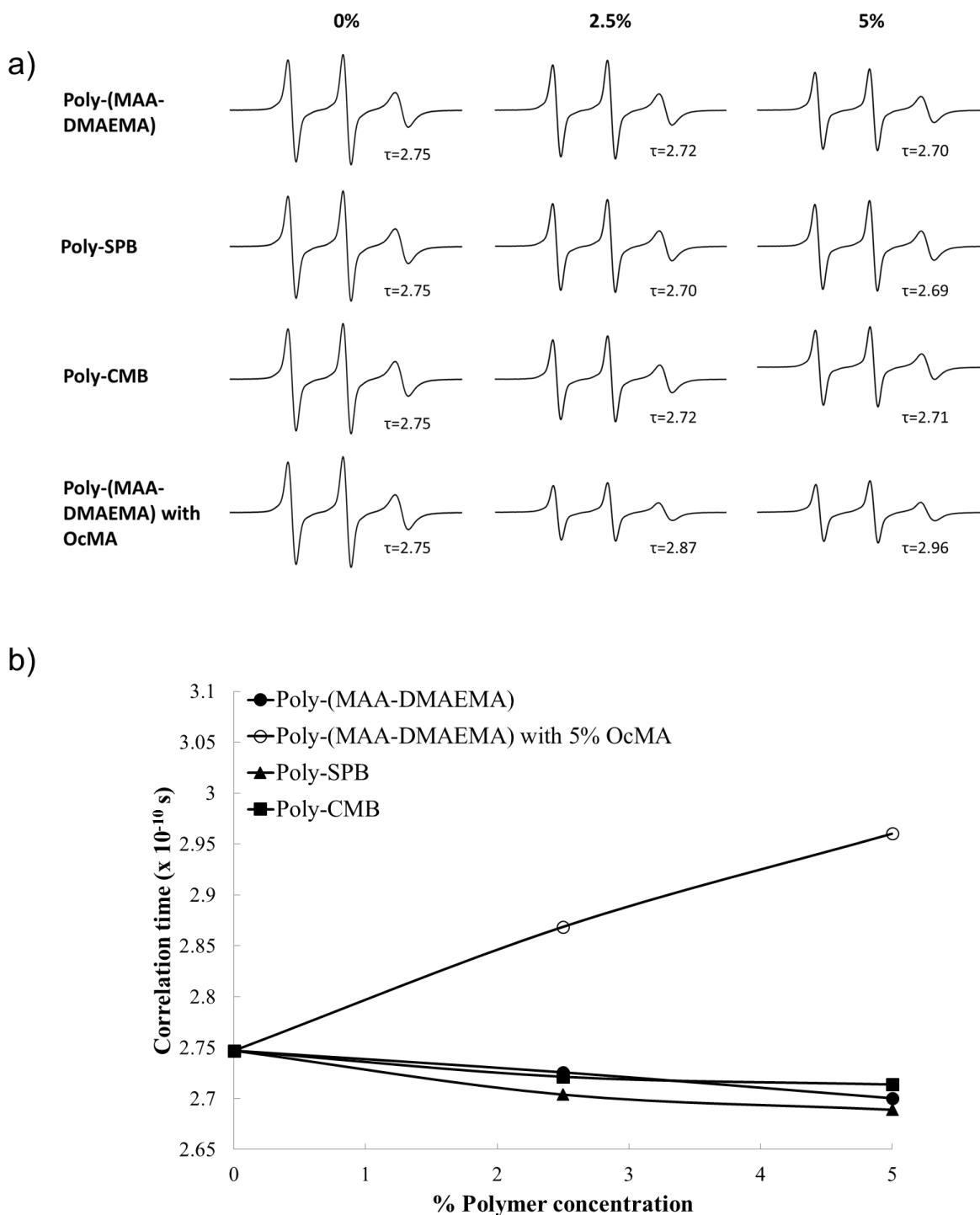


**Figure 3.13.** a) ESR spectra of 16-DSA (1 mol %) intercalated in EPC in the presence of various polymers at different polymer concentrations. Numbers below denote the correlation time ( $\tau$ ) and b) Polyampholyte concentration dependence of correlation time  $\tau$  for 16-DSA (1 mol %) intercalated into unilamellar dispersions of EPC in PBS buffer (pH 7.4).

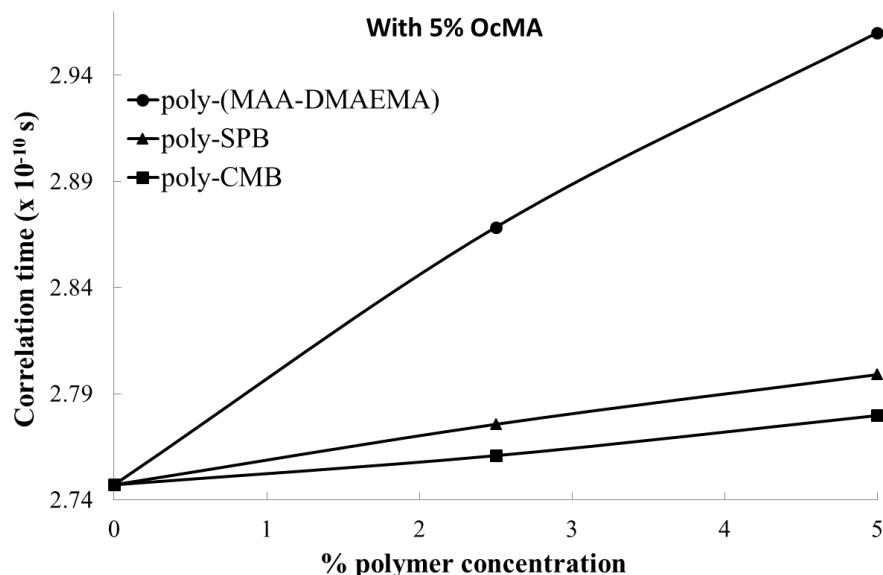


**Figure 3.14.** Hydrophobic polyampholytes (with 5 % OcMA) concentration dependence of correlation time  $\tau$  for 16-DSA (1 mol %) intercalated into unilamellar dispersions of EPC in PBS buffer (pH 7.4).

A schematic representation of the localization of different polyampholytes around cell membrane is presented in Fig. 3.15. Poly-SPB is present near the polar (hydrophilic) head region of the membrane. This was supported by the fact that a significant decrease in the order parameter of 5-DSA in the lipid bilayer was observed in the presence of poly-SPB. Apart from the electrostatic interaction, this may also be due to its extremely high hydrophilicity. Poly-(MAA-DMAEMA) is also placed near the polar region, suggested by a decrease in the order parameter, but is positioned slightly lower than poly-SPB, owing to its higher relative hydrophobicity. This was also supported by the observation that hydrophobic derivative poly-SPB disturbs correlation time to a greater extent as compared to poly-SPB. On the other hand, poly-(MAA-DMAEMA) with OcMA positions itself near the hydrophobic tail of the lipid membrane.

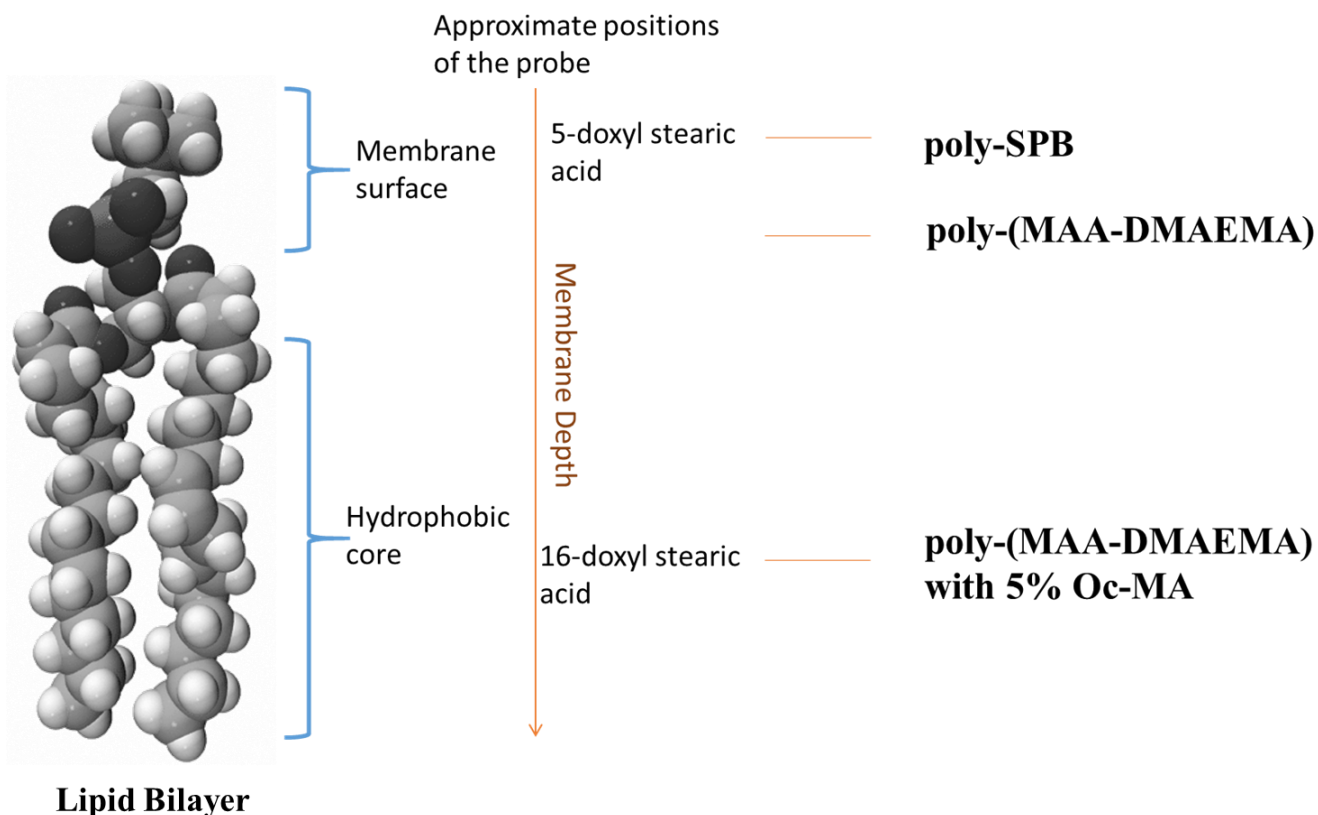


**Figure 3.15.** Schematic representation of membrane-polyampholyte interaction/localization.

From DSC and ESR studies, it has been established that cryoprotective polymers show greater interaction with cell membrane. This interaction might protect membrane from various freezing induced damages such as physical (mechanical) damage from ice recrystallization and chemical osmotic damages. To validate this, ice recrystallization inhibition studies were carried out using polyampholytes.

### 3.3.4 Ice recrystallization inhibition

Ice formation is not a desirable outcome during cryopreservation. Both intracellular and extracellular ice formation are extremely fatal to cells. Extracellular ice formation leads to mechanical damage to the cells and at the same time causes osmotic shock as a result of freezing of ice which leads to increase in concentration of extracellular solutes.<sup>42</sup> During the freezing process, small ice crystals are transformed into larger crystals by a process known as ice recrystallization. Recrystallization occurs because smaller ice crystals (which have bigger

curvature) tend to have lower melting point and hence melts at a higher annealing temperature (Kelvin effect). This released liquid water move to a neighboring (larger) ice crystal and refreezes and this new ice crystal will have higher melting point, which subsequently results in a matrix with more ice crystals which are larger in size.<sup>43</sup> Ice recrystallization damages cells and tissues during thawing due to membrane rupture and cell dehydration.<sup>44</sup> Splat cooling assay has been used by metallurgists for measuring recrystallization for years, but this technique was first employed to cryobiology by Knight et al.<sup>45</sup> This technique is usually used to determine the ice recrystallization inhibition (IRI) activity of any compound (Fig. 3.16a). Gibson and his co-workers have done extensive studies on ice recrystallization inhibit activity of polymers, including polyampholytes.<sup>26, 46-51</sup>

In the present study, we have employed modified splat assay. Fig. 3.16b depicts example micrograph of ice crystal wafer grown on PBS solution alone and a hydrophobic polyampholyte, poly-(MAA-DMAEMA) with 5 % BuMA. It can be clearly seen that the size of the ice crystals in the case of hydrophobic polymer is far smaller than when PBS is used.

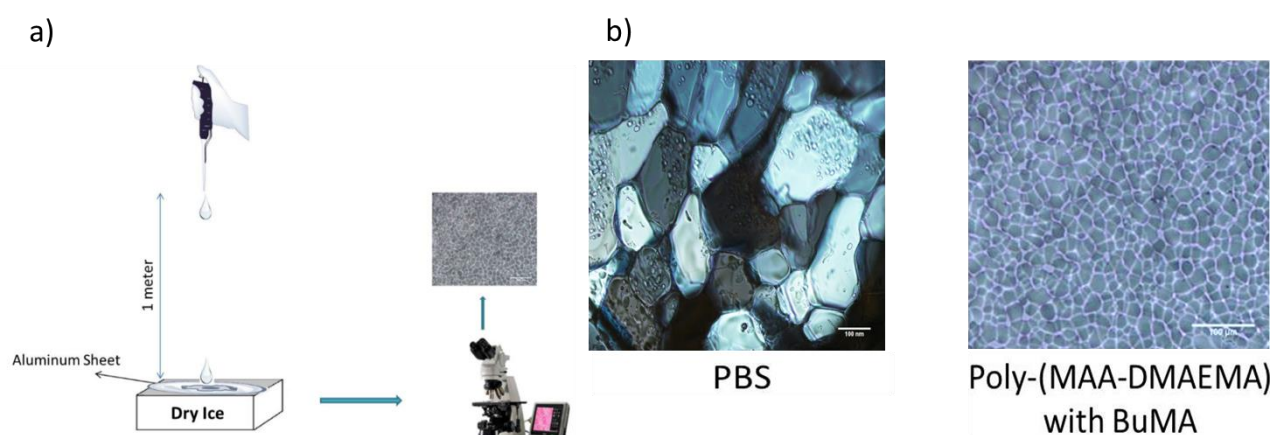


**Figure 3.16.** a) Schematic representation of the splat assay; b) Micrographs of poly-nucleated ice crystals in PBS alone and in the presence of poly-(MAA-DMAEMA) with BuMA, after 30 minutes annealing at  $-6^{\circ}\text{C}$  (scale bars =  $100\text{ }\mu\text{m}$ ).

Fig. 3.17 shows that all the three polyampholytes show IRI activity to a certain degree. This was supported by a previous report by Vorontsov et al., which argued that polyampholyte COOH-PLL also exhibits antifreeze property.<sup>52</sup> They also investigated the mechanism and found out that its antifreeze property is related to the hysteresis of growth rate and depression of freezing

point. They argued that in the event of ice crystallization, a non-steady-state behavior is displayed during the adsorption of large biological molecules and its rate is relatively slower than the process of embedding of crystal growth units. However, with the addition of hydrophobic monomer (BuMA), the size of the ice crystals reduced significantly in the case of poly-(MAA-DMAEMA), whereas no significant difference was observed in the case of poly-CMB and poly-SPB, which is again attributed to the low hydrophobicity of the BuMA and OcMA derivate of poly-SPB and poly-CMB (Table 3.2). This observation is also supported by ESR results. This behavior was corroborated by a report which showed that charge balance of polyampholytes is of foremost importance and mixtures with 1:1 ratio of cationic and anionic parts shows higher IRI activity. Additionally, they also suggested that mixed charge side chain polymers have higher efficiency than zwitterionic polymers.<sup>51</sup> Increasing the amount of hydrophobicity further (by introducing OcMA) led to a further decrease in the size of the crystal with MLGS around 2.6 % in the case of poly-(MAA-DMAEMA) which implied that this polymer inhibit recrystallization of ice almost completely. This is supported by a previous study where they have shown that IRI activity is dependent upon the presence of long alkyl chains and increased hydrophobicity<sup>53, 54</sup> and presence of hydrophobic domains in important for IRI activity.<sup>45, 46</sup> These polymers are believed to act like antifreeze proteins which bind to ice crystals irreversibly and inhibit their growth.<sup>55</sup> Studies have shown that the presence of hydrophobic domains in antifreeze glycoproteins with amphipathic character helps to repel additional water molecules which led to higher activity.<sup>48, 56, 57</sup> Another study with type III antifreeze protein demonstrated that hydrophobic groups may be involved in the energetics of the protein–ice interaction.<sup>48</sup> Studies by Deller et al. showed that synthetic polymers enhance cryopreservation of different kinds of cells by reducing ice crystal growth during thawing.<sup>58</sup> So, we can conclude that increase in cell viability with the increase in hydrophobicity of poly-(MAA-DMAEMA) is linked to its high IRI activity. In other words, hydrophobicity only enhances cell viability. Since poly-CMB in itself do not possess any cryoprotective property, hence even with the increase in hydrophobicity, no effect was observed.



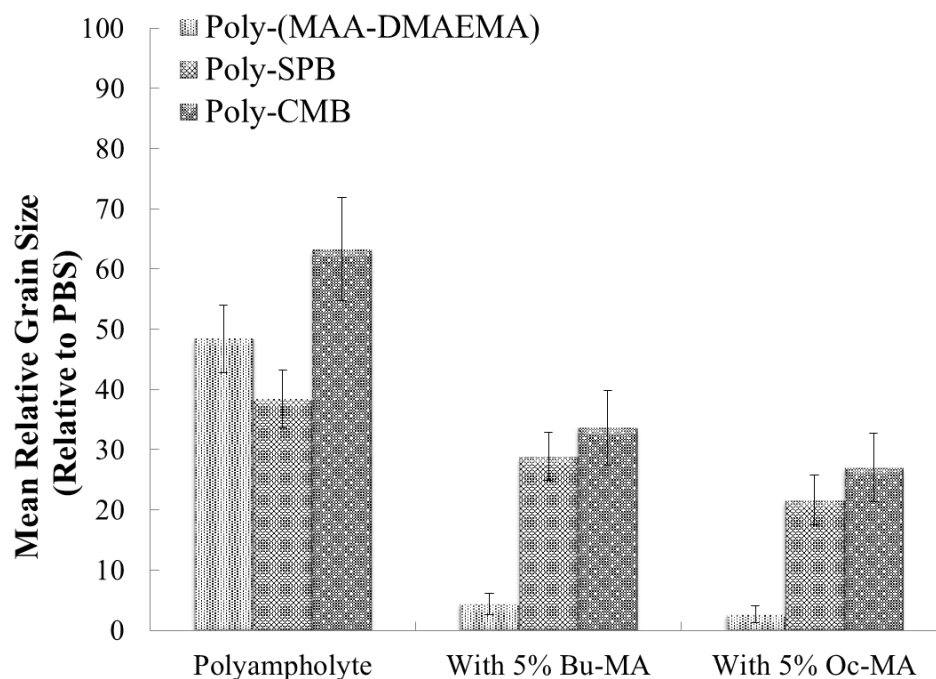


**Figure 3.17.** Ice recrystallization inhibition activity of poly-(MAA-DMAEMA), poly-SPB and poly-CMB and the effect of hydrophobicity at 10 % polymer concentration. Errors bars indicate the standard deviation of the mean.

After confirming that cryoprotective polymers interact more strongly with the cell membrane and this interaction is protective in nature, we intended to further validate this point by quantitatively analyzing the membrane damage after freezing in presence of different polymers.

### 3.3.5 Leakage Experiment

Fig. 3.18 shows that when no polyampholyte was added to the liposomes, maximum leakage was observed, due to the membrane damage/ lysis which resulted in the release of soluble marker (CF) enclosed in the liposome to the surrounding buffer. The leakage started to decrease with the addition of poly-(MAA-DMAEMA) and at 10 %, only around 35 % leakage was observed. This indicated that this polymer protect membrane during freeze-thaw process and the protection increases with increasing concentration of polymer. This is in good agreement with the cryopreservation results obtained with the same polymer. On the other hand, presence of poly-SPB also reduced the membrane leakage, but the extent of membrane protection was lesser



than poly-(MAA-DMAEMA). This again corresponds well with the cryopreservation results. Poly-CMB leads to very less reduction in leakage and no significant change was observed even with the increase in polymer concentration. This proves that poly-(MAA-DMAEMA) shows greatest membrane protection, followed by poly-SPB and poly-CMB do not exhibit any membrane protection ability. This explains the difference in the cryopreservation properties of different polyampholytes.

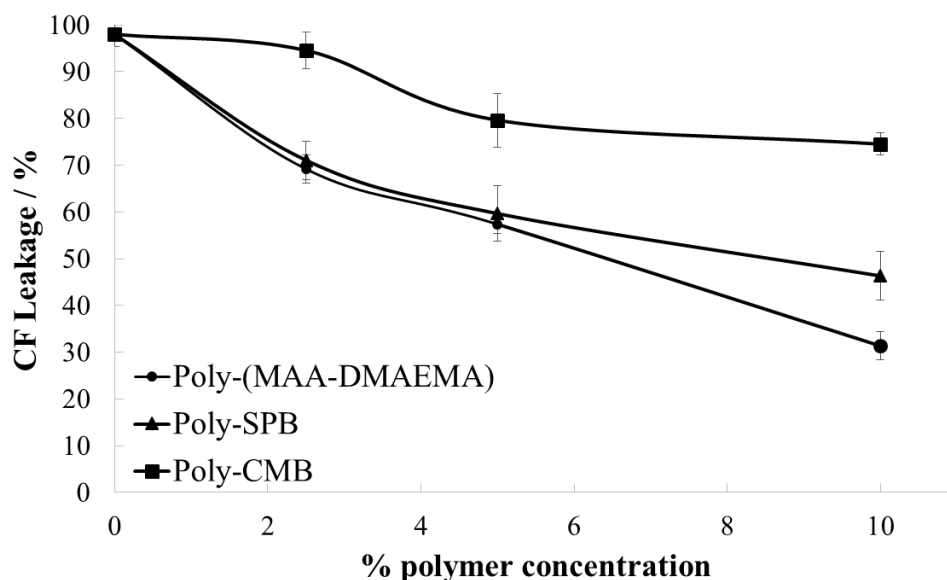


**Figure 3.18.** Protection of liposomes during freezing by different polyampholytes. CF leakage from liposomes cryopreserved with various polyampholytes solutions at different polymer concentrations. Data are expressed as the mean  $\pm$  SD for 3 independent experiments (5 samples each).

### 3.3.6 Polymer Chain Dynamics

Dynamic behavior of polymers is of particular importance, especially at low temperature, and there is a great relationship between molecular motion and structure. Molecular motion in polymers arises as a consequence of the interaction of thermal energy and cohesive forces between various fractions of the polymer chain. Interaction along chain as well as between adjacent chains is controlled by the structure of the polymer.<sup>59</sup>

Solid state NMR has the advantage that the orientation dependent (anisotropic) information is retained, as a result of which it can provide important information about packing arrangements,

molecular and supramolecular structure and also molecular dynamics. However, in solution NMR, anisotropic interactions are averaged by the rapid tumbling of molecules, whereas in solid state NMR, interactions like dipolar coupling and chemical shift dominates, which results in broadening of the spectral line width of nuclei in solids.<sup>60</sup> To solve this problem, magic angle spinning (MAS) NMR is applied. MAS involve rapidly rotating the sample about an axis oriented at  $54.7^\circ$  (magic angle) with respect to the external magnetic field (static field) which results in the suppression of anisotropic dipolar interactions (chemical shift broadening) by introducing artificial motions on the solid.<sup>61, 62</sup>

To elucidate the mechanism of cryopreservation, we studied the soluble state and mobility of the three different polymers by employing  $^1\text{H}$ -solid state NMR. In the case of poly-(MAA-DMAEMA), intact signals were observed initially at  $0^\circ\text{C}$ , and lowering the temperature resulted in the broadening of the peaks which led to decrease in the intensity of the peaks. After  $-20^\circ\text{C}$ , no peaks were detected (Fig. 3.19a). The disappearance of the peaks is due to intermolecular interactions among polymer chains and not due to precipitation. This interaction results in the formation of a possible reversible gel/matrix. So it can be hypothesized that the polymer forms soluble aggregates at very low temperature and traps water and salt and protects cells from stresses such as drastic changes in soluble space size and osmotic pressure at the temperatures at which cells are stored for cryopreservation. On the other hand, in the case of poly-SPB, although broadening of peaks were observed, but it was lesser than in the case of poly-(MAA-DMAEMA). At  $-20^\circ\text{C}$ , signals had a considerable intensity and even at  $-30^\circ\text{C}$ , signals persisted (Fig. 3.19b). So, the rate at which it forms soluble aggregates was lower than that of poly-(MAA-DMAEMA) and this could be linked to the lower cryoprotective efficiency of poly-SPB. When poly-CMB was analyzed, it was seen that almost all the peaks retained their mobility even at  $-40^\circ\text{C}$ , as a result of which it was unable to form reversible gel (Fig. 3.19c). This could be attributed to its extremely high propensity for cryopreservation. Here it was confirmed that cryoprotective polyampholytes act by forming a reversible gel which protects it from external factors.

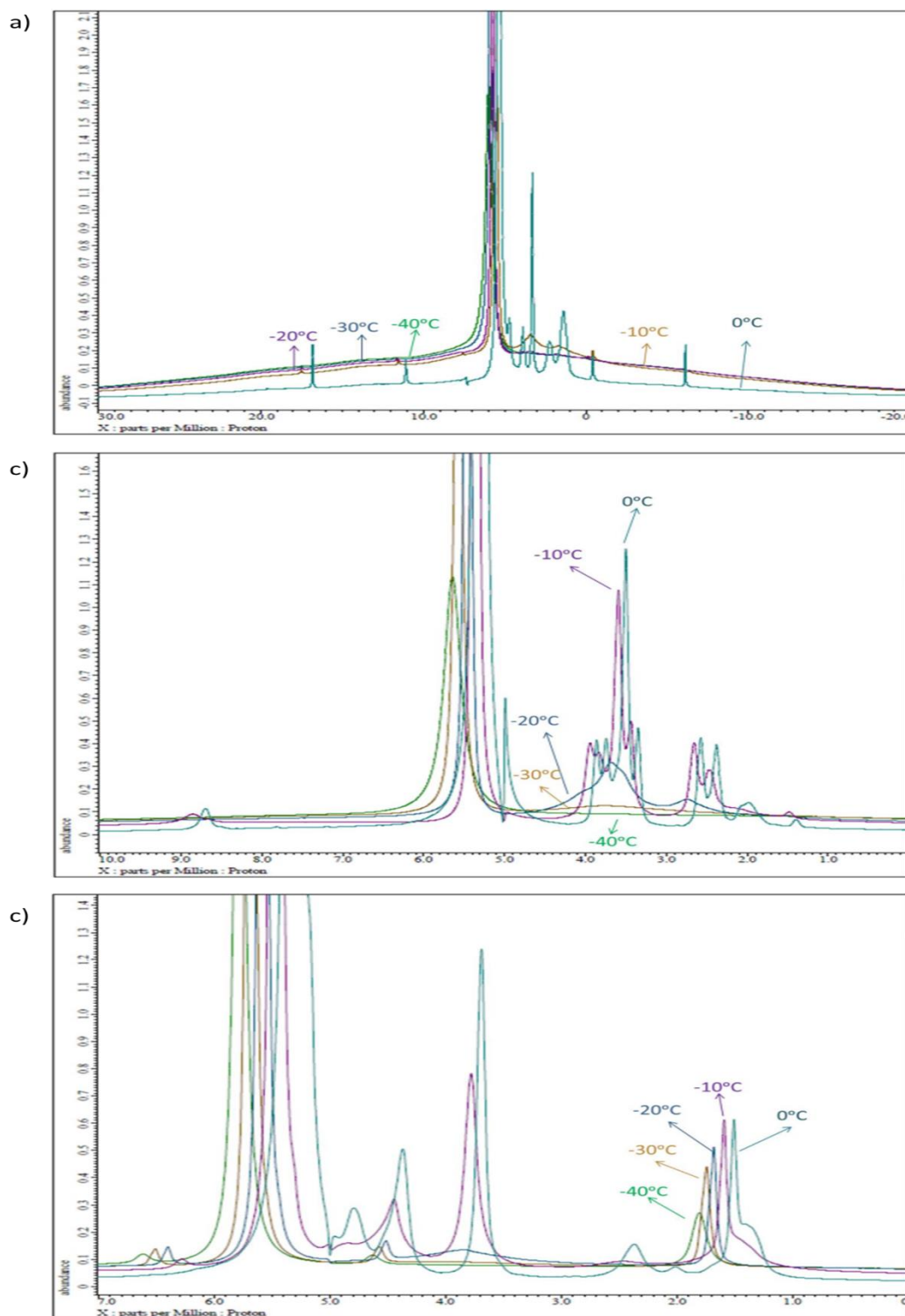


**Figure 3.19.**  $^1\text{H}$ -NMR spectra of a) poly-(MAA-DMAEMA), b) poly-SPB and c) poly-CMB in physiological saline solution (10 % w/v) during freezing.

### 3.4 Conclusion

In this study, we have demonstrated that synthetic polyampholytes can behave as excellent cryoprotective agents for cells, whose potential can be further augmented by supplementing the polyampholytes with small amount of hydrophobicity. Moreover, we also established that the mere presence of both the charges in a polymer is not sufficient enough to manifest cryoprotective property, polymer structure also influences its activity. This was indicated by the disparate cryoprotective property shown by different polyampholytes. This is due to the contrast in the interactions of different polymers with the cell membrane. Polymers showing higher cryoprotective properties showed greater interaction with the cell membrane, which was evident from the depression the phase transition temperature of the membrane and the greater penetration of the polymers inside the membrane. Membrane protection by cryoprotective polymers was further validated by the suppression of ice recrystallization (IRI activity), which is one of the primary reasons for membrane damage during cryopreservation. Hydrophobicity further enhances IRI activity. Leakage experiment confirmed the membrane protection during freezing directly affects the cryopreservation ability, with higher cryoprotective polymer showing greater membrane protection. Most importantly, we demonstrated that cryoprotective polymer acts by protecting cells from stresses such as drastic changes in soluble space size and osmotic pressure during freezing. Finally, the results show that synthetic polyampholytes can be tuned to be excellent CPAs where polymer structure and functionality determines their cryoprotective ability. Polymers cryopreserve cells by a synergistic effect where a lot of parameters are involved. With this study, mechanism of cryopreservation has been revealed which would enable for a more efficient molecular design of CPAs in future.

### 3.5 References

- 1 C. Polge, A. U. Smith and A. S. Parkes, A. S. *Nature*, 1949, **164**, 666.
- 2 J. E. Lovelock and M. W. Bishop, *Nature*, 1959, **183**, 1394–1395.
- 3 J. O. M. Karlsson and M. Toner, *Biomaterials*, 1996, **17**, 243-256.
- 4 M. E. Lynch and K. R. Diller, *Trans. ASME*, 1981, **81**, 229-232.
- 5 P. J. Mazur, *Gen. Physiol.*, 1963, **47**, 347-369.
- 6 D. Gao, J. K. Critser, *ILAR J.*, 2000, **41**, 187-196

- 7 H. Woelders, A. Matthijs and B. Engel, *Cryobiology*, 1997, **35**, 93–105.
- 8 P. Mazur, S. Leibo, J. Farrant, E. Chu, M. Hanna and L. Smith, Interactions of cooling rate, warming rate and protective additive on the survival of frozen mammalian cells. In *Ciba Foundation Symposium - The Frozen Cell*; Wolstenholme G. E. W., O'Connor M, Eds.; John Wiley & Sons, Ltd.: Chichester, UK, 2008, pp 69-88.
- 9 D. E. Pegg and M. P. Diaper, *Biophys. J.*, 1988, **54**, 471–488.
- 10 J. B. Mandumpal, C. A. Kreck and R. L. Mancera, *Phys. Chem. Chem. Phys.*, 2011, **13**, 3839-3842.
- 11 G. Clapisson, C. Salinas, P. Malacher, M. Michallet, I. Philip and T. Philip, *Bull. Cancer*, 2004, **91**, E97-102.
- 12 K. Matsumura and S. H. Hyon, *Biomaterials*, 2009, **30**, 4842-4849.
- 13 K. Matsumura, J. Y. Bae and S. H. Hyon, *Cell Transplant.*, 2010, **19**, 691-699.
- 14 M. Jain, R. Rajan, S. H. Hyon and K. Matsumura, *Biomater. Sci.*, 2014, **2**, 308-317.
- 15 K. Matsumura, F. Hayashi, T. Nagashima and S. H. Hyon, *J. Biomater. Sci. Polym. Ed.*, 2013, **24**, 1484-1497.
- 16 K. Matsumura, J. Y. Bae, H. H. Kim and S. H. Hyon, *Cryobiology*, 2011, **63**, 76-83.
- 17 R. Rajan, M. Jain and K. Matsumura, *J. Biomater. Sci., Polym. Ed.*, 2013, **24**, 1767-1780.
- 18 K. Matsumura, F. Hayashi, T. Nagashima and S. H. Hyon, *Cryobiol. Cryotechnol.*, 2013, **59**, 23–28.
- 19 R. C. MacDonald, R. I. MacDonald, B. P. M. Menco, K. Takeshita, N. K. Subbarao and L. R. Hu, *Biochim. Biophys. Acta.*, 1991, **1061**, 297–303.
- 20 C.-S. Lai and J. S. Schutzbach, *FEBS Lett.*, 1986, **203**, 153-156.
- 21 S. R. Wassall, T. M. Phelps, M. R. Albrecht, C. A. Langsford and W. Stillwell, *Biochim. Biophys. Acta, Biomembr.*, 1988, **939**, 393-402.
- 22 J. J. Yin, M. J. Smith, R. M. Eppley, S. W. Page and J. A. Sphon, *Biochim. Biophys. Acta, Biomembr.*, 1998, **1371**, 134-142.
- 23 J. Štrancar, In *ESR Spectroscopy in Membrane Biophysics*; Hemminga, M. A., Berliner, L. J., Eds.; Springer Science: New York, 2007; Chapter 3, 49–93.
- 24 M. I. Gibson, *Polym. Chem.*, 2010, **1**, 1141–1152.
- 25 F. Delaglio, S. Grzesiek, G. W. Vuister, G. Zhu, J. Pfeifer, A. Bax, *J. Biomol. NMR*, 1995, **6**, 277-293.

- 26 B. A. Johnson, *Methods Mol. Biol.*, 2004, **278**, 313-352.
- 27 H. Kitano, T. Kondo, T. Kamada, S. Iwanaga, M. Nakamura and K. Ohno, K. *Colloids Surf. B*, 2011, **88**, 455–462.
- 28 D. Q. Chapman, *Rev. Biophys.*, 1975, **8**, 185-235.
- 29 F. Szoka and D. Papahadjopoulos, *Annu. Rev. Biophys. Bioeng*, 1980, **9**, 467-508.
- 30 J. H. Crowe, F. A. Hoekstra and L. M. Crowe, *Annu. Rev. Physiol.* 1992, **54**, 579-599.
- 31 C. Cacela and D. K. Hinch, *Biophys. J.*, 2006, **90**, 2831–2842.
- 32 P. P. Borbat, A. J. Costa-Filho, K. A. Earle, J. K. Moscicki and J. H. Freed, *Science*, 2001, **291**, 266-269.
- 33 E. E. Kathmann and C. L. McCormick, *J. Polym. Sci., Part A: Polym. Chem.*, 1997, **35**, 231-242.
- 34 E. E. Kathmann and C. L. McCormick, *J. Polym. Sci., Part A: Polym. Chem.*, 2000, **35**, 243-253.
- 35 V. A. Levin, *J. Med. Chem.*, 1980, **23**, 682–684.
- 36 M. W. B. Bradbury, *Circ. Res.*, 1985, **57**, 213–222.
- 37 W. T. Cefalu and W. M. Pardridge, *J. Neurochem.*, **B**, **45**, 1954–1956.
- 38 A. Seelig, R. Gottschlich and R. M. Devant, *Proc. Natl. Acad. Sci. U. S. A.*, 1994, **91**, 68–72.
- 39 L. Mu and P. H. Seow, *Colloids Surf., B*, 2006, **47**, 90–97.
- 40 S. Ahmed, F. Hayashi, T. Nagashima, and K. Matsumura, *Biomaterials*, 2014, **35**, 6508-6518.
- 41 G. L. Smith and C. L. McCormick, *Macromolecules*, 2001, **34**, 918-924.
- 42 P. Mazur, *Am. J. Physiol.*, 1984, **247**, C125-C142.
- 43 C. A. Knight and J. G. Duman, *Cryobiology*, 1986, **23**, 256-262.
- 44 S. Zalis, M. B. Dolev and I. Braslavsky, *Cryobiology*, 2013, **67**, 438.
- 45 C. A. Knight, J. Hallett and A. L. D. Vries, *Cryobiology*, 1988, **25**, 55-60.
- 46 T. Congdon, R. Notman and M. I. Gibson, *Biomacromolecules*, 2013, **14**, 1578–1586.
- 47 R. C. Deller, T. Congdon, M. A. Sahid, M. Morgan, M. Vatish, D. A. Mitchell, R. Notman and M. I. Gibson, *Biomater. Sci.*, 2013, **1**, 478-485.
- 48 R. C. Deller, M. Vatish, D. A. Mitchell and M. I. Gibson, *Nat. Commun.*, 2014, **5**, 3244.
- 49 R. C. Deller, M. Vatish, D. A. Mitchell and M. I. Gibson, *ACS Biomater. Sci. Eng.*, 2015, **1**, 789–794.

- 50 T. Congdon, B. T. Dean, J. K. Wright, C. I. Biggs, R. Notman and M. I. Gibson, *Biomacromolecules*, 2015, **16**, 2820-2826.
- 51 D. E. Mitchell, M. Lilliman, S. G. Spain and M. I. Gibson, *Biomater. Sci.*, 2014, **2**, 1787-1795.
- 52 D. A. Vorontsov, G. Sazaki, S. H. Hyon, K. Matsumura and Y. Furukawa, *J. Phys. Chem. B*, 2014, **118**, 10240–10249.
- 53 C. J. Capicciotti, M. Leclere, F. A. Perras, D. L. Bryce, H. Paulin, J. Harden, Y. Liu and R. N. Ben, *Chem. Sci.*, 2012, **3**, 1408-1416.
- 54 A. K. Balcerzak, M. Febbraro and R. N. Ben, *RSC Adv.*, 2013, **3**, 3232-3236.
- 55 J. A. Raymond, A. L. DeVries, *Proc. Natl. Acad. Sci. U. S. A.*, 1977, **74**, 2589–2593.
- 56 Y. Tachibana, G. L. Fletcher, N. Fujitani, S. Tsuda, K. Monde and S. I. Nishimura, *Angew. Chem., Int. Ed.*, 2004, **43**, 856–862.
- 57 C. P. Garnham, R. L. Campbell and P. L. Davies, *Proc. Natl. Acad. Sci. U. S. A.*, 2011, **108**, 7363–7367.
- 58 F. D. Sönnichsen, C. I. DeLuca, P. L. Davies and B. D. Sykes, *Structure*, 1996, **4**, 1325–1337.
- 59 F. Heatley, Solid state NMR of polymers. In *Polymer International*; Mathias L. J. Eds.; Plenum Press: New York, 1991, vol. 30.
- 60 A. Alia, S. Ganapathy, H. J. M. D. Groot, *Photosynth. Res.*, 2009, **102**, 415–425.
- 61 E. R. Andrew, A. Bradbury, R. G. Eades, *Nature*, 1958, **182**, 1659.
- 62 I. J. Lowe, *Phys. Rev. Lett.*, 1959, **2**, 285–287.

## Chapter 4 ZWITTERIONIC POLYMER AS A NOVEL INHIBITOR OF PROTEIN AGGREGATION

### 4.1 Introduction

Protein instability is an ongoing challenge in the field of biopharmaceutics. With physical and chemical deterioration, protein aggregation is one of the foremost causes of protein instability.<sup>1</sup> Protein aggregation leads to an array of deleterious effects, including mitochondrial dysfunction and cell death, and can trigger serious neurodegenerative conditions such as Alzheimer's, Parkinson's, prion disease, and amyotrophic lateral sclerosis (ALS).<sup>2,3</sup> Protein aggregation involves formation of fibrous structures with a  $\beta$ -sheet conformation of misfolded proteins, known as amyloids.<sup>4</sup>

One cause of protein aggregation may be the physical association of protein molecules with each other. When changes in primary structure are involved, this is known as physical aggregation; when it is a result of new bond formation, it is known as chemical aggregation.<sup>1</sup> Both phenomena can occur simultaneously, leading to the formation of soluble or insoluble aggregates.<sup>5</sup>

One of the most commonly used and widely studied proteins is hen egg white lysozyme (HEWL). Its complete primary<sup>6</sup> and three-dimensional structures<sup>7</sup> are known; thus, it is also commonly used as a model system for aggregation studies. HEWL is a single polypeptide chain of 129 amino acid residues with four intramolecular disulphide bridges.<sup>8</sup> Many organic compounds (such as arginine,<sup>9-11</sup> proline,<sup>12</sup> and cyclodextrin<sup>13</sup>) and protein engineering techniques<sup>14</sup> have been used with some success to manage the refolding of proteins and inhibition of protein aggregation. Amphiphilic macromolecules have also been employed to inhibit amyloid formation for various proteins like HEWL.<sup>15</sup>

Polymers containing positive and negative groups (on different monomer units) are classified as polyampholytes<sup>16, 17</sup>. In contrast, zwitterionic polymers have anionic and cationic groups on the same monomer unit.<sup>18</sup> Due to the presence of a mixed charged state in zwitterionic polymers, they exhibit properties similar to those of proteins.<sup>19</sup>



Polyampholytes and zwitterionic polymers have unique antibiofouling<sup>20</sup> and cryoprotective properties,<sup>21-24</sup> which are strongly related to the interaction between polymer and water. They maintain the water structure<sup>25</sup> at the interface between polymer and material, due to the charge balance. Here, I propose the facile synthesis of a zwitterionic polymer via RAFT polymerization and the efficient inhibition of protein aggregation.

Living polymerization, developed by Michael Szwarc in the 1950s,<sup>26, 27</sup> has become an indispensable form of polymerization due to its potential to control various parameters such as architecture, molecular weight distribution, and functionality. This process eliminates transfer and termination reactions from chain growth polymerization. With the advent of living radical polymerization, also known as controlled radical polymerization (CRP),<sup>28-33</sup> it has become more convenient to react various kinds of monomers under different conditions. Of the three CRP types, namely ATRP), RAFT polymerization, and NMP, RAFT is one of the newest and most versatile forms that does not require transition metal, making polymers that are useful in biomaterial applications. RAFT involves degenerate reversible chain transfer<sup>34</sup> and is a robust method for developing complex macromolecular architectures.

In Chapter 2 and 3, I developed various polyampholytes with excellent cryoprotective properties that protect the cell membrane during freezing. These polyampholytes were biocompatible, and their behavior with respect to protein denaturation and folding has not been addressed. To our knowledge, there are few reports on the use of polymers for this purpose. Muraoka et al.<sup>35</sup> reported the use of the triangular-structured monodisperse polyethylene glycol to inhibit lysozyme aggregation, but synthesis requires 15 steps and various reagents. Tunacliffe et al. studied biological systems and found that Group 3 late embryogenesis abundant (G3LEA) proteins reduce aggregation of lysozymes during dehydration.<sup>36</sup> LEA proteins contain positive and negative charges, but are neutral or basic overall.<sup>37</sup> They were employed as molecular shields and chaperones.<sup>38-40</sup>

In this report, I synthesized a novel zwitterionic polymer, polysulfobetaine (Poly SPB), which inhibits thermal aggregation of lysozyme with greater efficiency than the corresponding monomers. I also compared its efficiency with other reagents known to inhibit protein aggregation. To our knowledge, this is the first report of the use of a synthetic zwitterionic polymer as a protein aggregation inhibitor.

## 4.1.1 Materials and Methods

### 4.1.2 Methods

Sulfobetaine was purchased from Osaka Organic Chemical (Osaka, Japan) and used without further purification. Lysozyme from chicken egg white, 2-(dodecylthiocarbonothioylthio)-2-methylpropionic acid, Thioflavin T (ThT), and *Micrococcus lysodeikticus* were purchased from Sigma-Aldrich. Azobisisobutyronitrile (AIBN) was purchased from Wako Pure Chemical Industries (Osaka, Japan). ND-195, ND-201, ND-211, and ND-256 were purchased from Anatrace, UK.

### 4.1.3 Synthesis of Poly-SPB

SPB (Osaka Organic Chemical, Osaka, Japan), 2-(dodecylthiocarbonothioylthio)-2-methylpropionic acid, and AIBN were dissolved in methanol-water (3:1 v/v %). The solution was then purged with nitrogen gas for 1 h and stirred at 70 °C. Samples were removed periodically (20 µL) and plunged in liquid nitrogen to quench the reaction and then the conversion at each reaction time was obtained by <sup>1</sup>H nuclear magnetic resonance (NMR) (Bruker AVANCE III 400MHz spectrometer, Bruker Biospin Inc., Switzerland). After 6 h, the reaction mixture was dialyzed against methanol and water for 24 h each with constant solvent exchange. The polymer was obtained after lyophilization.

### 4.1.4 Thioflavin T Assay

A stock solution of Thioflavin T (ThT) was prepared by adding 4 mg ThT to 5mL PBS and filtered through a 0.22 µm filter. The stock solution was diluted by adding 1 mL stock to 50 mL PBS to generate the working solution.<sup>41</sup> Lysozyme solution in PBS was then mixed with various reagents and heated to 90° C for 30 min; then, 2 mL of this solution was mixed with 100 µL ThT and fluorescence was observed with an excitation wavelength of 440 nm and emission wavelength of 480 nm (JASCO FP-6500). Increased intensity corresponds to amyloid formation due to ThT binding with amyloid fibrils.

### 4.1.5 Residual Enzyme Activity

Lysozyme solution in PBS was mixed with poly-SPB solution to achieve a final lysozyme concentration of 0.1 mg/mL. The solution was heated at 90°C for 30 min. *Micrococcus*

lysodeikticus (2 mL; 0.25 mg/mL in PBS) was placed in a quartz cuvette with 100  $\mu$ L lysozyme-polymer solution and mixed well. Turbidity was measured by UV-Vis spectrophotometry (UV-1600PC, Shimadzu Corporation, Kyoto, Japan) at 600 nm from 0 to 6 min with constant stirring at room temperature.<sup>42</sup>

#### 4.1.6 Transmission Electron Microscopy

Lysozyme (5 mg/mL) was dissolved in PBS with and without poly-SPB, and then incubated at 65°C for 14 days without agitation.<sup>43</sup> It was then diluted 10-fold for transmission electron microscopy (TEM). The sample (10  $\mu$ L) was placed on a copper grid (NS-C15 Cu150P; Stem, Tokyo, Japan). The grids were negatively stained with 2% phosphotungstic acid (Sigma Aldrich, Steinheim, Germany) for 1 min and then washed with two drops of distilled water, blotted, and air-dried. TEM images were collected on a Hitachi H-7100 system (Hitachi, Tokyo, Japan) with an accelerating voltage of 100 kV.

#### 4.1.7 Statistical Analysis

All data are expressed as mean  $\pm$  standard deviation (SD). All experiments were conducted in triplicate. The Tukey-Kramer test was used to compare the data shown in Fig. 4.8.

### 4.2 Results & discussion

#### 4.2.1 Characterization

Polysulfobetaine was synthesized from the zwitterionic monomer 3-((3-acrylamidopropyl)-dimethylammonio)-propane-1-sulfonate by RAFT polymerization (Fig. 4.1). Polymers were characterized using various techniques.

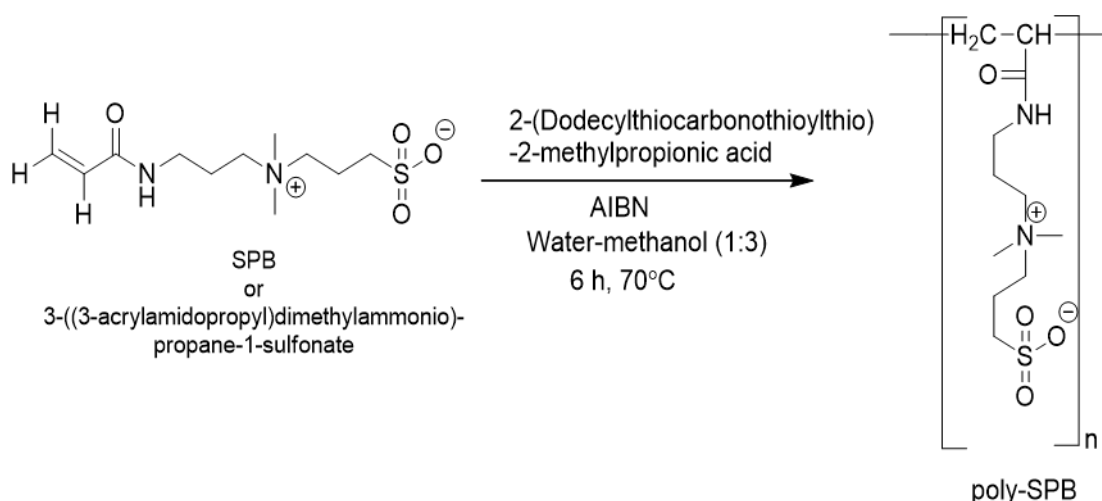


**Figure 4.1.** Synthesis of poly-SPB by RAFT polymerization.

$^1\text{H}$ - and  $^{13}\text{C}$ -NMR were used to analyze the chemical structure of the final product (polymer) obtained after purification (Fig. 4.2a & b). Attenuated total reflectance Fourier transform infrared (ATR-FTIR) spectroscopy (JASCO FT-IR-4200, Fourier Transform Infrared Spectrometer) revealed complete conversion of monomer to polymer with the loss of alkene stretching at around  $1627$  and  $3270\text{ cm}^{-1}$  (Fig. 4.3). Time dependent NMR spectrums were obtained after fixed intervals to calculate the rate of reaction and to ascertain the completion of reaction. Fig. 4.4a shows that the reaction initially proceeds rapidly and almost all of the monomer is converted to the corresponding polymer, represented by disappearance of the vinyl peaks at  $5.7$  and  $6.2$  ppm. Kinetic study of the polymerization (Fig. 4.4b) reaction revealed a first order kinetics, illustrated by a linear curve, representative of living polymerization<sup>44</sup>. Around 80% of the reaction was completed within the first two hours and all the monomer got converted into corresponding polymer in 6 hours, indicating completion of reaction.

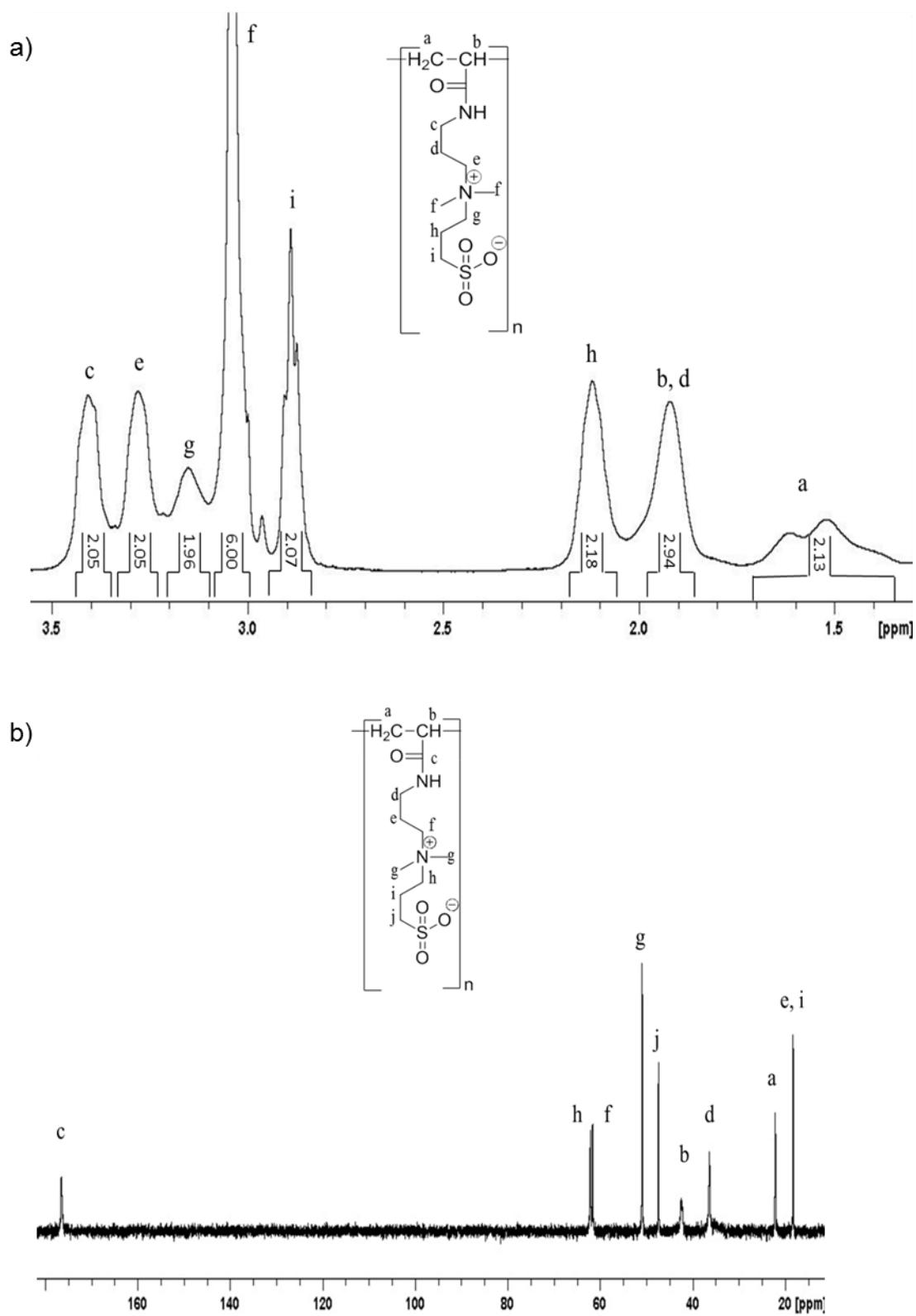


**Figure 4.2.** a)  $^1\text{H}$ -NMR and b)  $^{13}\text{C}$ -NMR of poly-SPB in  $\text{D}_2\text{O}$ .

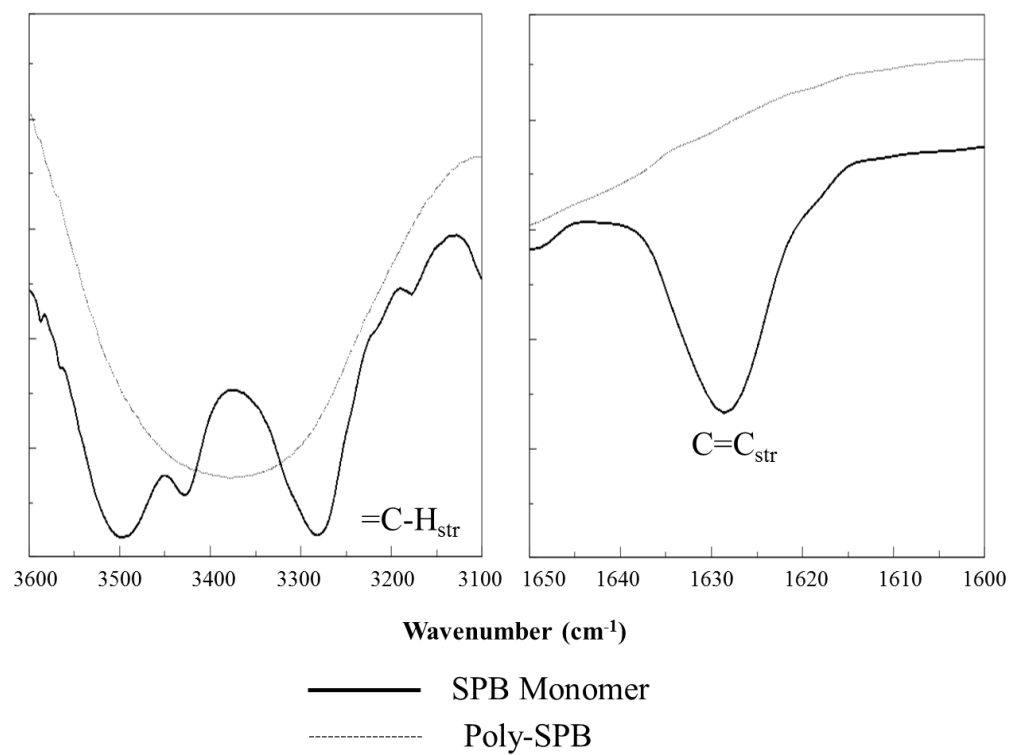


**Figure 4.3.** ATR-FTIR spectra of SPB monomer and poly-SPB.

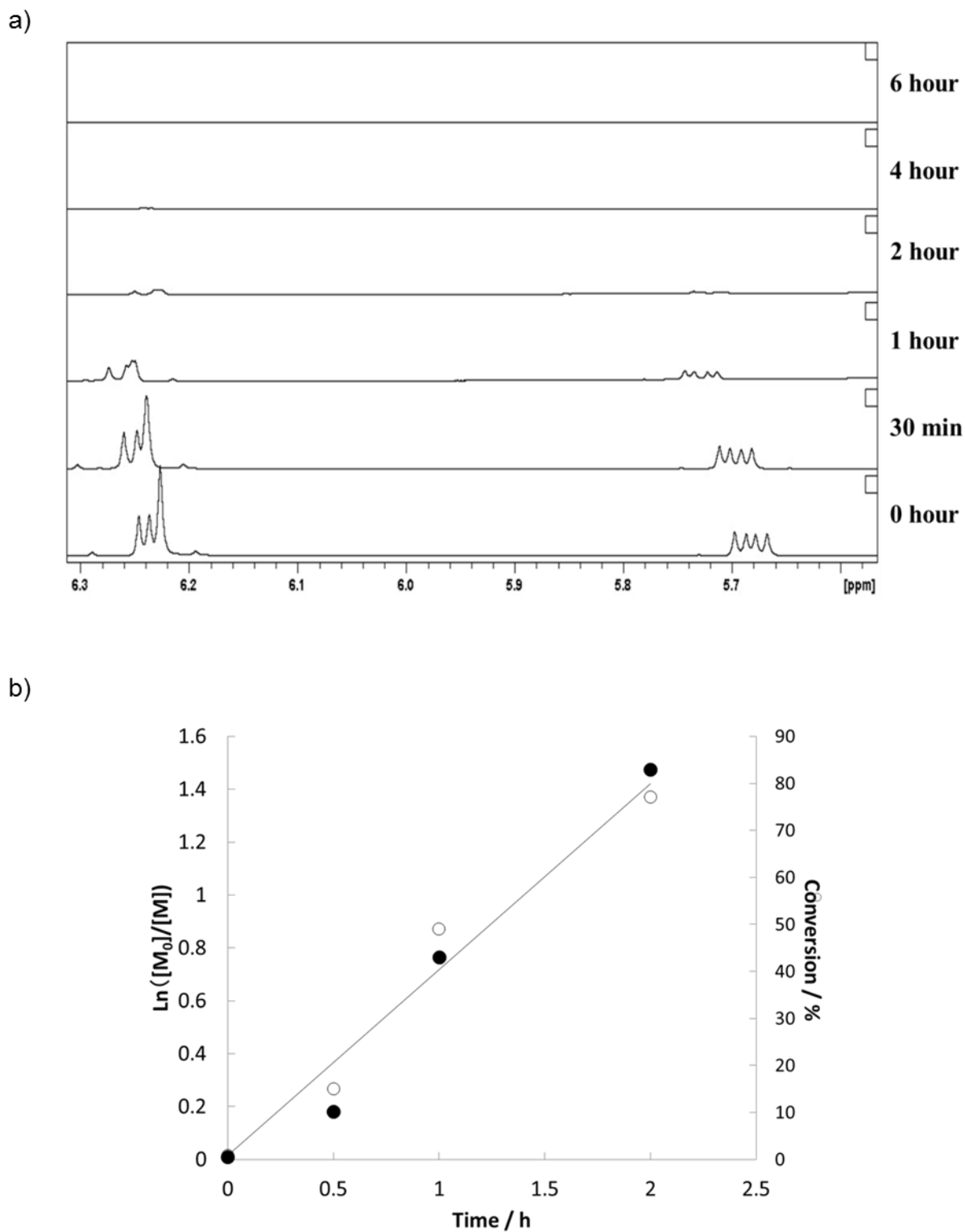


**Figure 4.4.** a) Time-dependent  $^1\text{H}$ -NMR and b) Kinetic plot for the polymerization of SPB by RAFT polymerization, followed by  $^1\text{H}$  NMR spectroscopy in  $\text{D}_2\text{O}$ .

#### 4.2.2 Protein aggregation Inhibition

A clear solution was obtained when lysozyme was dissolved in PBS (pH 7.4, 3 mg/mL) alone. The solution was heated to 90°C for 30 min, which resulted in aggregation of lysozyme (Fig. 4.5a). Addition of SPB monomer (10% w/v) partially inhibited lysozyme aggregation (Fig. 4.5b), and addition of poly-SPB yielded a slightly yellowish solution due to the nature of the polymer in PBS. When this solution was heated to 90°C for 30 min, no aggregates were seen (Fig. 4.5c). This was verified by spectrophotometry, which showed no significant change in absorbance in the visible region (500 nm). This experiment clearly demonstrated that poly-SPB inhibits thermal aggregation of lysozyme.

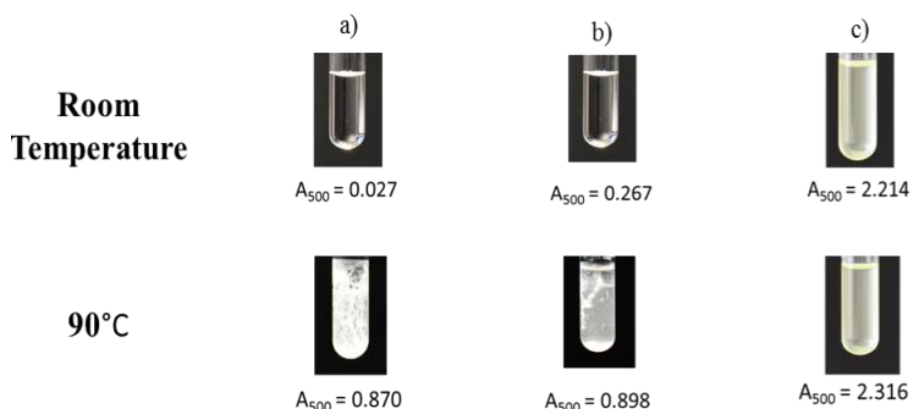


**Figure 4.5.** Photographs of lysozyme in PBS (3 mg/mL) at room temperature (top) and at 90° C (bottom); a) without additive; b) with 10 % SPB; c) with 10 % poly-SPB. Absorbance at 500 nm is shown below each image.

Lysozyme aggregation was also observed by circular dichroism (CD) spectroscopy (JASCO J-820, CD spectrometer). When a solution of lysozyme in PBS (0.5 mg/mL) containing no polymer was heated to 90° C, it exhibited a considerable decrease in the intensity of CD bands around 205 ( $\beta$ -sheet) and 225 nm ( $\alpha$ -helix), which corresponds to loss of the lysozyme secondary structure<sup>45-47</sup> (Fig. 4.6) and complete unfolding upon heating. The electrostatic interaction of poly-SPB with lysozyme was observed by zeta-potential which were recorded on Zetasizer 3000 (Malvern Instruments, Worcestershire, UK). They showed that poly-SPB has a slightly negative



surface charge which, combined with the positive charge of lysozyme possesses, produces a weak and reversible electrostatic interaction (Table 1).

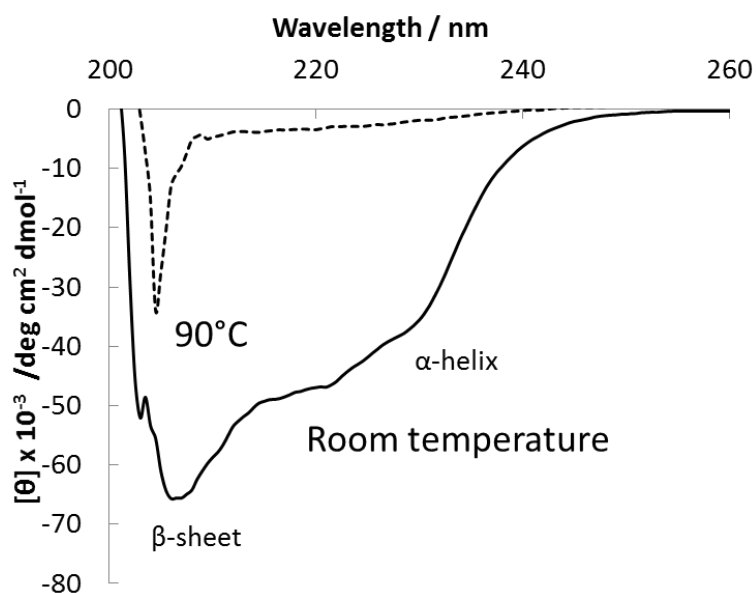


**Figure 4.6.** CD spectra of lysozyme (0.5 mg/mL) in PBS buffer at 30° C and 90° C.

**Table 4.1.** Zeta Potential values at pH 7. (Numbers in parenthesis indicate the final concentration (w/v) %).

Sample	Zeta Potential (mV)
Lysozyme (0.33)	5.24
Poly-SPB (0.67)	-4.79
Lysozyme (0.33) + Poly-SPB (0.67)	-4.18

### 4.2.3 Amyloid Fibril Formation

TEM revealed the formation of amyloid fibrils on heating of lysozyme (Fig. 4.7a). Fibrils were long, dense and straight, representing amyloid morphology<sup>48</sup>. When poly-SPB was added to the lysozyme and heated, no fibril formation was observed. Hence, addition of poly-SPB completely blocked fibrillation (Fig. 4.7b).

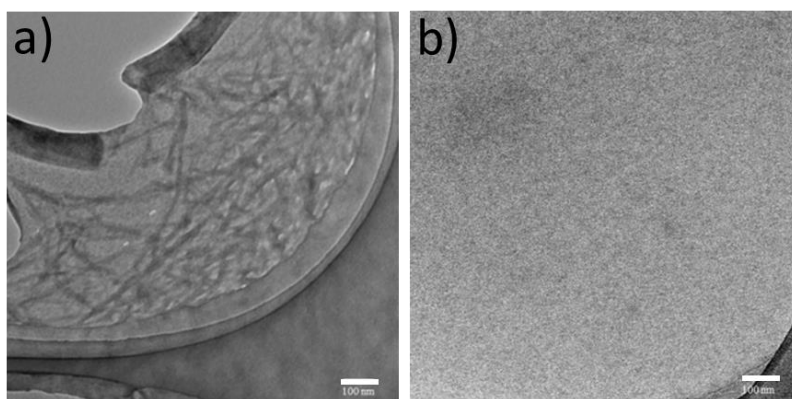


**Figure 4.7.** TEM images of lysozyme solution after incubation at 90° C a) in PBS alone, and b) with poly-SPB. Scale bars represent 100 nm.

Amyloid aggregation inhibition was quantitatively analyzed by the Thioflavin T assay. Lysozyme in PBS containing poly-SPB showed very high inhibition of protein aggregation (amyloid fibril formation) with an efficiency that increased with increasing polymer concentrations. At 10 % polymer concentration, ~96 % inhibition was observed (Fig. 4.8a). This represented significantly greater efficiency than the monomer SPB and other commercially available reagents such as non-detergent sulfobetaines (NDSBs)<sup>49-53</sup> and L-arginine hydrochloride<sup>54, 55</sup> (Fig. 4.8b).

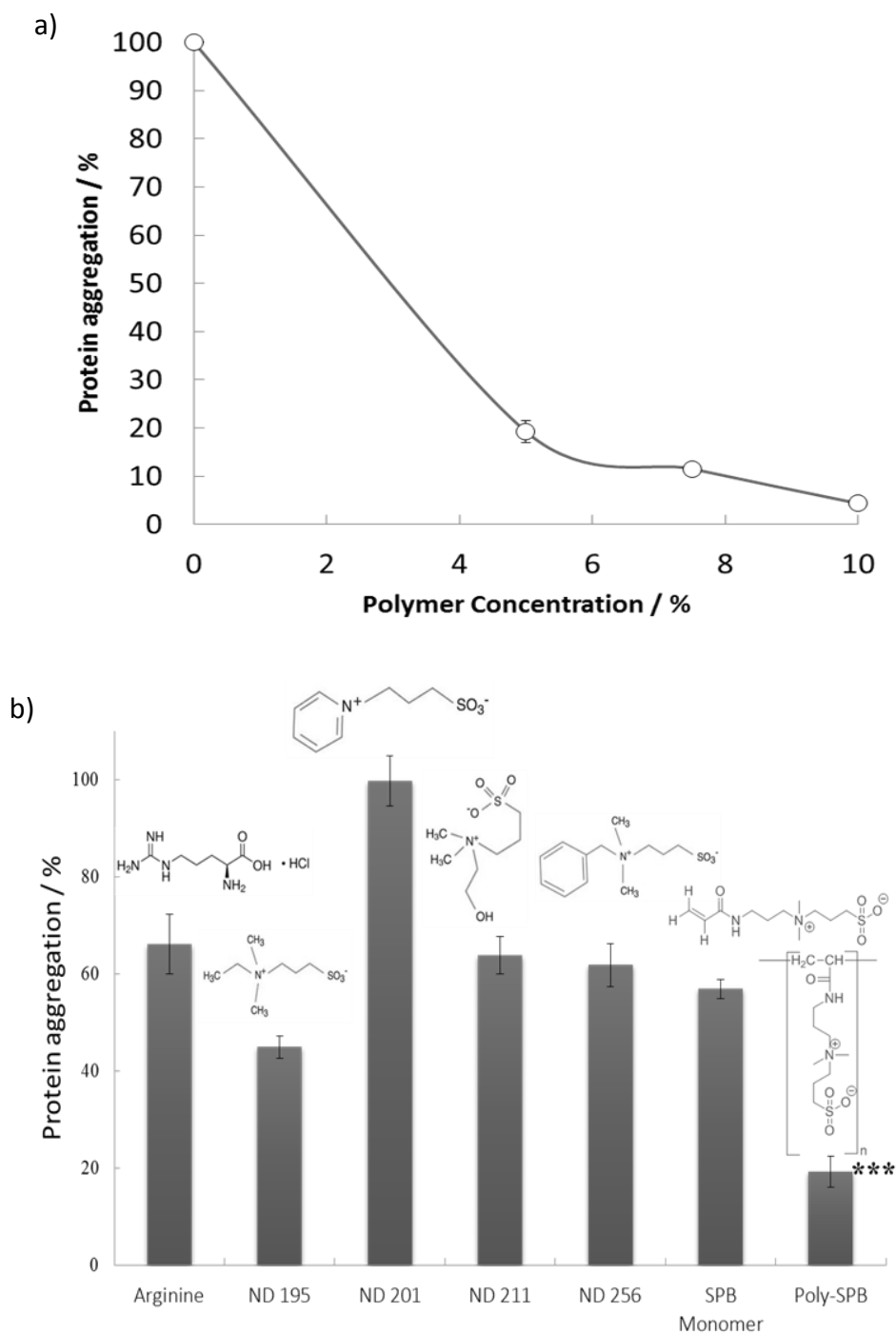


**Figure 4.8.** a) Protein aggregation of lysozyme (0.5 mg/mL) when heated to 90° C for 30 minutes a) in the presence of poly-SPB at various polymer concentrations, and b) in the presence of various reagents (5 % w/v). Data are expressed as the mean  $\pm$  SD of 3 independent experiments (5 samples each) \*\*\* $P < 0.001$  vs. all other reagents.

#### 4.2.4 Enzymatic Activity

The enzymatic activity of lysozyme after heating was also studied by using gram-positive *Micrococcus lysodeikticus* to assess the ability of poly-SPB to inhibit thermal aggregation. When lysozyme acts on the cell suspension, the turbidity of the suspension decreases and sample absorbance undergoes a drastic diminution. I monitored the reduction in turbidity caused by action of lysozyme on the cell suspension resulting in degradation of the bacterial cell wall as a decrease in absorbance at 600 nm (Fig. 4.9a). Residual lysozyme activity increased with increasing concentrations of poly-SPB: at 15 % poly-SPB (w/v %), lysozyme retained more than 85 % activity (Fig. 4.9b), more than has been reported elsewhere.<sup>35</sup> This confirms that poly-SPB is an efficient inhibitor of lysozyme aggregation that also prevents irreversible mis-folding.

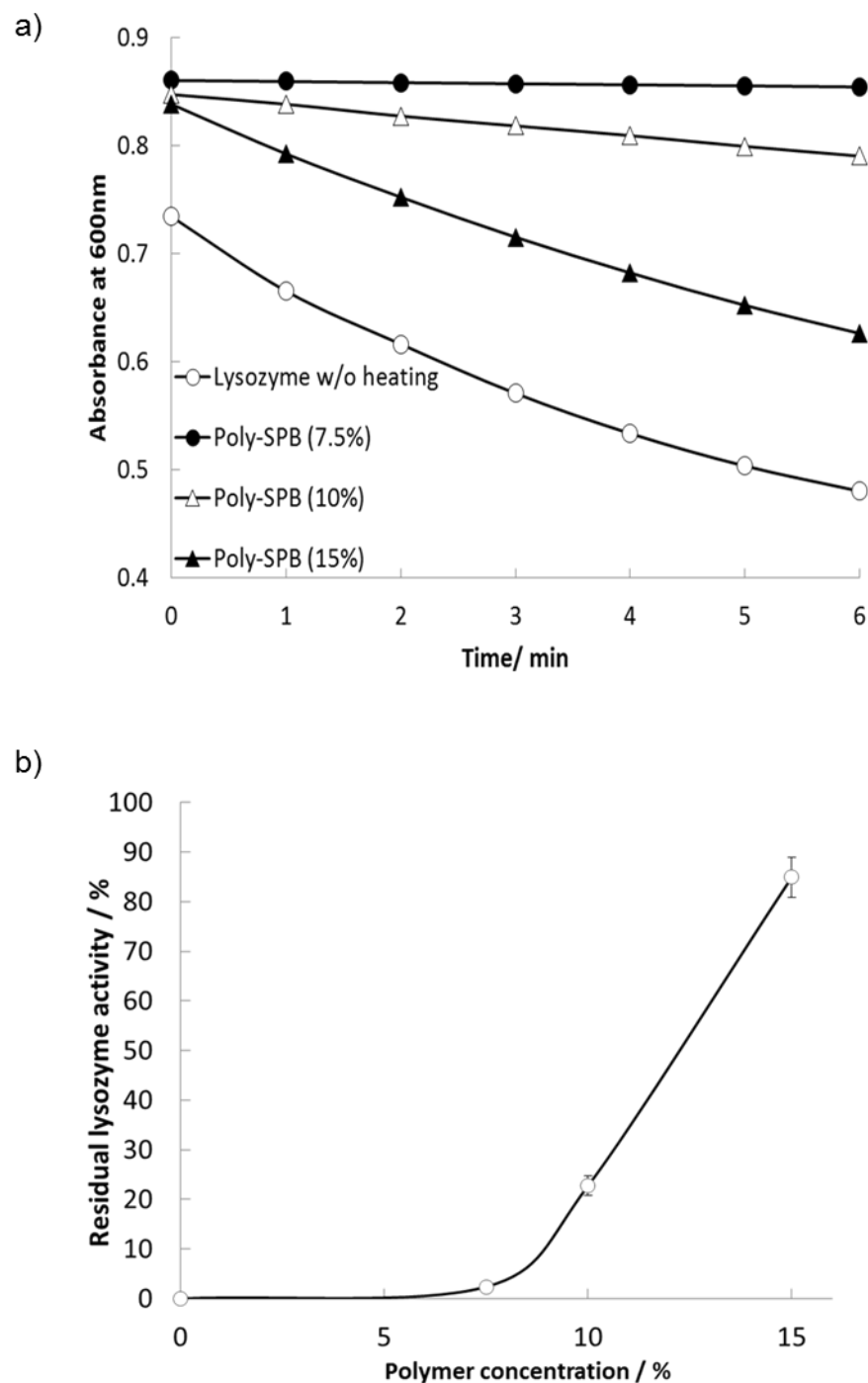


**Figure 4.9.** a) Rate of inactivation of lysozyme when heated to 90° C when lysozyme in PBS (open triangle, slope = 0.0418); with 15 % poly-SPB (closed triangle, slope = 0.0355); with 10 % poly-SPB (open circle, slope=0.0095) and with 7.5 % poly-SPB (closed circle, slope = 0.001), and b) Enzymatic activity of lysozyme after treatment at 90 °C in the presence of poly-SPB. Data are expressed as the mean  $\pm$  SD of 3 independent experiments (5 samples each).

## 4.2.5 Preservation of Secondary Structure

### 4.2.5.1 ATR-FTIR

These studies revealed a change in the secondary structure of lysozyme upon aggregation. The amide I peak corresponding to a  $\beta$ -sheet<sup>56</sup> shifted to a lower-frequency band position (Fig. 4.10) suggesting an increase in  $\beta$ -structure in the fibrils.<sup>57</sup> Addition of poly-SPB prevented any change in secondary structure.

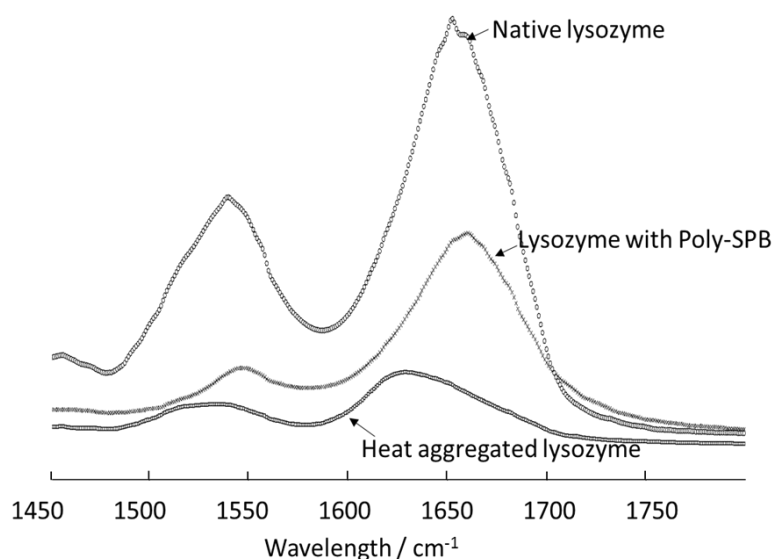


**Figure 4.10.** ATR-FTIR of native lysozyme in the presence of poly-SPB and lysozyme (aggregated) after heating at 90 °C for 30 min.

### 4.2.5.2 <sup>1</sup>H-NMR

Conformational states of lysozyme before and after heating were analyzed by <sup>1</sup>H-NMR. Due to the anisotropic magnetic fields of the aromatic or carbonyl groups, folded proteins show an extensive range of chemical shifts. On the other hand, a relatively narrow range of chemical shifts is shown by denatured proteins, due to their transformation to a random-coil conformation.<sup>58</sup> <sup>1</sup>H-NMR of lysozyme solution in D<sub>2</sub>O exhibits a wide range of signals. After heating the solution to 90 °C for 30 min, all the peaks disappeared (Fig. 4.11a). This finding suggests that, after heating, the lysozyme is transformed into a random coil state and has lost its secondary structure. In contrast, addition of monomer to the lysozyme aids in partial retention

of the secondary structure (Fig. 4.11b). A mixture of lysozyme with poly-SPB resulted in many signals over a wide range of chemical shifts and almost all the peaks were retained (Fig. 4.11c). The signals at the up-field and down-field regions persisted with considerable intensities, indicating the lysozyme remained dissolved and retained a partial higher-order structure. Most of the proton signals can be assigned to their corresponding amino acids.<sup>59</sup> Signals observed in the high magnetic field region correspond to the amino acid residues located in the secondary structures<sup>60, 61</sup> ( $\alpha$ -helix,  $\beta$ -sheet, and loop) and the retention of these signals even after heating reveals that poly-SPB stabilizes the partial higher-order structure of lysozyme, which in turn improves enzyme solubility at higher temperatures.

Protein aggregation or denaturation is usually caused by water stress.<sup>62</sup> Under extreme conditions such as heating, drying, and desiccation, proteins undergo severe dehydration due to hydrophobic aggregation of the unfolded or denatured states, thus leading to aggregation.<sup>63</sup> Because Poly-SPB shows weak and reversible interaction with proteins,<sup>29</sup> it acts as a molecular shield, reducing collisions between aggregating species and maintaining the water structure.<sup>34</sup>

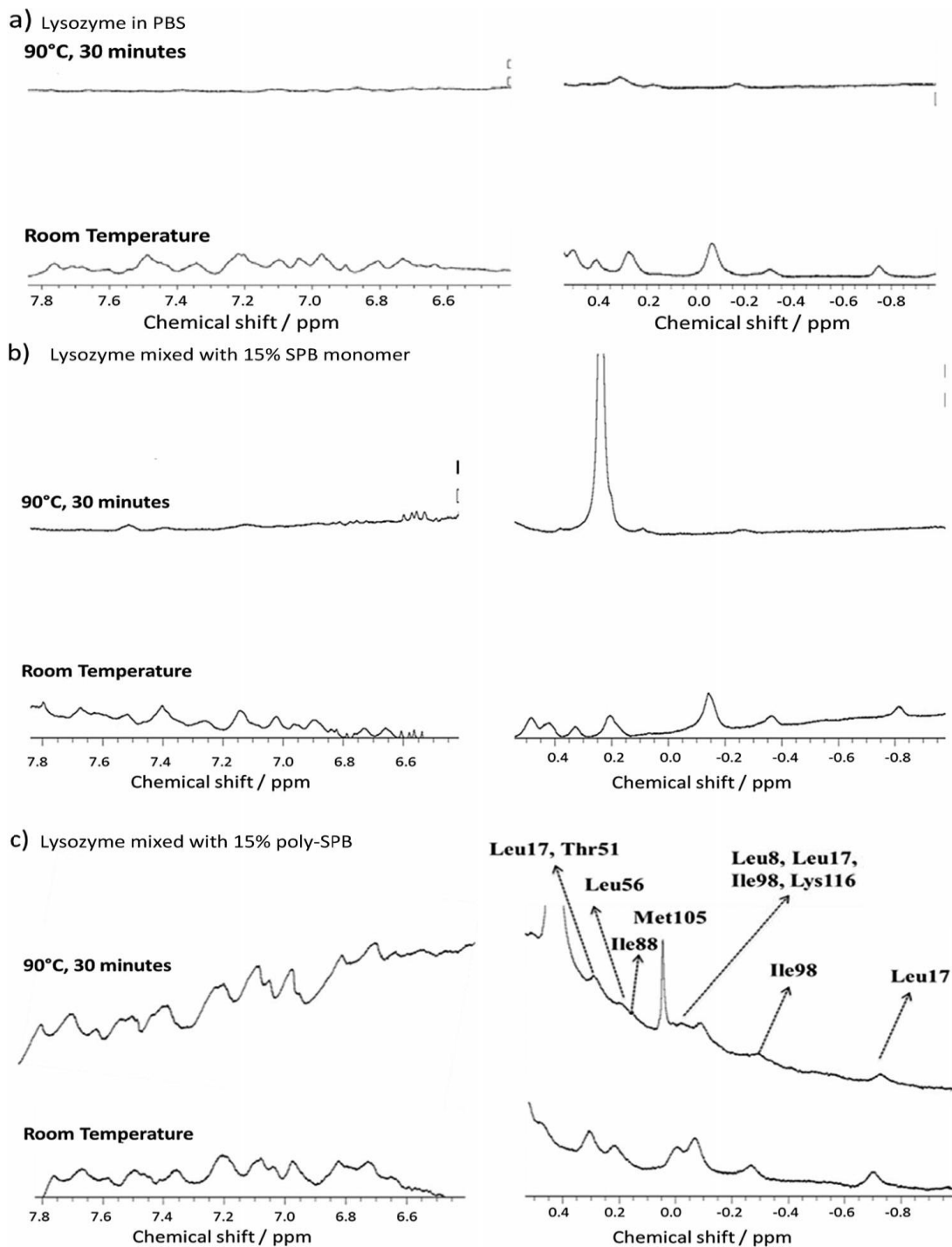


**Figure 4.11.** a)  $^1\text{H}$  NMR spectra of a mixture of a) lysozyme in PBS, b) lysozyme mixed with monomer SPB, and c) lysozyme mixed with poly-SPB at room temperature and after heating to 90 °C for 30 min.



### 4.3 Conclusion

In summary, I have shown that a zwitterionic polymer is an efficient inhibitor of thermal aggregation of lysozyme. To our knowledge, this is the first report of a zwitterionic polymer being used to inhibit protein aggregation. Poly-SPB stabilizes lysozyme and preserves its higher-order structure. The solubility of lysozyme in the presence of poly-SPB was retained even at higher temperatures, thus inhibiting lysozyme aggregation. Amyloid fibril formation was also suppressed. I believe that additional study of substituted poly-SPB, sulfobetaines with different alkyl chain lengths, and conversion into a nanogel may greatly improve the efficiency of this artificial molecular chaperone. Further studies are in progress to elucidate the mechanism by which aggregation is suppressed.

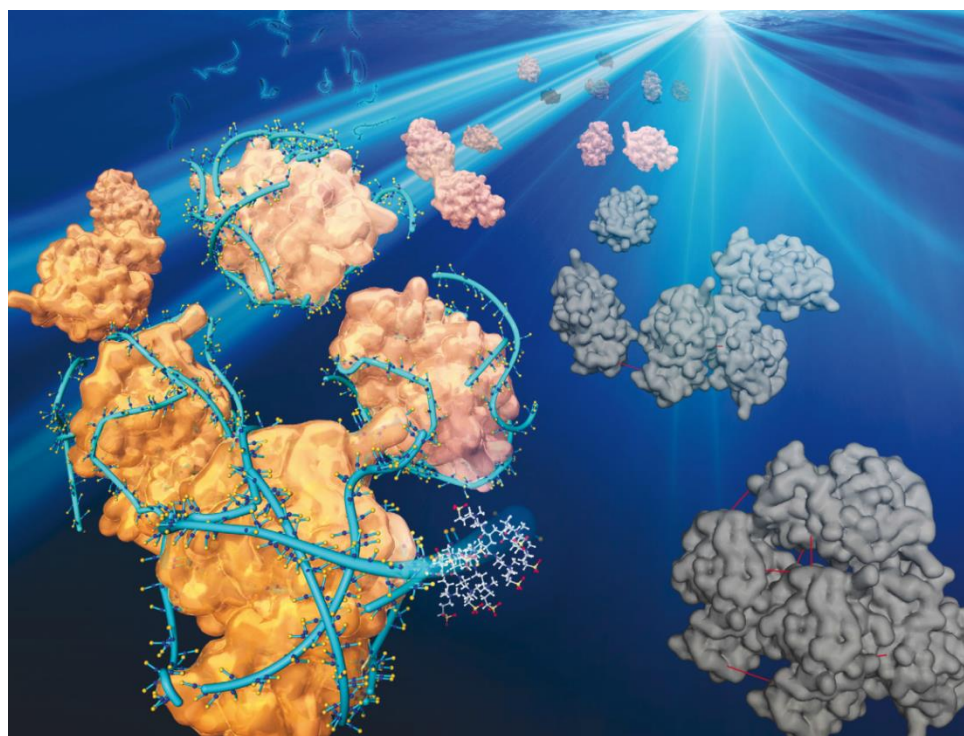


**Figure 4.12.** Schematic representation of the interaction between poly-SPB and lysozyme leading to the protection of lysozyme during heating.

### 4.4 References

- 1 W. Wang, *Int. J. Pharm.*, 1999, **185**, 129–188.
- 2 C. A. Ross and M. A. Poirier, *Nat. Med.*, 2004, **10**, S10–S17.
- 3 P. T. Lansbury and H. A. Lashuel, *Nature*, 2006, **443**, 774–779.

- 4 E. H. Koo, P. T. Lansbury, Jr., and J. W. Kelly, *Proc. Natl. Acad. Sci. U.S.A.*, 1999, **96**, 9989-9990.
- 5 V. Sluzky, J. A. Tamada, A. M. Klibanov, and R. Langer, *Proc. Natl. Acad. Sci. U S A.*, 1991, **88**, 9377–9381.
- 6 R. E. Canfield, *J. Biol. Chem.*, 1963, **238**, 2698–2707.
- 7 C. C. F. Blake, D. F. Koenig, G. A. Mair, A. C. T. North, D. C. Phillips and V. R. Sarma, *Nature*, 1965, **206**, 757–761.
- 8 L. R. Wetter and H. F. Deutsch, *J. Biol. Chem.*, 1951, **192**, 237–242.
- 9 S. Taneja and F. Ahmad, *Biochem. J.*, 1994, **303**, 147-153.
- 10 D. Das, J. Kriangkum, L. P. Nagata, R. E. Fulton and M. R. Suresh, *J. Virol. Meth.*, 2004, **117**, 169-177.
- 11 R. Asano, T. Kudo, K. Makabe, K. Tsumoto and I. Kumagai,, *FEBS Lett.*, 2002, **528**, 70–76.
- 12 D. Samuel, T. K. Kumar, G. Ganesh, G. Jayaraman, P. W. Yang, M. M. Chang, V. O. Trivedi, S. L. Wang, K. C. Hang, D. K. Chang and C. Yu, *Protein Sci.*, 2000, **9**, 344-352.
- 13 N. Karuppiyah and A. Sharma, *Biochem. Biophys. Res. Commun.*, 1995, **21**, 6066-6072.
- 14 J. D. Pedelacq, E. Piltch, E. C. Liong, J. Berendzen, C. Y. Kim, B. S. Rho, M. S. Park, T. C. Terwilliger and G.S. Waldo, *Nat. Biotechnol.*, 2002, **9**, 927–932.
- 15 S. Y. Ow, I. Bekard, A. Blencowe, G. G. Qiao and D. E. Dunstan, *J. Mater. Chem. B*, 2015, **3**, 1350-1359.
- 16 S. E. Kudaibergenov, *Adv. Polym. Sci.*, 1999, **144**, 115-197.
- 17 E. A. Bekturov, S. E. Kudaibergenov, S. R. Rafikov, *J. Macromol. Sci. Rev. Macromol. Chem. Phys.*, 1990, **C30**, 233-303.
- 18 A. B. Lowe and C. L. McCormic, *Chem. Rev.*, 2002, **102**, 4177–4189.
- 19 M. Bernards and Y. He, *J. Biomater. Sci. Polym. Ed.*, 2014, **25**, 1479-1488.
- 20 H. Kitano, T. Kondo, T. Kamada, S. Iwanaga, M. Nakamura and K. Ohno, *Colloids Surf. B*, 2011, **88**, 455-462.
- 21 K. Matsumura and S. H. Hyon, *Biomaterials*, 2009, **30**, 4842-4849.
- 22 R. Rajan and K. Matsumura, *J. Biomater. Sci. Polym. Ed.*, 2013, **24**, 1767-1780.
- 23 R. Rajan and K. Matsumura, *Cryobiol. Cryotechnol.*, 2014, **60**, 99-103.
- 24 M. Jain, R. Rajan, S. H. Hyon and K. Matsumura, *Biomater. Sci.*, 2014, **2**, 308-317.

- 25 H. Kitano, T. Mori, Y. Takeuchi, S. Tada, M. G. Ide, Y. Yokoyama and M. Tanaka, *Macromol. Biosci.*, 2005, **5**, 314–321.
- 26 M. Szwarc, M. Levy, R. Milkovich, *J. Am. Chem. Soc.*, 1956, **78**, 2656–2657.
- 27 M. Szwarc M, *Nature*, 1956, **176**, 1168–1169.
- 28 J. Chiefari, Y. K. Chong, F. Ercole, J. Krstina, J. Jeffery, T. P. T. Le, R. T. A. Mayadunne, G. F. Meijs, C. L. Moad, G. Moad, E. Rizzardo and S. H. Thang, *Macromolecules*, 1998, **31**, 5559-5562
- 29 G. Moad, E. Rizzardo, S. H. Thang, *Aust. J. Chem.*, 2005, **58**, 379-410.
- 30 J. S. Wang and K. Matyjaszewski, *J. Am. Chem. Soc.*, 1995, **117**, 5614–5615.
- 31 M. Kato, M. Kamigaito, M. Sawamoto and T. Higashimura, *Macromolecules*, 1995, **28**, 1721–1723.
- 32 W. Tang, N. V. Tsarevsky and K. Matyjaszewski, *J. Am. Chem. Soc.*, 2006, **128**, 1598–1604.
- 33 R. B. Grubbs, C. J. Hawker, J. Dao and J. M. J. Fréchet, *Angew. Chem. Int. Ed. Engl.*, 1997, **36**, 270.
- 34 M. Semsarilar and S. Perrier, *Nat. Chem.*, 2010, **2**, 811–820.
- 35 T. Muraoka, K. Adachi, M. Ui, S. Kawasaki, N. Sadhukhan, H. Obara, H. Tochio, M. Shirakawa and K. Kinbara, *Angew. Chem. Int. Ed.*, 2013, **52**, 2430-2434.
- 36 T. Furuki, T. Shimizu, S. Chakrabortee, K. Yamakawa, R. Hatanaka, T. Takahashi, T. Kikawada, T. Okuda, H. Mihara, A. Tunnacliffe and M. Sakurai, *Biochim. Biophys. Acta, Proteins Proteomics*, 2012, **1824**, 891-897.
- 37 M. J. Wise and A. Tunnacliffe, *Trends Plant Sci.*, 2004, **9**, 13–17.
- 38 S. Chakrabortee, R. Tripathi, M. Watson, G. S. K. Schierle, D. P. Kurniawan, C. F. Kaminski, M. J. Wise and A. Tunnacliffe, *Mol. Biosyst.*, 2012, **8**, 210-219.
- 39 S. Chakrabortee, Y. Liu, L. Zhang, H. R. Matthews, H. Zhang, N. Pan, C. R. Cheng, S. H. Guan, D. A. Guo, Z. Huang, Y. Zheng and A. Tunnacliffe, *Biochem. J.*, 2012, **442**, 507-515.
- 40 S. Chakrabortee, F. Meersman, G. S. K. Schierle, C. W. Bertoncini, B. McGee, C. F. Kaminski and A. Tunnacliffe, *Proc. Natl. Acad. Sci. U.S.A.*, 2010, **107**, 16084-16089.
- 41 S. Taneja and F. Ahmad, *Biochem. J.*, 1994, **303**, 147-153.

- 42 M. Kudou, K. Shiraki, S. Fujiwara, T. Imanaka and M. Takagi, *Eur. J. Biochem.*, 2003, **270**, 4547-4554.
- 43 S. Feng, X. H. Song and C. M. Zeng, *FEBS Lett.*, 2012, **586**, 3951-3955.
- 44 J. Chiefari, Y.K. Chong, F. Ercole, J. Krstina, J. Jeffery, T.P.T. Le, R. T. A. Mayadunne, G. F. Mejis, C. L. Moad, G. Moad, E. Rizzardo and S. H. Thang, *Macromolecules*, 1998, **31**, 5559–5562.
- 45 G. Holzwarth and P. Doty, *J. Am. Chem. Soc.*, 1965, **20**, 218-228.
- 46 N Greenfield and G. D. Fasman, *Biochemistry*, 1969, **8**, 4108-4116.
- 47 S. Y. Venyaminov, I. A. Baikarov, Z. M. Shen, C. S. C. Wu and J. T. Yang, *Anal Biochem.*, 1993, **241**, 17-24.
- 48 M. R. Krebs, D. K. Wilkins, E. W. Chung, M. C. Pitkeathly, A. K. Chamberlain, J. Zurdo, C. V. Robinson, and C. M. Dobson, *J. Mol. Biol.*, 2000, **300**, 541–549.
- 49 M. E. Goldberg, N. E. Bezançon, L. Vuillard and T. Rabilloud, *Fold. Des.*, 1996, **1**, 21–27.
- 50 L. Vuillard, T. Rabilloud, R. Leberman, C. B.Colominas and S. Cusack, *FEBS Lett.*, 1994, **353**, 294-296.
- 51 L. Vuillard, D. Madern, B. Franzetti and T. Rabilloud, *Anal. Biochem.*, 1995, **230**, 290–294.
- 52 L. Vuillard, C. B. Breton and T Rabilloud, *Biochem. J.*, 1995, **305**, 337–343.
- 53 L. Vuillard, B. Baalbaki, M. Lehmann, S. Nørager, P. Legrand and M. Roth, *J.Cryst Growth*, 1996, **168**, 150-154.
- 54 D. Shah and A. R. Shaikh, *AIChE J.*, 2011, **27**, 513-520.
- 55 S. Tomita, Y. Nagasaki and K. Shiraki, *Biotechnol. Bioeng.*, 2012, **109**, 2543-552.
- 56 J. Kong and S. Yu, *Acta Biochim. Biophys. Sinica*, 2007, **39**, 549-559.
- 57 B. Shivu, S. Seshadri, J. Li, K. A. Oberg, V. N. Uversky and A. L. Fink, *Biochemistry*, 2013, **52**, 5176-5183.
- 58 J. Cavanagh and W. J. Fairbrother, A. G. Palmer III, M. Rance and N. J. Skelton, *Protein NMR Spectroscopy: Principles and Practice*, 2nd ed., Academic Press, San Diego, 2006.
- 59 J. Boyd, C. M. Dobson and C. Redfield, *Eur. J. Biochem.*, 1985, **153**, 383-396.
- 60 Y. Wang, T. C. Y. Wang, T. C. Bjorndahl and D. S. Wishart, *J. Biomol. NMR*, 2000, **17**, 83–84.

- 61 J. C. Cheetham, P. J. Artymiuk and D. C. Phillips, *J. Mol. Biol.*, 1992, **224**, 613–628.
- 62 K. Goyal, L. J. Walton and A. Tunnacliffe, *Biochem J.*, 2005, **388**, 151-157.
- 63 A. L. Fink, *Fold. Des.*, 1998, **3**, R9-R23.

## Chapter 5 CORE-SHELL NANOGELS AS EFFECTIVE SUPPRESSOR OF PROTEIN AGGREGATION

### 5.1 Introduction

The term microgel was coined by Baker in his report published in 1949.<sup>1</sup> The etymology of the word comes from two different parts- “micro” and “gel”. The term micro represents the size of the compound and is defined as having size in the range of 10-1000 nm.<sup>2</sup> On the other hand, the term gel represent the propensity of these particles to swell in a suitable solvent. When the size of the particle is in the nano range, then these particles are termed as “nanogels”. These gels are usually formed by chemical or physical crosslinking. Nanogels are mostly composed of synthetic polymers. Nanogels are the nano-sized counterpart of hydrogels.

Akiyoshi and his group were one of the pioneers in the field of nanogels (although they did not strictly refer to their particles as nanogels). In 1993, they synthesized hydrophobized polysaccharides, mainly cholesterol (CHP) modified pullulan.<sup>3</sup> Because of the increased hydrophobicity due to the cholesterol moiety, and the compound underwent self-aggregation in water, resulting in the formation of nanoparticles. Since then, they have published a series of reports on such nanogels. They have also carried out extensive research on the application of CHP based nanogels as artificial molecular chaperones in which the proteins were trapped inside the nanogels and they could be released when cyclodextrin was added.<sup>4, 5</sup>

Nanogels have been employed for a wide range of applications in the field of bioengineering,<sup>6</sup> diagnostics,<sup>7, 8</sup> drug delivery, sensing,<sup>9</sup> etc. Recently Gota et al. developed a nanogel based thermometer for measuring intracellular temperature.<sup>10</sup> Although nanogels have been used for various applications, its greatest application was observed as a delivery vehicle. Various research groups have used nanogels for delivering drugs in the body. Nanogels certainly have an edge over their macroscopic counterparts when it comes to their application as delivery vehicles. Nanogels have greater drug loading capacity than macrogels, high stability, and can incorporate various materials like drugs, peptides, nucleic acid, etc.<sup>11</sup> In addition, various responsive nanogels have also been developed.<sup>12-15</sup>

## 5.2 Materials and Methods

### 5.2.1 Methods

Sulfobetaine monomer was purchased from Osaka Organic Chemical (Osaka, Japan) and used without further purification. 2-(dodecylthiocarbonothioylthio)-2-methylpropionic acid was purchased from Sigma-Aldrich. Azobisisobutyronitrile (AIBN) was purchased from Wako Pure Chemical Industries (Osaka, Japan). AIBN was recrystallized with methanol before using. N-butyl methacrylate (BuMA) was purchased from NOF Corporation (Tokyo, Japan). The inhibitor from BuMA was removed prior to use by passing it through inhibitor remover column (prepacked column, Sigma-Aldrich). Ethylene glycol dimethacrylate was purchased from TCI (Tokyo, Japan). 4–4'-Azobis-(4-cyanovaleric acid) (V-501, initiator) was purchased from TCI (Tokyo, Japan).

### 5.2.2 Synthesis of Poly-SPB

Polymers of different degrees of polymerization (DP) were synthesized by varying the ratio of monomer to RAFT agent. As an example of synthesis of polymer with DP 200, the brief procedure was: SPB) monomer (12 mmol), 2-(dodecylthiocarbonothioylthio)-2-methylpropionic acid (0.6 mmol) and AIBN (0.12 mmol) were dissolved in 60 mL methanol-water mixture (3:1 v/v %). The solution was then purged with nitrogen gas for 1 hour and stirred at 70 °C. After 6 hours, the reaction mixture was dialyzed using a membrane of MWCO 14,000 (Viskase Companies. Inc., Illinois, United States of America) against methanol and water successively for 24 hours each with regular change of solvent. The polymer was then obtained after lyophilization.

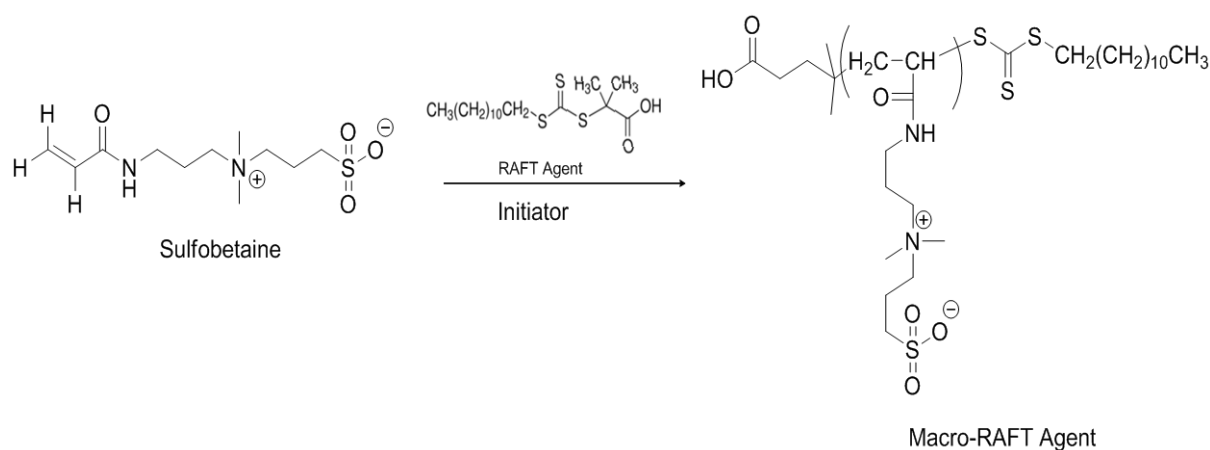


**Figure 5.1.** Synthesis of Macro-CTA (poly-SPB).

### 5.2.3 Synthesis of core-shell nanogels

Nanogels with different polymers of different DP were synthesized. As an example of synthesis nanogel with polymer of DP 200, the brief procedure was: poly-SPB (0.2 g), SPB (1.477 g), ethylene glycol dimethacrylate (21  $\mu$ L) and V-501 (4 mg) were dissolved in 50 mL milliQ water. The reaction mixture was then purged with nitrogen gas for 1 hour and stirred at 70°C. After 24 hours, the solution was then dialyzed using a membrane of MWCO 50,000 (Spectra/Por® Membrane, Spectrum Labs, United States of America) against water for 3 days with regular change of water. The final product was then obtained by lyophilization.<sup>16</sup>

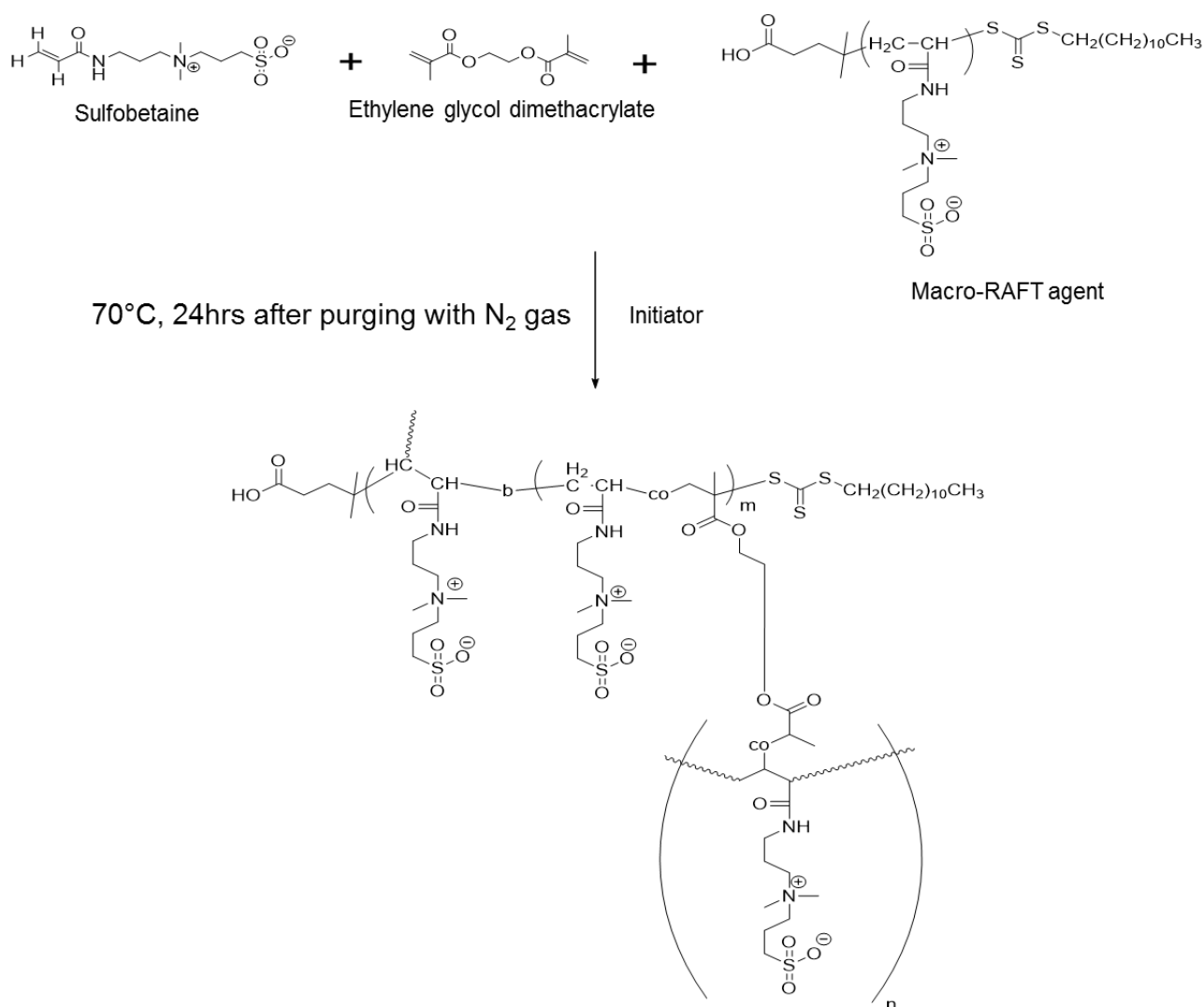


**Figure 5.2.** Synthesis of core-shell nanogel of poly-SPB.



### 5.2.4 Synthesis of Nanogel (with BuMA in the core)

Nanogels with different polymers of different DP were synthesized. As an example of synthesis nanogel with polymer of DP 200, the brief procedure was: poly-SPB (0.2 g), SPB (1.477 g), BuMA (44.4  $\mu$ L), ethylene glycol dimethacrylate (21  $\mu$ L) and V-501 (4 mg) were dissolved in 60 mL water-methanol mixture (5:1 v/v %). The reaction mixture was then purged with nitrogen gas for 1 hour and stirred at 70°C. After 24 hours, the solution was then dialyzed using a membrane of MWCO 50,000 (Spectra/Por® Membrane, Spectrum Labs, United States of America) against water for 3 days with regular change of water. The final product was then obtained by lyophilization.<sup>16</sup>

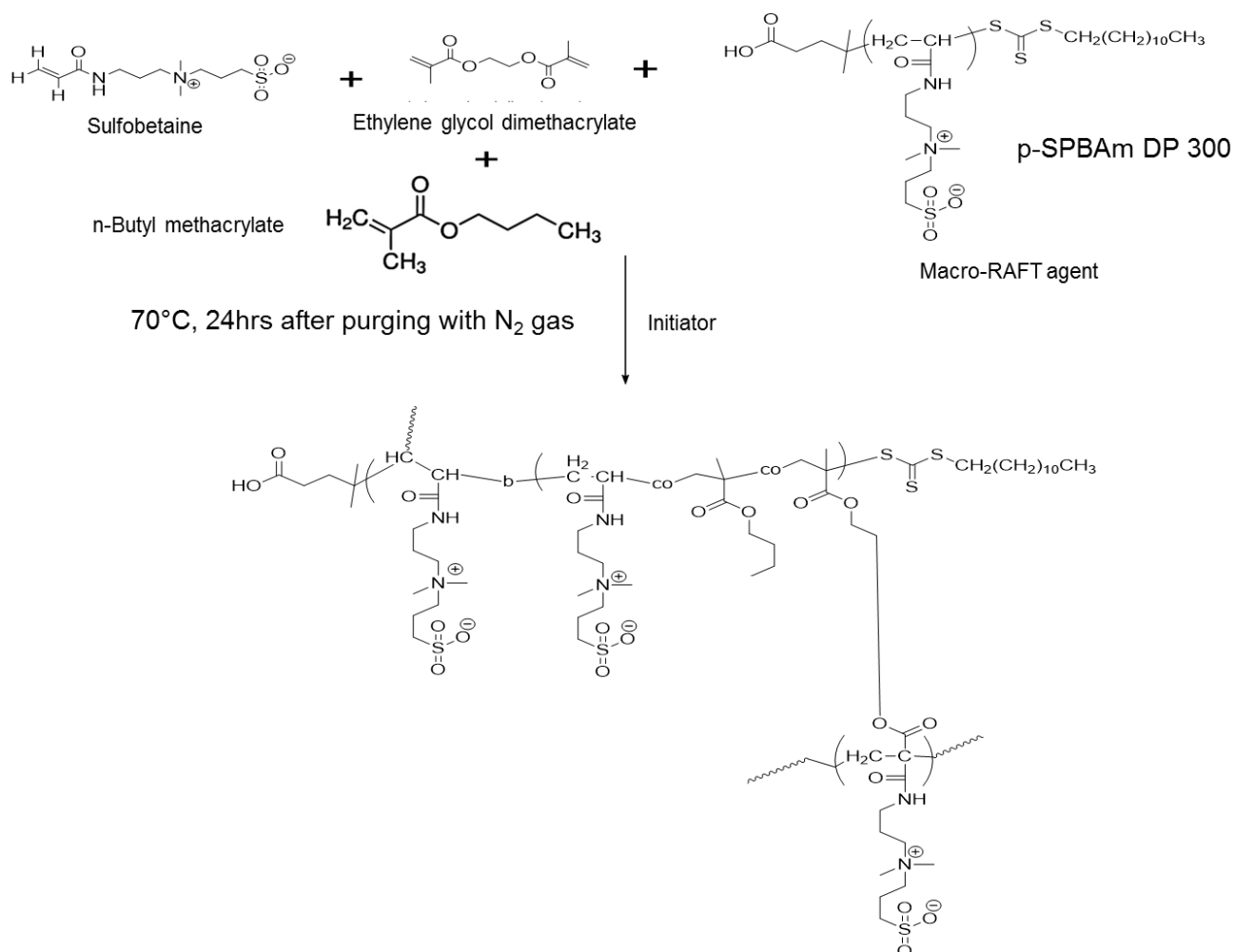


**Figure 5.3.** Synthesis of core-shell nanogel of poly-SPB with BuMA in the core.

### 5.2.5 Molecular Weight Determination

The molecular weight and distribution (polydispersity index, PDI) of the polymers were determined by gel permeation chromatography (GPC, column, BioSeps2000; Phenomenex, Inc., CA, USA) and was measured using Shimadzu high-performance liquid chromatography data system incorporating a refractive index detector. NaBr solution (pH 7.4, 0.1 M) was used as the mobile phase (flow rate, 1 mL min<sup>-1</sup>) and Pullulan (Shodex Group, Tokyo, Japan) was used as the standard.

### 5.2.6 Thioflavin T Assay

A stock solution of Thioflavin T (ThT) was prepared by adding 4 mg ThT to 5 mL PBS and filtered through a 0.22 µm filter. The stock solution was diluted by adding 1 mL stock to 50 mL PBS to generate the working solution.<sup>17</sup> Lysozyme solution in PBS was then mixed with various reagents and heated to 90°C for 30 min; then, 2 mL of this solution was mixed with 100 µL ThT and fluorescence was observed with an excitation wavelength of 440 nm and emission wavelength of 480 nm (JASCO FP-6500). Increased intensity corresponds to amyloid formation due to ThT binding with amyloid fibrils.

### 5.2.7 Residual Enzyme Activity

Lysozyme solution in PBS was mixed with poly-SPB solution to achieve a final lysozyme concentration of 0.1 mg/mL. The solution was heated at 90 °C for 30 min. *Micrococcus lysodeikticus* (2 mL; 0.25 mg/mL in PBS) was placed in a quartz cuvette with 100 µL lysozyme-polymer solution and mixed well. Turbidity was measured by UV-Vis spectrophotometry (UV-1600PC, Shimadzu Corporation, Kyoto, Japan) at 600 nm from 0 to 6 min with constant stirring at room temperature.<sup>18</sup>

## 5.3 Results and Discussion

### 5.3.1 Characterization

Polymers were prepared under various conditions and were characterized with <sup>1</sup>H NMR and GPC. Completion of the reaction was monitored by <sup>1</sup>H-NMR by observing the loss of vinyl

protons of the monomer. Conversion of the monomer to the corresponding polymer and the ratio of the initial concentration and at any given time during the reaction,  $\ln([M]_0/[M])$  were also evaluated using  $^1\text{H-NMR}$ .<sup>19</sup> Fig. 5.4 shows that polymer with both DP's showed almost a linear curve, representing living polymerization.

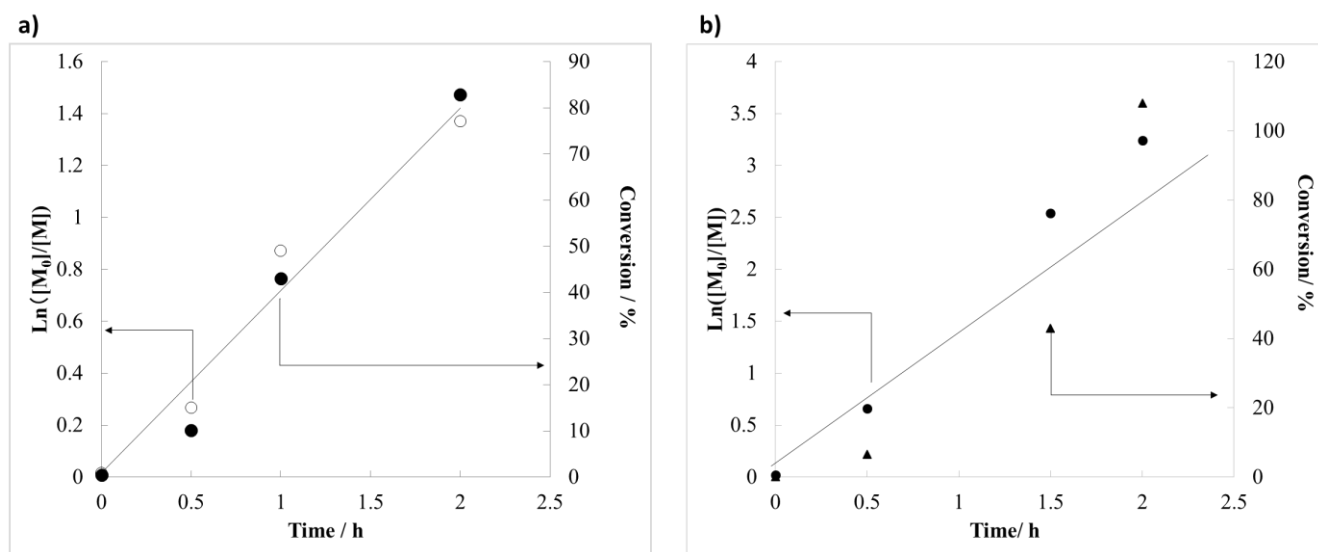


**Figure 5.4.** Kinetic plot of Poly-SPB with a) DP 20 and b) DP 200.

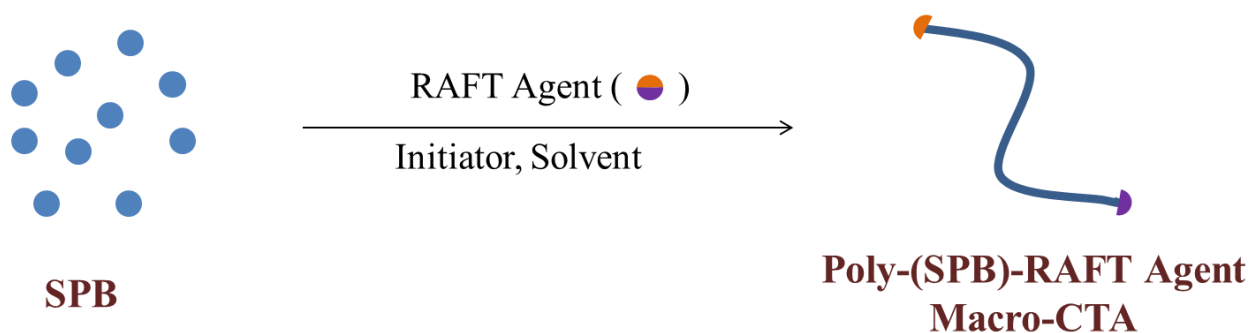
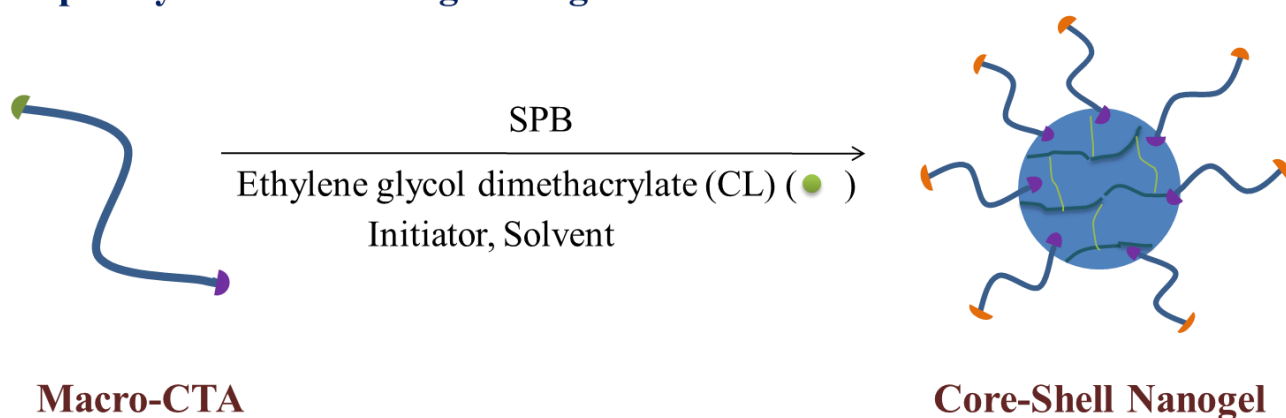
Polymers with two degree of polymerization were prepared by changing the molar ratio of Monomer and raft agent. The two polymers prepared are summarized in Table 5.1.

**Table 5.1.** Characteristics of the poly-(SPB) prepared via RAFT polymerization.

Macro-CTA (Poly-SPB	Molar ratio <sup>a)</sup>	$M_n \times 10^{-3}$	$M_w/M_n$
DP 20	100:1:5	5.5	1.18
DP 200	1000:1:5	36.2	1.59

a) [monomer]:[initiator]:[RAFT agent]

The nanogels were synthesized using a two-step scheme where the macro-CTA developed is combined with the SPB in presence of a radical cross linker and initiator (Fig. 5.5).

**Step 1. Synthesis of Macro-CTA****Step 2. Synthesis of Nanogel using Macro-CTA and Cross-linker**

**Figure 5.5.** Schematic Representation of nanogel formation.

No additional RAFT agent is required for this step, as the Macro-CTA acts as the new RAFT agent, thus creating a nanoparticle with poly-SPB shell and cross linker and poly-SPB (with and without BuMA) as the core. Different nanogels were synthesized using the two macro-CTAs of different molecular weights. They are summarized in Table 5.2.

**Table 5.2.** Characteristics of the nanogels prepared via RAFT polymerization.

Nanogel	Macro-CTA	% BuMA
NGA		0
NGB	DP 20	5
NGC		10
NGD		0
NGE	DP 200	5
NGF		10

### 5.3.2 Enzymatic Activity

The enzymatic activity of lysozyme after heating was also studied by using gram-positive *Micrococcus lysodeikticus* to assess the ability of the nanogels to inhibit thermal aggregation. When lysozyme acts on the cell suspension, the turbidity of the suspension decreases and sample absorbance undergoes a drastic diminution. We monitored the reduction in turbidity caused by action of lysozyme on the cell suspension resulting in degradation of the bacterial cell wall as a decrease in absorbance at 600 nm. Fig. 5.6 showed that all the nanogels show more than tenfold efficiency than poly-SPB. Increase in the molecular weight of the macro-CTA also leads to higher efficiency as can be seen by comparing the enzymatic activity in the presence of NGA and NGD. Since protein aggregation with poly-SPB is linked with its antibiofouling ability, there the increase in efficiency is due to greater antibiofouling property. Shorter polymer chains show antibiofouling property by virtue of the formation of hydration layer due to their hydrophilicity. In contrast, in longer polymer chains, presence of stearic repulsion (from flexible polymer chains) in addition to the formation of hydration layer enables them to have greater antibiofouling property.<sup>20, 21</sup> Addition of hydrophobicity also leads to increase in activity, as is evident by the increased retention when heated in presence of nanogels with BuMA. Also nanogels with 10 % BuMA show higher activity than nanogels with 5% BuMA (Fig. 5.6). This could be due to the fact that increased hydrophobicity leads to the suppression of the hydrophobic aggregation of the unfolded or denatured states.<sup>22, 23</sup>

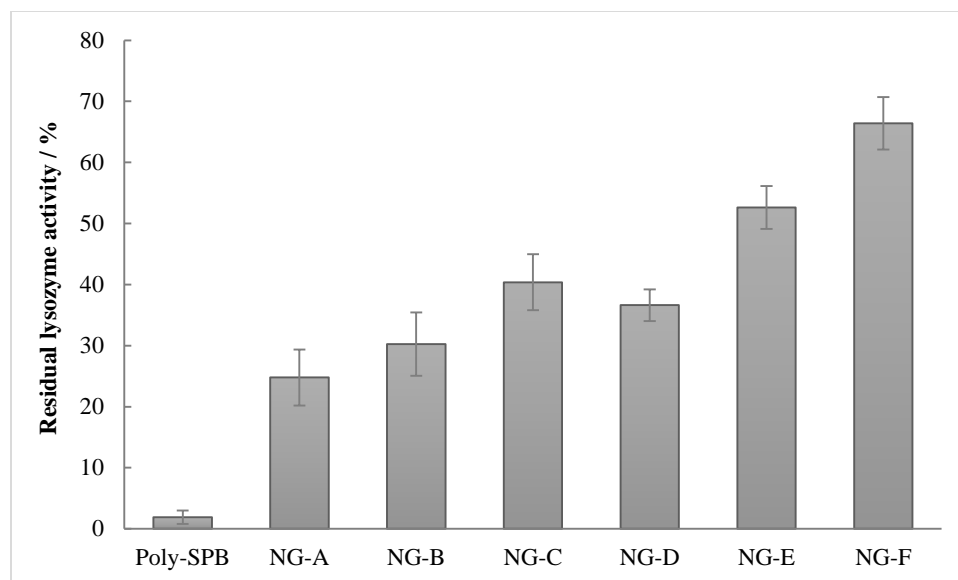


**Figure 5.6.** Enzymatic activity of lysozyme after treatment at 90 °C in the presence of different nanogels at 5% polymer concentration (w/v %). Data are expressed as the mean  $\pm$  SD of 3 independent experiments.

### 5.3.3 Amyloid Fibril Formation

Chapter 4 revealed that lysozyme on heating form amyloid fibrils. Therefore, amyloid aggregation inhibition by nanogels was quantitatively analyzed by the Thioflavin T assay. Lysozyme in nanogels containing poly-SPB showed very high inhibition of protein aggregation (amyloid fibril formation) with an efficiency that increased. The trends observed with inhibition of fibril formation was similar to the trend obtained in the residual enzymatic activity studies. Increase in molecular weight and hydrophobicity led to an increase in the amyloid formation suppression.

Efficiency of nanogels was higher than that of poly-SPB. Since poly-SPB was shown to have higher activity than other commercially available reagents such as non-detergent sulfobetaines (NDSBs)<sup>24-28</sup> and L-arginine hydrochloride,<sup>29, 30</sup> therefore, it be inferred that nanogels show significantly higher efficiency than all these compounds.

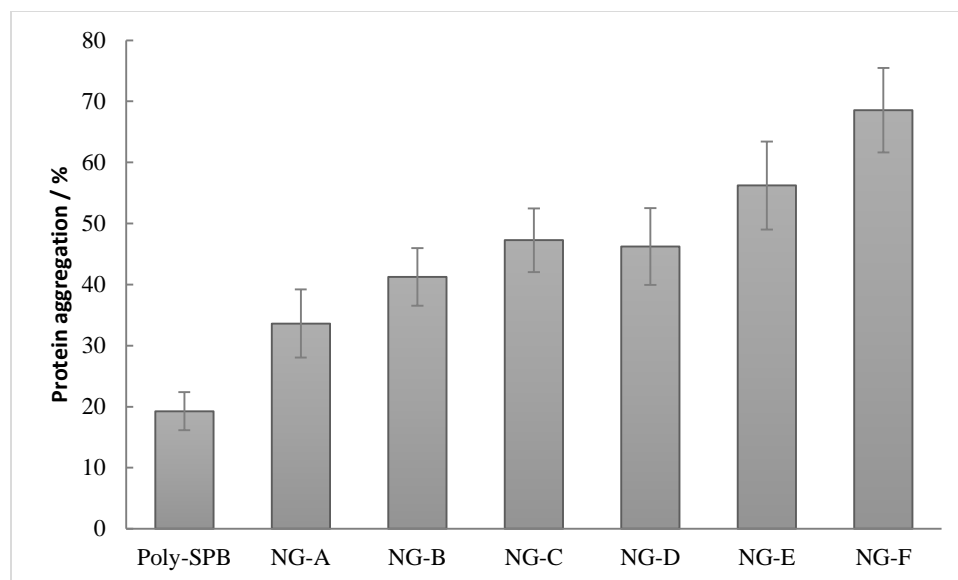


**Figure 5.7.** Protein aggregation inhibition of lysozyme (0.5 mg/mL) when heated to 90 °C for 30 minutes in the presence of different nanogels at 5% concentration (w/v %). Data are expressed as the mean  $\pm$  SD of 3 independent experiments.

## 5.4 Conclusion

In summary, I have shown that transforming a polymer, which itself shows efficiency against protein aggregation, into a nanogel can increase the overall efficiency of the system manifold. It was seen that synthesis of a core-shell nanogel can be easily achieved by employing a chemical cross-linker. The efficiency of the nanogel can be enhanced by increasing the molecular weight of the macro-CTA. Introduction of hydrophobicity to the nanogel also resulted in increased protection against protein aggregation. The nanogel is believed to act as an artificial molecular chaperone and increase the stability of lysozyme even at elevated temperatures. Further studies are warranted to explain the molecular mechanism behind such a remarkable efficiency of such nanogels.

## 5.5 References

- 1 W. O. Baker, *Ind. Eng. Chem.*, 1949, **41**, 511–520.
- 2 P. C. Hiemenz, and R. Rajagopalan, (eds) *Principles of Colloid and Surface Chemistry*, 3rd edn, revised and expanded, CRC Press, 1997.

- 3 K. Akiyoshi, S. Deguchi, N. Moriguchi, S. Yamaguchi and J. Sunamoto, *Macromolecules*, 1993, **26**, 3062-3068.
- 4 Y. Nomura, M. Ikeda, N. Yamaguchi, Y. Aoyama and K. Akiyoshi, *FEBS Lett.*, 2003, **553**, 271-276.
- 5 K. Ikeda, T. Okada, S. Sawada, K. Akiyoshi and K. Matsuzaki, *FEBS Lett.*, 2006, **580**, 6587-6595.
- 6 C. Hayashi, U. Hasegawa, Y. Saita, H. Hemmi, T. Hayata, K. Nakashima, Y. Ezura, T. Amagasa, K. Akiyoshi and M. Noda, *J. Cell. Physiol.*, 2009, **220**, 1–7.
- 7 M. Oishi, S. Sumitani and Y. Nagasaki, *Bioconjugate Chem.*, 2007, **18**, 1379–1382.
- 8 U. Hasegawa, S. M. Nomura, S. C. Kaul, T. Hirano and K. Akiyoshi, *Biochem. Biophys. Res. Commun.*, 2005, **331**, 917–921.
- 9 H. S. Peng, J. A. Stolwijk, L. N. Sun, J. Wegener and O. S. Wolfbeis, *Angew. Chem. Int. Ed.*, 2010, **49**, 4246–4249.
- 10 C. Gota, K. Okabe, T. Funatsu, Y. Harada and S. Uchiyama, *J. Am. Chem. Soc.*, 2009, **131**, 2766–2767.
- 11 N. Singh, Nisha, V. Gill and P. Gill, *Am. J. Adv. Drug Delivery*, 2013, **1**, 271-276.
- 12 S. V. Vinogradov, E. V. Batrakova and A. V. Kabanov, *Colloids Surf.*, 1999, **16**, 291–304.
- 13 J. K. Oh, R. Drumright, D. J. Siegwart and K. Matyjaszewski, *Prog. Polym. Sci.*, 2008, **33**, 448–477.
- 14 Y. Sasaki and K. Akiyoshi, *Chem. Rec.*, 2010, **10**, 366-76.
- 15 K. Reamdonck, J. Demeester and S. D. Smedt, *Soft Matter*, 2009, **5**, 707–715
- 16 Y. Kotsuchibashi and R. Narain, *Polym. Chem.*, 2014, **5**, 3061-3070.
- 17 S. Taneja and F. Ahmad, *Biochem. J.*, 1994, **303**, 147-153.
- 18 M. Kudou, K. Shiraki, S. Fujiwara, T. Imanaka and M. Takagi, *Eur. J. Biochem.*, 2003, **270**, 4547-4554.
- 19 H. Kitano, T. Mori, Y. Takeuchi, S. Tada, M. G. Ide, Y. Yokoyama and M. Tanaka, *Macromol. Biosci.*, 2005, **5**, 314–321.
- 20 D. Lazos, S. Franzka and M. Ulbricht, *Langmuir*, 2005, **21**, 8774-84.
- 21 H. Zhang and M. Chiao, *J. Med. Biol. Eng.*, 2015 **35**, 143–155.
- 22 R. Wetzels, *Trends Biotechnol.*, 1994, **12**, 193–198.
- 23 A. L. Fink, *Fold. Des.*, 1998, **3**, R9-R23.



- 24 M. E. Goldberg, N. E. Bezançon, L. Vuillard and T. Rabilloud, *Fold. Des.*, 1996, **1**, 21–27.
- 25 L. Vuillard, T. Rabilloud, R. Leberman, C. B.Colominas and S. Cusack, *FEBS Lett.*, 1994, **353**, 294-296.
- 26 L. Vuillard, D. Madern, B. Franzetti and T. Rabilloud, *Anal. Biochem.*, 1995, **230**, 290–294.
- 27 L. Vuillard, C. B. Breton and T Rabilloud, *Biochem. J.*, 1995, **305**, 337–343.
- 28 L. Vuillard, B. Baalbaki, M. Lehmann, S. Nørager, P. Legrand and M. Roth, *J.Cryst. Growth*, 1996, **168**, 150-154.
- 29 D. Shah and A. R. Shaikh, *AIChE J.*, 2011, **27**, 513-520.
- 30 S. Tomita, Y. Nagasaki and K. Shiraki, *Biotechnol. Bioeng.*, 2012, **109**, 2543-552.

## Chapter 6 SUMMARY AND OUTLOOK

### 6.1 Conclusion

This thesis addresses the feasibility of synthetic polyampholytes to be employed for various biomaterial applications. The polyampholytes were synthesized using the relatively simple process of RAFT polymerization which made it easier to control molecular mass and the polydispersity index. These polyampholytes showed excellent efficiency towards various biomaterial applications and displayed their excellent biocompatibility.

**In Chapter 2**, I developed a synthetic polyampholyte made of methacrylic acid and 2-(dimethylamino)ethyl methacrylate (Poly-MAA-DMAEMA) and showed that it can efficiently cryopreserve various types of cells without the requirement for any other cryoprotectants. Additionally, introduction of hydrophobicity and an increase in molecular weight promoted cell viability after thawing. Leakage experiments suggested that polyampholytes protected the cell membrane during cryopreservation, and this effect was enhanced by increased hydrophobicity. Moreover, due to low cytotoxicity, these polyampholytes have the potential to replace the conventionally used cryoprotective agent DMSO. This was the first study of its kind which showed that it is possible to design a polymeric cryoprotectant using appropriate polymerization techniques that will protect the cell membrane during freezing.

**In Chapter 3**, I intended to elucidate the molecular mechanism of cryopreservation. This was achieved by synthesizing two more polyampholytes along with poly-(MAA-DMAEMA). One of those polyampholytes didn't show any cryoprotective property at all (poly-CMB) and the second one showed intermediate cryoprotective property (poly-SPB). This contrasting behavior led us to understand the molecular mechanism of cryopreservation. Various studies were carried out to investigate the effect on cell membrane and how polymer chain dynamics is affected during and after the freeze-thawing process. The results suggested that polyampholytes with high cryoprotective property interacts more strongly with the cell membrane and this enables it to protect it from freezing damage. One of the primary causes of cell death which is ice recrystallization, is also avoided by using cryoprotective polyampholytes. Introduction of hydrophobicity further eliminates the recrystallization of ice. Also it was concluded from solid

state NMR that they protect cells from stresses such as drastic changes in soluble space size and osmotic pressure.

**In Chapter 4**, I intended to explore other applications of synthetic polyampholytes. I was able to successfully develop a novel zwitterionic polymer which showed remarkable efficiency against protein aggregation. Lysozyme did not aggregate when heated in the presence of this polymer, and its efficiency was higher than some of the previously well-known reagents. Presence of poly-SPB in lysozyme solution suppressed amyloid formation and also helped in retention of its enzymatic activity, even after prolonged heating. Poly-SPB facilitated retention of partial higher order structures and lysozyme solubility at higher temperatures. The high efficiency of the polyampholyte was ascribed to its ability to prevent collisions between aggregating species by acting as a molecular shield.

**In Chapter 5**, I modified the zwitterionic polymer used in Chapter 4 and developed a core shell nanogel using a chemical cross-linker. I varied the molecular weight and the hydrophobicity of the nanogels. The nanogels obtained showed remarkable efficiency against thermal aggregation of lysozyme. Its efficiency was much higher than zwitterionic polymer prepared in chapter 4. It could achieve similar or even higher efficiency at significantly lower concentrations. This is the first such study, where such a nanogel system has been developed which shows excellent activity against protein aggregation.

## 6.2 Outlook and Scope

I believe I have been successfully able to develop synthetic polyampholytes which can have various biomaterial applications. I have demonstrated that it is very easy to develop synthetic polyampholytes *via* RAFT polymerization and is very easy to control the molecular weight and the functionality of the polymers. Due to the synthetic nature of these polymers, they offer a set a set of advantages over peptide (or amino acid) based polyampholytes because its synthetic nature facilitates modification of surface hydrophobicity and hydrophilicity, as well as easy control over molecular weight and polydispersity.

In Chapter 2 and 3, I demonstrated that synthetic polyampholytes possess remarkable cryoprotective properties and I also elucidated the mechanism. The polymers are biocompatible

and protect cell membrane during freezing. Its mechanism of cryopreservation is different from that of DMSO. Poly-(MAA-DMAEMA) under appropriate conditions of hydrophobicity and molecular weight is a potent CPA and has the potential to be used clinically in future. Additionally, the understanding of the membrane interaction can lead to the development of numerous polymer based CPAs in the future which can then be employed for preserving 2D and 3D cell containing constructs.

In chapter 4 and 5, I developed a novel polymer based system which protects proteins under extreme stress, this leading to suppression of protein aggregation. Previously, only small organic molecules were used for such a study, but in Chapter 4, I showed that a synthetic polymer can also be effective against protein aggregation. The higher efficiency of this polymer than other reagents can revolutionize the field of protein biopharmaceutics where more polymer, particularly zwitterionic polymers can be successfully employed.

In Chapter 5, the development of nanogels based on poly-SPB clearly demonstrated the ability of such a system to be used for protein biopharmaceutics. The efficiency of the nanogels was surprisingly very high and requires only small amount to be effective against protein aggregation. Further studies on how poly-SPB and its corresponding nanogels protect the protein can pave the path for the development of much more effective systems. For the cure of several ailments, proteins are delivered to the body, but most of the proteins undergo aggregation and forms fibril which cause unnecessary damage and several other complications. Hence, these nanogels can be used in conjunction with the proteins and can be delivered safely to the body.

These are just two of the properties of synthetic polyampholytes. They exhibit a range of other properties like temperature and pH responsiveness, anti-biofouling, drug delivery, etc. All the applications can be studied in the future.

Although these polymers have broad range of applications that covers different areas of biomaterial science, but these are model systems only. It is a fundamental study which describes the different methodologies to develop polyampholytes for various applications. In order to use them for clinical applications, in-vivo study need to be carried out. I believe my study has broadened the basic understanding of the hydrogels. This has covered some pit-holes in the research field. I expect my study will assist in the development of better systems in the future.

## ACHIEVEMENTS

### Main Publications

- 1 **Robin Rajan**, Minkle Jain and Kazuaki Matsumura, “Cryoprotective properties of completely synthetic polyampholytes via reversible addition-fragmentation chain transfer (RAFT) polymerization and the effects of hydrophobicity”, **Journal of Biomaterials Science, Polymer Edition**, Taylor & Francis Group , 24, 2013, 1767-1780.
- 2 **Robin Rajan** and Kazuaki Matsumura, “Preparation of Novel Synthetic Cryoprotectants”, **Cryobiology and Cryotechnology**, 60, 2014, 99-103.
- 3 **Robin Rajan** and Kazuaki Matsumura, “A zwitterionic polymer as a novel inhibitor of protein aggregation”, **Journal of Materials Chemistry B**, Royal Society of Chemistry, 3, 2015, 5683—5689.
- 4 **Robin Rajan**, Fumiaki Hayashi, Toshio Nagashima and Kazuaki Matsumura, “Toward a Molecular Understanding of the Mechanism of Cryopreservation: Cell Membrane Interactions and Hydrophobicity”, **Biomacromolecules**, American Chemical Society, 17, 2016, 1882-93.

### Related Publications

- 1 Minkle Jain, **Robin Rajan**, Suong-Hyu Hyon and Kazuaki Matsumura, “Hydrogelation of dextran-based polyampholytes with cryoprotective properties via click chemistry” **Biomaterials Science**, Royal Society of Chemistry, 2 (3), 2014, 308-317.
- 2 Kazuaki Matsumura, Minkle Jain and **Robin Rajan**, Cell and Materials Interface in Cryobiology and Cryoprotection in Cell and Material Interface: **Advances in Tissue Engineering, Biosensor, Implant, and Imaging Technologies**, Edited by Nihal Engin Vrana, CRC Press, Taylor & Francis Group, 2015. **(Book Chapter)**
- 3 **Robin Rajan** and Kazuaki Matsumura, “Synthetic Polyampholytes Based Cryoprotective Agents by Reversible Addition Fragmentation Chain Transfer Polymerisation”, **MRS Proceedings**, Cambridge University Press, 2013.

## ACKNOWLEDGEMENT

*"The dream begins, most of the time, with a teacher who believes in you, who tugs and pushes, and leads you onto the next plateau, sometimes poking you with a sharp stick called truth."*

--Dan Rather

I am highly indebted to my supervisor **Associate Prof. Dr. Kazuaki Matsumura** as he was with me at every step of my research. It is only due to his constant guidance, advice and support that I am able to complete this project. I am blessed to have had someone like him as my mentor and guide. His guidance not only increased my knowledge but also helped me in successfully overcoming my difficulties. I would also like to thank him for being open to my ideas and for encouraging and helping me to shape my interest.

Besides my supervisor I would also like to thank my sub supervisor Prof. Dr. Noriyoshi Matsumi for his support during my doctoral study. I also express my sincere and deep sense of gratitude to Prof. Dr. Shinya Maenosono, School of Materials Science, JAIST, who was my minor research supervisor, for not only providing me with the necessary laboratory facilities for my work but for also constantly encouraging and guiding me. I would to thank Prof. Dr. Tatsuo Kaneko, Associate Prof. Dr. Yuki Nagao, Prof. Dr. Masahiro Takagi and Prof. Dr. Koichi Kato for all their critical comments and valuable suggestions during my preliminary defense.

Special appreciation goes to my friend, Dr. Minkle Jain, who always supported me in all my endeavors. I would like to thank her for always being by my side and for being someone I could rely on. It was her positive criticism and questioning that helped me to think rationally and to come up with magical solutions each time I thank her for assisting me in setting up difficult reactions and in all my other laboratory work.

Finally I would also like to thank my parents and my brother for the incredible amount of support that they have given me throughout my research career. Doing this without their encouragement and prayers, would've been impossible. I would also like to dedicate this thesis to my parents as a tribute to their encouragement, support and love towards me.